

**EVALUATION OF INCIPIENT MOTION
CRITERIA FOR ROCK IN RENO MATTRESSES
AND RIP RAP**

Francis W. Stoffberg



**EVALUATION OF INCIPIENT MOTION
CRITERIA FOR ROCK IN RENO MATTRESSES
AND RIP RAP**

By Francis W. Stoffberg

**Thesis presented in partial fulfilment of the
requirements for the degree of Master of Engineering
at the University of Stellenbosch**

Study Leader: Prof. G. R. Basson

December 2005

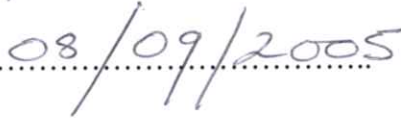
DECLARATION

I, the undersigned, hereby declare that the work contained in this thesis is my own original work and that I have not previously in its entirety or in part submitted it at any university for a degree.

Signature:

A handwritten signature in blue ink, appearing to be 'J. J. Lee', written over a dotted line.

Date:08/09/2005.....

A handwritten date '08/09/2005' in blue ink, written over a dotted line.

ABSTRACT

There has always been some debate in the past about the most effective and economical type of revetment to be used to combat or prevent erosion in rivers and channels. Some of the most common materials used for these mitigation measures are gabions, Reno mattresses and rip rap.

A study done by the Colorado State University (CSU, 1984), comprised hydraulic tests of Reno mattresses used as a channel bed revetment. The results were compared with those of rip rap.

This thesis mainly deals with the evaluation of incipient motion conditions for rock used in Reno mattresses and as rip rap. In this thesis the results of the CSU study and the design criteria of Maccaferri are evaluated and compared with the results obtained when applying the stream power theory and the Shields' theory with respect to incipient motion.

This thesis includes the theory with respect to incipient motion conditions, background to the CSU study and comparisons of the results of the CSU study and Maccaferri's design criteria with theoretical calculations. A cost comparison of Reno mattresses and rip rap as channel bed revetment measures, as well as conclusions and recommendations with regard to the design and use of these options, are also included.

The frame of reference for this thesis is the set of CSU test results. The calibrations achieved, proposals made and accuracy of conclusions thus depend on those results.

OPSOMMING

Daar is nog altyd in die verlede gedebatteer omtrent die mees effektiewe en ekonomiese tipe bekleding wat gebruik moet word ten einde erosie in riviere en kanale teen te werk of te verhoed. 'n Paar van die mees algemene materiale wat vir hierdie bekampingsmaatreëls aangewend word, is skanskorwe, skanskorfmatrasse en rip-rap (rotsbekleding of stortklip).

'n Studie is deur die Colorado State University (CSU, 1984) gedoen waarvolgens hidrouliese toetse uitgevoer is op skanskorfmatrasse as kanaalbodem bekleding. Die resultate is met dié van rip-rap vergelyk.

Hierdie tesis handel hoofsaaklik oor die evaluering van die begin van beweging van klip wat in skanskorfmatrasse en rip-rap gebruik word. In hierdie tesis word die resultate van die CSU studie asook die ontwerp kriteria van Maccaferri geëvalueer en vergelyk met die resultate verkry vanaf die stroomdrywingsteorie en die Shields teorie, ten opsigte van begin van beweging.

Hierdie tesis sluit in die teorie betreffende die toestand tydens begin van beweging, 'n agtergrond van die CSU studie en 'n vergelyking van resultate van die CSU studie en Maccaferri se ontwerp kriteria met dié verkry van teoretiese berekeninge. 'n Kostevergelyking tussen skanskorfmatrasse en rip-rap as bekleding vir kanaalbodems, sowel as gevolgtrekkings en voorstelle met betrekking tot die ontwerp en gebruik van hierdie opsies, is ook ingesluit.

Die verwysingsraamwerk van hierdie tesis is vasgestel deur die CSU studie toetse. Die kalibrasie bereik, voorstelle wat gemaak word en die akkuraatheid van gevoltrekkings is dus binne daardie perke gedoen.

INDEX

EVALUATION OF INCIPIENT MOTION CONDITIONS FOR ROCK USED IN RENO MATTRESSES AND RIP RAP

| ITEM | DESCRIPTION | PAGE |
|-------|---|------|
| | DECLARATION | i |
| | ABSTRACT | ii |
| | OPSOMMING | iii |
| | INDEX | iv |
| | LIST OF SYMBOLS | vii |
| | LIST OF TABLES | x |
| | LIST OF FIGURES | xiii |
| | ACKNOWLEDGEMENT | xvi |
| 1. | INTRODUCTION | 1 |
| 2. | INCIPIENT MOTION THEORY | 2 |
| 2.1 | Introduction | 2 |
| 2.2 | Physical Characteristics Of Sediment | 3 |
| 2.2.1 | Size | 3 |
| 2.2.2 | Shape | 4 |
| 2.2.3 | Uniformity | 5 |
| 2.2.4 | Settling velocity | 6 |
| 2.2.5 | Cohesiveness | 7 |
| 2.2.6 | Angle of repose | 8 |
| 2.3 | Types Of Motion | 9 |
| 2.4 | Factors Influencing The Motion Of Any Particular Particle | 9 |

| | | |
|-------|--|----|
| 2.5 | Intensity Of Motion | 10 |
| 2.6 | Models Of Incipient Motion In Terms Of Flow-related Parameters | 11 |
| 2.6.1 | Introduction | 11 |
| 2.6.2 | Incipient motion in terms of flow velocity | 11 |
| 2.6.3 | Incipient motion in terms of shear stress | 12 |
| 2.6.4 | Incipient motion in terms of stream power | 16 |
| 2.7 | Incipient Motion On Sloping Beds | 27 |
| 2.8 | Layer Thicknesses Of Rip Rap And Reno Mattress Revetments | 30 |
| 3. | BACKGROUND OF STUDY DONE BY COLORADO STATE UNIVERSITY (CSU) | 32 |
| 3.1 | Introduction | 32 |
| 3.2 | Objectives Of The CSU Study | 32 |
| 3.3 | Test Program | 33 |
| 3.3.1 | Scale-model testing | 33 |
| 3.3.2 | Full-scale testing | 39 |
| 3.4 | Analysis Of Results | 42 |
| 3.4.1 | Hydraulics of mattress channels | 42 |
| 3.4.2 | Incipient motion conditions | 46 |
| 3.4.3 | Deformation of mattresses under high flow conditions | 48 |
| 3.5 | Summary And Conclusions Of CSU Study | 49 |
| 4. | COMPARISON OF CSU STUDY RESULTS WITH THAT OF STREAM POWER THEORY, BASED ON THE LIU DIAGRAM, AND SHIELD'S THEORY AS FORECASTERS FOR INCIPIENT MOTION OF ROCK IN RIP RAP | 51 |
| 4.1 | Introduction | 51 |
| 4.2 | Assumptions | 52 |
| 4.3 | Comparison Of Results | 52 |
| 4.3.1 | Comparison of results in terms of stream power | 52 |
| 4.3.2 | Comparison of results in terms of Shield's parameter (shear stress) | 62 |

| | | |
|-------|--|-----|
| 4.4 | Comparison Of Proposed Rip Rap Layer And Reno Mattress Thicknesses | 65 |
| 4.4.1 | Rip rap | 65 |
| 4.4.2 | Reno mattresses | 73 |
| 4.5 | Reno Mattresses: Proposals Of This Thesis Versus Proposals By Maccaferri | 81 |
| 4.6 | Combination Of Results | 85 |
| 5. | PARAMETER SENSITIVITY | 86 |
| 6. | COST ANALYSIS | 90 |
| 7. | SUMMARY OF RESULTS | 93 |
| 8. | CONCLUSIONS AND RECOMMENDATIONS | 97 |
| 9. | REFERENCES | 100 |

ANNEXURES

- ANNEXURE A : Table A-1: Dimensions of Model-Scale and Full-Scale Mattresses Tested in CSU Study
- ANNEXURE B : Relationship between Reno Mattress Thickness and Rock Particle Diameter
- ANNEXURE C : Figures C-1 to C-2 and Table C-1: Maccaferri Design Criteria for revetments using Reno Mattresses (Maccaferri, 2004 and Papetti, 1985)
- ANNEXURE D : Figures D-1 to D-4: Comparison of Rip Rap Layer and Reno Mattress Thicknesses between Various Methods Used for CSU Tests A to D to Just Resist Particle Motion
- ANNEXURE E : Figures E-1 to E-4: Relationship of Sensitive Parameters to Each Other for Minimum Conditions to Just Resist Particle Motion Based on Data of CSU Tests A to D
- ANNEXURE F : Figures F-1 to F-4: Comparative Costs for Rip Rap and Reno Mattresses Based on CSU Tests A to D

LIST OF SYMBOLS

| SYMBOL | DESCRIPTION | UNIT |
|--------------|--|---------------------|
| a | Largest triaxial dimension of sediment particle | (m or mm) |
| A | Cross sectional flow area | (m ²) |
| b | Intermediate triaxial dimension of sediment particle | (m or mm) |
| c | Shortest triaxial dimension of sediment particle | (m or mm) |
| C_D | Coefficient of drag | |
| CSU | Colorado State University | |
| d | Sediment diameter | (m or mm) |
| d_i | Median diameter of any particular size fraction | (m or mm) |
| d_s | Diameter of sphere having the same surface area as a particular particle | (m or mm) |
| d_v | Diameter of sphere having the same volume as a particular particle | (m or mm) |
| $d_{\%}$ | Sediment diameter where % indicates the percentage of particles finer by mass than the indicated value | (m or mm) |
| d_{50} | Median diameter | (m or mm) |
| d_{max} | Maximum nominal sediment diameter | (m or mm) |
| \bar{d} | Mean diameter | (m or mm) |
| D | Hydraulic mean depth, hydraulic depth, or flow depth | (m) |
| F | Froude number | |
| F_D | Drag force | (N) |
| $F_{D,cr}$ | Critical drag force for any given slope | (N) |
| $F_{D,cr,0}$ | Critical drag force for a horizontal slope | (N) |
| g | Gravitational acceleration ($\approx 9,81$) | (m/s ²) |
| k | Absolute roughness of bed material | (m) |
| k_{β} | Correction factor for a longitudinal slope | |
| k_{γ} | Correction factor for a transverse slope | |

| | | |
|----------------------|---|---------------------------|
| n | Manning roughness coefficient | ($\text{s/m}^{1/3}$) |
| n_b | Manning roughness coefficient for flume bed | ($\text{s/m}^{1/3}$) |
| P | Wetted perimeter normal to the direction of flow | (m) |
| p_i | Percentage by mass of any particular size fraction | (%) |
| P_r | Applied stream power required | (N) |
| P_t | Stream power applied | (N) |
| $P_{t(l)}$ | Stream power applied for laminar flow | (N) |
| $P_{t(t)}$ | Stream power applied for turbulent flow | (N) |
| Q | Discharge, flow rate | (m^3/s) |
| r | Rip rap layer thickness | (m or mm) |
| R | Hydraulic radius ($= A/P$) | (m) |
| R_b | Hydraulic radius acting on the flume bed | (m) |
| Re | Reynolds number ($= \rho v R / \mu = v R / \nu$) | |
| Re_* | Particle Reynolds number | |
| R_0 | Radius of turbulent eddies next to stream bed | (m) |
| S | Slope | (m/m) |
| S_0 | Bed slope | (m/m) |
| SANRAL | South African National Roads Agency Limited | |
| t | Reno mattress thickness | (m or mm) |
| v | Average velocity ($= Q/A$) | (m/s) |
| v_* | Shear velocity of sediment particle | (m/s) |
| v_{ss} | Settling velocity of sediment particle | (m/s) |
| $\frac{v_*}{v_{ss}}$ | Movability number | |
| v_y | Velocity in vertical direction | (m/s) |
| $W_{\%}$ | rock weight for which the % of the rock indicated is smaller by weight | (N/m^3) |
| x | Horizontal distance from the origin in the direction of flow | (m) |
| y | Vertical height above origin | (m) |
| y_0 | Ordinate where velocity is mathematically = 0 ($y_0 = k/30$) | (m) |

| | | |
|-----------------|--|-------------------------|
| β | Longitudinal slope of bed in the direction of flow | (degrees) |
| γ | Transverse slope of bed normal to the direction of flow | (degrees) |
| λ | Porosity | |
| η | Ratio of applied unit stream power to unit power required to suspend (move) particle | |
| η_l | Ratio of applied unit stream power to unit stream power required to suspend a particle in a laminar boundary | |
| η_t | Ratio of applied unit stream power to unit stream power required to suspend a particle in a turbulent boundary | |
| θ | Shield's parameter | |
| θ_c | Critical Shield's parameter | |
| μ | Dynamic viscosity of water ($= \rho \nu \approx 10^{-3}$) | (Pa.s) |
| ν | Kinematic viscosity of water ($= \mu/\rho \approx 10^{-6}$) | (m ² /s) |
| ρ | Density of water (≈ 1000) | (kg/m ³) |
| ρ_s | Particle density | (kg/m ³) |
| σ | Standard deviation | |
| τ | Shear stress | (Pa, N/m ²) |
| τ_c | Critical bed shear stress for incipient motion | (Pa, N/m ²) |
| τ_0 | Shear stress at the bed (boundary) | (Pa, N/m ²) |
| $\tau_{0,cr}$ | Critical bed shear stress at any slope | (Pa, N/m ²) |
| $\tau_{0,cr,0}$ | Critical bed shear stress on a horizontal bed | (Pa, N/m ²) |
| ϕ_r | Angle of repose | (degrees) |
| ψ | Slope correction factor | |

LIST OF TABLES

| REF. | TITLE | PAGE |
|------|---|------|
| 2.1 | Particle size classification (Armitage & McGahey, 2003 and Simons and Şentürk, 1977) | 4 |
| 2.2 | Values for angle of repose for quartzitic material (Armitage, 2002) | 8 |
| 3.1 | Model-to-prototype scaling ratios | 34 |
| 3.2 | Scale-model mattress test data in the 2,44 m flume (CSU, 1984) | 36 |
| 3.3 | Manning's roughness coefficient for the model-scale mattresses tests conducted in the 2,44 m flume (CSU, 1984) | 37 |
| 3.4 | Run sequence for Test A: 150 mm nominal thick mattress (1,22 m flume) | 38 |
| 3.5 | Run sequence for Test B: 230 mm nominal thick mattress (1,22 m flume) | 38 |
| 3.6 | Run sequence for Test C: 300 mm nominal thick mattress (1,22 m flume) | 39 |
| 3.7 | Run sequence for Test D: 450 mm nominal thick mattress (1,22 m flume) | 39 |
| 3.8 | Test run sequence – discharge, velocity, depth measurements for the 150 mm full-scale mattress tests (CSU, 1984) | 40 |
| 3.9 | Test run sequence – discharge, velocity, depth measurements for the 230 mm full-scale mattress tests (CSU, 1984) | 41 |
| 3.10 | Determination of 230 mm mattress properties, roughness coefficient, n_b and bed shear stress, τ_b (CSU, 1984) | 41 |
| 3.11 | Critical velocities for various mattress thicknesses determined from the CSU study compared with the velocities suggested by Agostini and Papetti (CSU, 1984) | 46 |

| | | |
|------|---|----|
| 3.12 | Required mattress thickness as determined from laboratory tests compared to that suggested for rip rap (CSU, 1984) | 48 |
| 4.1 | Comparison between CSU study, Shields & Stream Power based on the Liu Diagram for 150 mm Mattress (Test A) | 56 |
| 4.2 | Comparison between CSU study, Shields & Stream Power based on the Liu Diagram for 230 mm Mattress (Test B) | 57 |
| 4.3 | Comparison between CSU study, Shields & Stream Power based on the Liu Diagram for 300 mm Mattress (Test C) | 58 |
| 4.4 | Comparison between CSU study, Shields & Stream Power based on the Liu Diagram for 450 mm Mattress (Test D) | 59 |
| 4.5 | Movability Numbers for motion incipency, using the Stream Power theory | 61 |
| 4.6 | Shield's parameter for motion incipency, using Shield's theory | 63 |
| 4.7 | Comparative values of shear stress and Shield's parameter obtained from the CSU tests done (CSU, 1984) and those calculated theoretically | 64 |
| 4.8 | Rip rap: Required rock size and layer thickness that will just resist motion (at point of motion incipency) using the slopes and flow depths as per CSU Test A | 68 |
| 4.9 | Rip rap: Required rock size and layer thickness that will just resist motion (at point of motion incipency) using the slopes and flow depths as per CSU Test B | 69 |
| 4.10 | Rip rap: Required rock size and layer thickness that will just resist motion (at point of motion incipency) using the slopes and flow depths as per CSU Test C | 70 |
| 4.11 | Rip rap: Required rock size and layer thickness that will just resist motion (at point of motion incipency) using the slopes and flow depths as per CSU Test D | 71 |
| 4.12 | Reno mattresses: Required rock size and mattress thickness that will just resist motion (at point of motion incipency) using the slopes, flow depths, velocities and shear stresses as per CSU Test A | 77 |

| | | |
|------|---|----|
| 4.13 | Reno mattresses: Required rock size and mattress thickness that will just resist motion (at point of motion incipency) using the slopes, flow depths, velocities and shear stresses as per CSU Test B | 78 |
| 4.14 | Reno mattresses: Required rock size and mattress thickness that will just resist motion (at point of motion incipency) using the slopes, flow depths, velocities and shear stresses as per CSU Test C | 79 |
| 4.15 | Reno mattresses: Required rock size and mattress thickness that will just resist motion (at point of motion incipency) using the slopes, flow depths, velocities and shear stresses as per CSU Test D | 80 |
| 4.16 | Comparative rock sizes for Reno mattresses obtained by applying Shield's theory, Stream Power theory and from Maccaferri's design graphs | 82 |
| 4.17 | Comparative Reno mattress thicknesses obtained by applying Shield's theory, Stream Power theory and from Maccaferri's design graphs | 84 |
| 6.1 | Unit costs used in cost analysis | 91 |
| 7.1 | Comparative minimum required layer thickness, r , and cost per m^2 for rip rap to just resist motion (at incipient motion condition) as per CSU Test B | 95 |
| 7.2 | Comparative minimum required thicknesses, t , and cost per m^2 for Reno mattresses to just resist motion (at incipient motion condition) as per CSU Test B | 95 |
| 8.1 | Recommended Movability number, v^*/v_{ss} , for design of mean rock size | 98 |
| 8.2 | Recommended Shield's parameter, θ , for design of mean rock size | 98 |

LIST OF FIGURES

| REF. | TITLE | PAGE |
|------|---|------|
| 2.1 | The Shield's diagram for incipient motion (Armitage, 2002) | 13 |
| 2.2 | Schematic long section of uniform flow showing depth of flow, D , velocity profile, v , shear stress distribution, τ , bed slope S_0 , and water element ABCE (Rooseboom, 1974 and 1992) | 17 |
| 2.3 | Long section of uniform flow in a stream showing the distribution of stream power made available, $\rho g S_0 v$, and stream power applied, $\tau dv/dy$ (Rooseboom, 1974) | 18 |
| 2.4 | The Rooseboom criteria for incipient motion (based on Liu diagram) (Rooseboom, 1974 & 1992) | 26 |
| 2.5 | The Armitage criteria for incipient scour (based on Liu diagram) (Armitage, 2002) | 26 |
| 3.1 | Comparison between the measured and calculated Manning's roughness coefficient (CSU, 1984) | 43 |
| 3.2 | Average velocity distribution for selected model-scale mattress tests in the 1,22 m flume (CSU, 1984) | 44 |
| 3.3 | Relationship between shear stress, velocity and hydraulic radius (CSU, 1984) | 45 |
| 3.4 | Critical velocity that indicates rock movement as a function of mattress thickness (CSU, 1984) | 47 |
| 3.5 | Critical shear stress versus mattress / rip rap thickness (CSU, 1984) | 48 |
| 4.1 | Values of movability numbers and particle Reynolds numbers for the 150 mm, 230 mm, 300 mm, and 450 mm mattresses plotted on the Liu diagram together with the criteria of Rooseboom (1974 and 1992) and Armitage (2002) | 54 |
| 4.2 | Detail "A": see Figure 4.1 | 55 |

| | | |
|------|---|----|
| 4.3 | Rip rap layer thicknesses as proposed in this thesis using Shield's theory versus that using stream power theory | 66 |
| 4.4 | Required rip rap layer thicknesses for Test A | 68 |
| 4.5 | Required rip rap layer thicknesses for Test B | 69 |
| 4.6 | Required rip rap layer thicknesses for Test C | 70 |
| 4.7 | Required rip rap layer thicknesses for Test D | 71 |
| 4.8 | Recommended rip rap size for different methods applied to CSU test data - Tests A to D (CSU, 1984) | 72 |
| 4.9 | Median rock diameter sizes required for Reno mattresses as proposed in this thesis using Shield's theory versus that using stream power theory | 74 |
| 4.10 | Reno mattress thicknesses as proposed in this thesis using Shield's theory versus that using stream power theory | 75 |
| 4.11 | Required Reno mattress thicknesses for Test A | 77 |
| 4.12 | Required Reno mattress thicknesses for Test B | 78 |
| 4.13 | Required Reno mattress thicknesses for Test C | 79 |
| 4.14 | Required Reno mattress thicknesses for Test D | 80 |
| 4.15 | Rock sizes for Reno mattresses as proposed by Maccaferri, obtained graphically (Maccaferri, 2004), versus that proposed in this thesis, based on Shield's theory and Stream Power theory, for CSU Tests A to D (CSU, 1984) | 83 |
| 4.16 | Reno mattress thicknesses as proposed by Maccaferri, obtained graphically (Maccaferri, 2004), versus that proposed in this thesis, based on Shield's theory and Stream Power theory, for CSU Tests A to D (CSU, 1984) | 85 |
| 5.1 | The relationship of flow velocity to bed shear stress for minimum conditions to just resist particle motion (at point of motion incipency) based on data of CSU tests A to D (see Tables 4.8 to 4.15 and Figures 4.4 to 4.7 & 4.11 to 4.14) | 87 |

| | | |
|-----|---|----|
| 5.2 | The relationship of bed shear stress to Froude number for minimum conditions to just resist particle motion (at point of motion incipency) based on data of CSU tests A to D (see Tables 4.8 to 4.15 and Figures 4.4 to 4.7 & 4.11 to 4.14) | 88 |
| 5.3 | The relationship of flow velocity to Froude number for minimum conditions to just resist particle motion (at point of motion incipency) based on data of CSU tests A to D (see Tables 4.8 to 4.15 and Figures 4.4 to 4.7 & 4.11 to 4.14) | 88 |
| 6.1 | Cost comparison between rip rap and Reno mattresses, based on the layer thicknesses proposed in Tables 4.8 to 4.15 and Figures 4.4 to 4.7 and 4.11 to 4.14 | 92 |
| 7.1 | Comparative costs for rip rap and Reno mattresses for minimum required layer thicknesses to just resist motion (at incipient motion condition) as per CSU Test B (see Tables 3.5, 4.2, 4.9 and 4.13, as well as Figures 4.5 and 4.12) | 94 |

ACKNOWLEDGEMENT

I gratefully acknowledge my study leader, Professor Gerrit Basson of the Civil Engineering Department at the University of Stellenbosch, who provided me with the opportunity to do this thesis, and for his assistance and guidance during the execution thereof.

EVALUATION OF INCIPIENT MOTION CRITERIA FOR ROCK IN RENO MATTRESSES AND RIP RAP

1. INTRODUCTION

Sediment transport is a major problem in the control and utilisation of surface water all over the world. Various problems in this regard are encountered in the design of irrigation and drainage structures, in the improvement or stabilization of rivers and channels, in flood control, in the planning and design of dams, in the maintenance of harbour channels, and in the control of soil and beach erosion.

A study, including hydraulic tests, was done by the Colorado State University (CSU, 1984) with regard to the stability of Reno (or gabion) mattresses when used as river and canal revetments. Details with respect to the CSU study are discussed in Chapter 3.

The objectives of this thesis are as follows:

- to compare and evaluate the results of the study done by the CSU with results obtained by applying known models of incipient motion, based on flow-related parameters, such as velocity, bed shear stress and stream power.
- to compare the results obtained from the Colorado State University with those obtained from the methodology given in the SANRAL Road Drainage Manual, and
- to theoretically test which parameters are the most sensitive with respect to the above-mentioned methods, i.e., which parameter has the biggest influence on incipient motion of rock inside Reno mattresses and of rock used for rip rap.

The theory of sediment movement is briefly discussed in Chapter 2, and although the theory of both suspended and bed load sediment transport are covered, the latter is more applicable to the above-mentioned objectives.

2. INCIPIENT MOTION THEORY

2.1 Introduction

This chapter reviews incipient motion – the conditions under which the movement of sediment, and hence scour, will commence. Scour is not only the principle cause of failure of many bridges and culverts, it is also the principle cause of failure of countless other hydraulic structures, including sub-standard gabion, Reno mattress and rip rap revetments. The opposite mechanism, namely deposition, is also a cause of failure of many others. Incipient motion can thus also be seen as the nominal boundary between scour and deposition. Incipient motion is hard to define as it refers to some “threshold of motion”.

The threshold of sediment motion cannot be defined with absolute precision. As the velocity of flow over an initially stationary bed of sediment is steadily increased, there is no point at which sediment movement suddenly becomes general. There is first a condition in which a grain or particle is detached from the bed every few seconds, and the movement could possibly be ascribed to the unstable initial position of each particular grain or particle. Then, as the velocity is increased, particle movement gradually becomes more frequent until it is general over the whole bed. The transition to general movement can, in certain cases, be rapid.

Incipient motion is dependent on the physical characteristics of the sediment particles, and factors such as shape, uniformity, settling velocity, cohesiveness and the angle of repose (internal friction angle) all play a role. The physical characteristics of sediment are discussed in section 2.2.

Incipient motion can be described in terms of flow velocity, bed shear stress and unit stream power, and the influence of these parameters on incipient motion is described in section 2.6.

The conditions for incipient motion are clearly affected by the slope of the bed, both in the longitudinal and transverse directions. Some attention is therefore given to factors that have been used to adjust the incipient motion parameters developed for flat beds to those that apply for slopes (see section 2.7).

2.2 Physical Characteristics Of Sediment

2.2.1 Size

Particle size is probably the most important parameter in defining incipient motion. Smaller particles will generally be moved more easily by the flow than larger ones. It is generally assumed that sediment particles are reasonably spherical, although particle shapes could be very different in reality.

Some definitions of sediment diameter are as follows:

- Sieve diameter: the length of the side of a square opening through which the particle will just pass.
- Nominal diameter: the diameter of a sphere of equal volume.
- Sedimentation diameter: the diameter of a sphere of the same density and the same settling velocity in the same fluid at the same temperature.
- Standard fall diameter: as for sedimentation diameter except that the sphere has a density of 2650 kg/m^3 , the liquid is quiescent distilled water of infinite extent, and the temperature is 24°C .
- Triaxial dimensions: the length of the three orthogonal dimensions a , b and c , where a is generally the longest dimension and c the shortest.

The most common particle size classification is given in Table 2.1.

Table 2.1: Particle size classification (Armitage & McGahey, 2003 and Simons and Şentürk, 1977)

| Class | Size (mm) |
|------------------|------------------|
| Boulders | >256 |
| Cobbles | 64 to 256 |
| Gravel | 2 to 64 |
| Very course sand | 1 to 2 |
| Coarse sand | 0.5 to 1.0 |
| Medium sand | 0.25 to 0.5 |
| Fine sand | 0.125 to 0.25 |
| Very fine sand | 0.062 to 0.125 |
| Silt | 0.004 to 0.062 |
| Clay | 0.00024 to 0.004 |
| Colloids | < 0.00024 |

2.2.2 Shape

Abrasion in the natural transport process tends to round sediment particles and the roundness is an indication of how far the particle has travelled. Since it is generally assumed that sediment particles are reasonably spherical, it is necessary to define a shape factor to take into account the deviation from the spherical. The most common shape factor is that of Corey (Simons and Şentürk, 1977), defined as:

$$SF = \frac{c}{\sqrt{ab}} \quad (2.1)$$

where, a = longest dimension
 c = shortest dimension

Naturally worn quartz particles have a Corey shape factor of about 0,7 (Simons and Şentürk, 1977).

A perfect sphere has a shape factor of 1.0, while values below 1.0 would indicate increasing deviation from a perfect sphere. The Corey shape factor generally works well, except that a cube also has a shape factor of 1.0. To overcome this problem, the diameter of a sphere having the same surface area as that of the particle is defined as d_s , and the diameter of a sphere having the same volume as that of the particle as d_v (Armitage and McGahey, 2003). Equation (2.1) then becomes:

$$SF = \frac{d_s c}{d_v \sqrt{ab}} \quad (2.2)$$

2.2.3 Uniformity

Sediment uniformity is the measure of the distribution of the particle sizes. Since sediment particle sizes are usually determined by sieve analysis, giving the percentage of material by mass passing one sieve diameter, but retained on one size smaller. Statistical parameters such as the mean, standard deviation, skewness, etc. may be determined from this.

The most common definitions are as follows:

- Median diameter (d_{50}):
The particle diameter that is exceeded by exactly 50% of the material by mass. If the size distribution is skewed, d_{50} is usually calculated from the average of the $d_{15.9}$ and $d_{84.1}$ values (Simons and Şentürk, 1977):

$$d_{50} = \frac{d_{15.9} + d_{84.1}}{2} \quad (2.3)$$

- Mean diameter: (\bar{d}):

The arithmetic mean of the particle sizes:

$$\bar{d} = \frac{\sum p_i d_i}{100} \quad (2.4)$$

where, d_i = the median diameter of any particular size fraction

p_i = the percentage by mass of that fraction

- Standard deviation (σ):

$$\sigma = \frac{\sum p_i \sqrt{d_i - \bar{d}^2}}{100} \quad (2.5)$$

where, d_i = the median diameter of any particular size fraction

p_i = the percentage by mass of that fraction

\bar{d} = the mean diameter

Alternatively, d_{50} is substituted for \bar{d} .

2.2.4 Settling velocity

The “settling velocity”, also called the “fall velocity”, is generally defined as the average terminal settling velocity of a particle falling alone in quiescent, distilled water of infinite extent. The settling velocity depends on the size, shape, surface roughness and density of the particle, and on the density and viscosity of the fluid. Other factors that can also have an influence are the fluid turbulence, particle concentration and the presence of boundaries.

The primary variable defining the interaction of sediment transport with the bed, banks or suspension in the fluid is the settling velocity of sediment particles.

At the terminal velocity of a particle, the weight, buoyancy force and drag force are in equilibrium. The settling velocity can be defined as follows (Chadwick & Morfett, 1998 and Armitage, 2002):

$$v_{ss} = \sqrt{\frac{4}{3} \left(\frac{\rho_s - \rho}{\rho} \right) \frac{g d}{C_D}} \quad (2.6)$$

where,

- v_{ss} = the settling velocity (m/s)
- ρ_s = particle density (kg/m³)
- ρ = density of the fluid (kg/m³)
- g = gravitational acceleration (= 9,81 m/s²)
- d = sediment diameter (d_{50} or \bar{d} can be used alternatively) (m)
- C_D = drag coefficient

The settling velocity of objects with unusual shapes must be determined experimentally.

2.2.5 Cohesiveness

Sediment can be classified into two principle types, namely non-cohesive and cohesive materials:

- Non-cohesive materials consist of individual particles, such as boulders, cobbles, gravel and sand. The weight of the particles is the dominant force determining transportability.
- Cohesive materials usually contain very fine particles, such as silt and clay. These particles have very high surface to mass ratios. Because of the very large surface area, electro-chemical forces tend to bind these particles together into a coherent

mass. Once the electro-chemical bonds between cohesive particles have been broken down and the particles are carried into suspension, cohesive particles generally behave similarly to non-cohesive materials.

This study will focus exclusively on non-cohesive particles, as rock is used in Reno mattresses and rip rap.

2.2.6 Angle of repose

The “angle of repose”, ϕ_r , also called the “angle of internal friction”, is the angle of maximum slope that can be sustained by the sediment particles on the bed or sides of a channel or river under the critical equilibrium condition of incipient sliding, i.e., before sliding commences.

The angle of repose is largely a function of sediment size, shape and porosity (fraction of sediment volume occupied by voids, i.e., air or water). In general, ϕ_r increases with increasing sediment size, increasing angularity and decreasing porosity.

Values for ϕ_r , for quartzitic material, are shown in Table 2.2.

Table 2.2: Values for angle of repose for quartzitic material (Armitage, 2002).

| Size (d_{50}) (mm) | Angle of repose (ϕ_r) | |
|---------------------------|------------------------------|---------|
| | Rounded | Angular |
| ≤ 1 | 30^0 | 35^0 |
| 5 | 32^0 | 37^0 |
| 10 | 35^0 | 40^0 |
| 50 | 37^0 | 42^0 |
| ≥ 100 | 40^0 | 45^0 |

Values of ϕ_r for other materials should be determined experimentally.

2.3 Types Of Motion

Incipient motion can be one of several types:

- Sliding
- Rolling
- Saltating (hopping)
- Suspension

Taken together, the above-mentioned types of movement constitute sediment transport. In general, sediment particles will roll or slide before saltating, and they will saltate before being carried in suspension. Bed load refers to sediment that is moving in the close vicinity of the bed of a channel or river, i.e., sliding, rolling and saltating. Suspended load accounts for the remainder of the transported sediment material.

2.4 Factors Influencing The Motion Of Any Particular Particle

The movement or possibility of movement of any particular particle can be influenced by one or more of the following factors:

- An uneven boundary. Each particle is surrounded by other particles having their own unique characteristics, such as size, shape, orientation and location. The surrounding particles all contribute to the flow regime around the particle under consideration, e.g., the particle might rest in the turbulent wake cast off by an upstream particle, or be shielded by it. The issue even becomes more complicated in the presence of ripples and / or dunes, where the location of the particle relative to the bed is important.
- The particular particle may touch other particles at a number of points. Sometimes the particle is supporting other particles that might prevent it from moving when

movement would have otherwise taken place; alternatively the presence of other particles would hinder sliding.

- In the case of non-uniform sediment, which is usually the case with all natural sediments, smaller particles on the surface of the bed might be swept away leaving a bed comprising of much coarser material, which protects the underlying sediment layers. This phenomenon is called “armouring”.
- In the case of cohesive particles, the electro-chemical bonds between the particles have to be broken down partially or fully, to initiate any movement.
- In the case where more than one particle starts moving at a particular instant, they start to interact with the fluid and hence with each other, and may even collide, in which case dispersive forces are created.
- Seepage from or into a river or channel bed can give rise to “seepage pressure”, which could either enhance or prohibit sediment motion.
- The particle may be located on a longitudinal or transverse slope, which will tend to reduce the force required to set it in motion.

2.5 Intensity Of Motion

Three intensities of motion near the incipient motion condition can be defined as (Simons & Şentürk, 1977 and Armitage & McGahey, 2003):

- “Weak movement”: Only a few particles are in motion on the bed. The particles moving on 1 cm² can be counted.
- “Medium movement”: This is a condition in which the particles of mean diameter begin to move. The movement is not local in character and the bed continues to be plane (motion not strong enough to affect bed configurations).
- “General movement”: This is a condition where the whole mixture of sediment particles is in motion, and the movement occurs in all parts of the bed at all times.

2.6 Models Of Incipient Motion In Terms Of Flow-related Parameters

2.6.1 Introduction

When flow over movable boundaries of a river or channel has hydraulic conditions exceeding the critical condition for motion of the bed material, sediment transport (scour) will commence. It is however sometimes difficult to determine the point of incipience. The region near the solid boundary is of particular interest, since this is where the largest changes in the flow parameters are taking place and where sediment motion is initiated.

Various simplified models have been developed, of which most are based on a single flow-related parameter that plays the dominant role in determining whether motion will take place or not. The three most used flow-related parameters are:

- flow velocity,
- bed shear stress, and
- stream power.

These three flow-related parameters will form the basis of the subsequent incipient motion theory review, with the main emphasis being placed on the stream power approach.

2.6.2 Incipient motion in terms of flow velocity

In the past many researchers tried to link incipient motion to some flow velocity. Average velocities are convenient to use and relatively easy to measure. The problem with linking the average flow velocity to incipient motion, is that drag forces and lift forces are dependent on the velocity distribution and not the average velocity. For instance, for the same average velocity, a deep channel will have smaller velocity gradients than a shallow channel, and a higher average flow velocity will be required to start sediment motion in a deep channel than would be required for an identical shallow channel.

Local flow velocities in the vicinity of the sediment particle should rather be used. The problem though is that it is very difficult to measure as the particles generally lie in regions of exceptionally high velocity gradients, and it is difficult to determine the effective boundary location due to irregular roughness elements and the change in the nature of the boundary layer.

2.6.3 Incipient motion in terms of shear stress

Shields is a familiar name in the field of sediment transport and river hydraulics and is referred to by most researchers in the field of sediment transport. The work of Shields included experiments, which covered developed sediment motion, as well as incipient motion (Henderson, 1966).

Shields determined, via dimensional analysis, that the drag force, F_D , was a function of the particle diameter, the particle density, the fluid viscosity, the bed form, the Particle Reynolds Number, Re_* , and the bed shear stress, τ_0 . Resistance to motion was assumed to depend only upon the form of the bed and the immersed weight of the particles (Armitage and McGahey, 2003).

From the above Shields deduced the “Shield’s parameter”, θ , which is also called the “Shields entrainment function” or the “dimensionless mobility factor”. The Shield’s parameter is a function of the Particle Reynolds Number, Re_* , and is defined as follows:

$$\theta = \frac{\tau_0}{(\rho_s - \rho)gd_{50}} = \frac{\rho v_*^2}{(\rho_s - \rho)gd_{50}} \quad (2.7)$$

If τ_c is the critical bed shear stress for incipient motion, then the critical Shield's parameter, θ_c , is expressed as:

$$\theta_c = \frac{\tau_c}{(\rho_s - \rho)gd_{50}} \quad (2.8)$$

The Shield's diagram for incipient motion is shown in Figure 2.1. The Shield's diagram is one of the best known criteria depicting the boundary between flow conditions under which cohesionless bed material will be transported and those under which such material will not be transported. Shields attempted to calculate the value of bed shear stress at which the extrapolated transport rate was zero. A drawback of the Shield's diagram is that the shear velocity forms part of both the parameters used on the diagram's axes, which means that trial and error solutions are required.

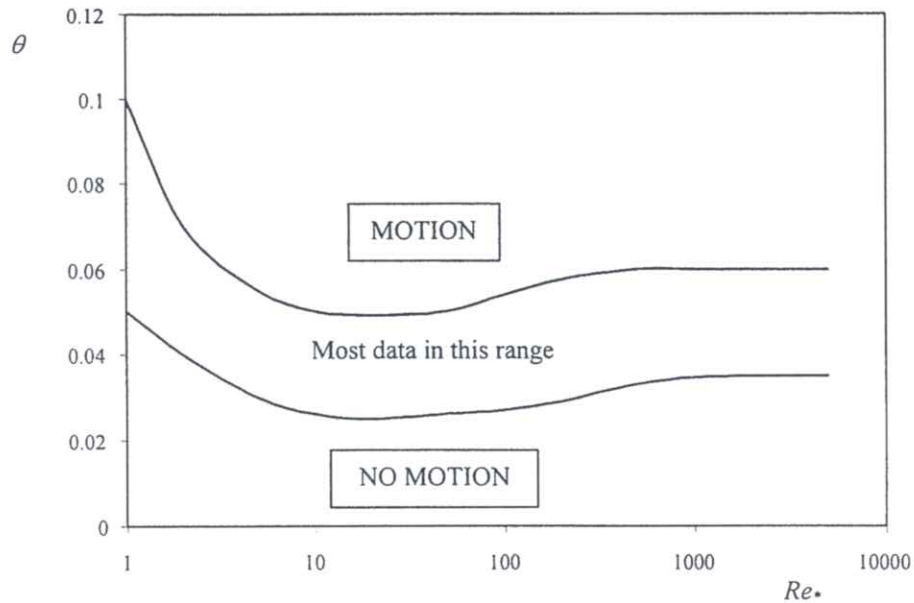


Figure 2.1: The Shield's diagram for incipient motion (Armitage, 2002)

For flat bed and uniform flow conditions, there is a laminar boundary flow region in which the Shield's parameter varies inversely as Re_* , a transitional region, and a region of fully developed turbulence in which the Shield's parameter is reasonably constant (0.056) (Henderson, 1966).

White (Henderson, 1966) has attempted to analyse the threshold condition by considering the equilibrium of a single typical particle. He suggested that in laminar flow the resultant drag force, F_D , having a greater surface drag component than in turbulent flow, would act at a higher level (Henderson, 1966 and Simons and Şentürk, 1977). If so, the effect would be to reduce the critical value of the bed shear stress, τ_0 , explaining the dip in Shield's curve in Figure 2.1. In turbulent flow it is expected that the drag force will act at a certain fixed level, causing the Shield's parameter to be constant, as shown in Figure 2.1.

The methodology given in the SANRAL Road Drainage Manual (1997) for the determining of rip rap rock size for channel beds is based on the constant Shield's parameter value of 0.056 in the turbulent region (when $Re_* > 400$) on the Shield's diagram in Figure 2.1, and can be derived as follows:

from Eq. 2.7:
$$\theta = \frac{\tau_0}{(\rho_s - \rho)gd_{50}} = 0.056 \quad (2.9)$$

but
$$\tau_0 = \rho gRS_0 = \rho gDS_0 \quad (2.10)$$

substitute (2.10) in (2.9):
$$\frac{\rho gDS_0}{(\rho_s - \rho)gd_{50}} = 0.056$$

with $\rho_s = 2650 \text{ kg/m}^3$:
$$\frac{DS_0}{1,65d_{50}} = 0.056$$

hence at threshold condition:
$$d_{50} = 10.823DS_0 \approx 11DS_0 \quad (2.11)$$

Rip rap rock for bed protection against erosion has hence to be sized for:

$$d_{50} > 11DS_0 \quad (2.12)$$

By using a relationship deduced by Lane, the diameter of rock required to protect the side slopes of channels and rivers can be calculated as follows (SANRAL, 1997):

$$d_{50} > \frac{8,3DS_0}{\cos \gamma \sqrt{1 - \frac{\tan^2 \gamma}{\tan^2 \phi_r}}} \quad (2.13)$$

where,

- ϕ_r = angle of repose of the sediment particle (degrees)
- γ = side slope of channel or river normal to flow (degrees from horizontal)
- D = flow depth (m)
- S_0 = longitudinal bed slope of the channel (m/m)

Because of increasing erosive capabilities of flow around bends, the values for rock sizes calculated, by using equations 2.12 and 2.13, should be increased by the following percentages where rip rap revetments are provided at bends and curves in the channel or river (SANRAL, 1997):

- Gently curving channel 30%
- Sharply curving channel 60%

2.6.4 Incipient motion in terms of stream power

Fluid mechanics has to be understood in order to deal with the interactive processes which are involved with the transportation of sediment by fluids. Traditionally, this understanding was based on the laws of conservation of:

- mass (e.g. continuity equation)
- energy (e.g. Bernoulli equation)
- momentum (e.g. momentum-force equation)

An additional law, namely the law of conservation of:

- power

allows a clearer insight into the transport of sediment (Rooseboom 1974 and 1992).

The derivations of equations that follow, are based on a homogeneous fluid under uniform flow conditions, which means that the bed slope, water surface slope and energy gradient are parallel.

The motion of sediment and water requires energy. In open channel flow, the energy source is potential energy that becomes available as water flows downstream. The rate at which this energy becomes available, is represented by the “available stream power”. This energy is then applied to move the water over the stream bed, and the rate of energy application is represented by the “applied stream power”. The total available stream power at a section in a stream is equal to the total applied stream power at that section, and this is the basis of the conservation of power. It is a dynamic equilibrium, which means that if the applied stream power changes due to changes of bed conditions, the conditions in the stream will change as well, changing the available stream power. The total stream power will remain the same ($\equiv \rho g S_0 Q$).

2.6.4.1 Available stream power

Consider uniform stationary flow of water in a channel with infinite width, small longitudinal slope, S_0 , and depth of flow, D . A small element of water, ABCE (shown exaggerated in Figure 2.2) of unit volume moves downstream at velocity, v . The weight of the unit volume is equal to ρg . The rate at which this small element loses height (Rooseboom, 1992 and Simpson, 1997):

$$= v \sin\beta \quad (2.14)$$

where, v = velocity in direction of bed slope (m/s)
 β = angle of bed to the horizontal (degrees)

At small angles, $\sin\beta = \tan\beta = \beta = S_0$, which is the bed slope. Hence the velocity in the vertical direction:

$$v_y = vS_0 \quad (2.15)$$

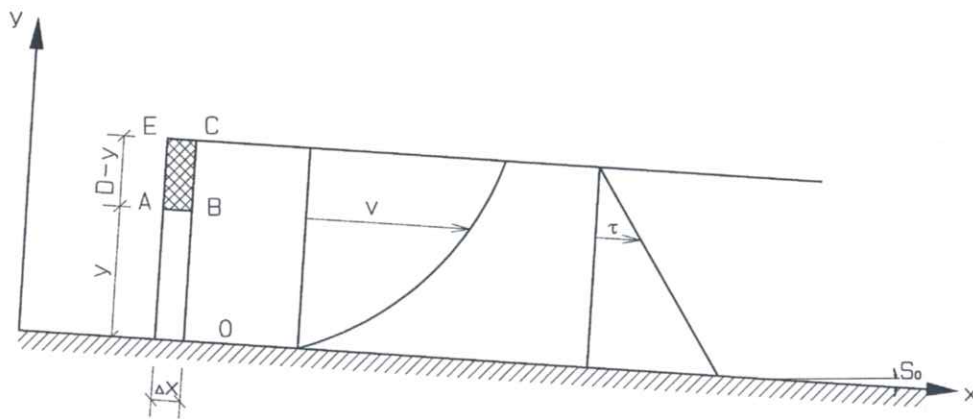


Figure 2.2: Schematic long section of uniform flow showing depth of flow, D , velocity profile, v , shear stress distribution, τ , bed slope S_0 , and water element ABCE. (Rooseboom, 1974 and 1992)

The potential energy loss per unit volume of water per unit time, which is the available stream power per unit volume (see Figure 2.3), can be expressed as:

$$\text{Available stream power per unit volume} = \rho g S_0 v \quad (\text{N.m/s/m}^3) \quad (2.16)$$

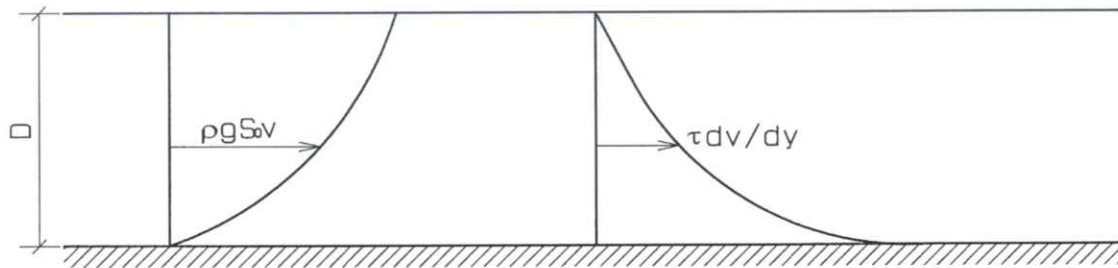


Figure 2.3: Long section of uniform flow in a stream showing the distribution of stream power made available, $\rho g S_0 v$, and stream power applied, $\tau dv/dy$. (Rooseboom, 1974).

The only variable changing in the above equation is v (see Figures 2.2 and 2.3). The water at the surface can be expected to be moving the fastest, which means that the stream power available at the surface is the highest. Water touching the bed can be expected to stand still, and hence the available stream power here is zero. The amount of stream power made available for a given slope and discharge, is independent of the mode (laminar mode or turbulent mode) of flow.

2.6.4.2 Applied stream power

The energy made available is used to overcome the resisting force of the river bed on the water flowing downstream. Flow can occur in laminar mode or turbulent mode.

To understand applied stream power, shear stress and its variation with depth must be considered (see Figure 2.2). With uniform flow at average point velocity, v , there is no acceleration. The forces acting on any element of fluid are thus in equilibrium, which means that opposing forces must be equal to driving forces.

Taking the element ABCE, as shown in Figure 2.2, with height $(D-y)$, length Δx and unit width, the forces acting on the sides of the element are due to water pressure and are equal in magnitude, with the result that there is no net force. With β the slope of the stream bed with the horizontal, $\sin\beta$ at small values of β is equal to the slope, S_0 .

The “shear force” represents the resistance to movement encountered by the element, acting along the lower plane of the element, and can be expressed as follows:

$$\text{Shear force} = \tau \Delta x = \rho g(D-y) \Delta x S_0 \quad (2.17)$$

The “shear stress”, τ , which is the shear force per unit area, is expressed as:

$$\text{Shear stress} = \tau = \rho g(D-y) S_0 \quad (2.18)$$

Shear stress increases linearly from zero at the surface to a maximum value at the bed, equal to ρgDS_0 , as shown in Figure 2.2, irrespective of what flow conditions exist. The only variable at any section of uniform flow is y .

The velocity changes with height above the bed. The deformation of the packets of water requires energy, and thus energy is made available by the loss in potential of the water packets as they move downstream. The stream power applied (equivalent to power per unit volume) at a depth, y , in the stream, is shown in Figure 2.3 and can be expressed as follows (Rooseboom, 1974 & 1992):

$$\text{Stream power applied: } P_t = \tau \frac{dv}{dy} \quad (\text{N.m/s/m}^3) \quad (2.19)$$

where, $\frac{dv}{dy}$ = the change in velocity with change in depth (m/s/m)

At the bed, the rate of change in velocity can be seen to be a maximum and the shear stress is also at a maximum.

As mentioned in paragraph 2.6.2, local flow velocities in the vicinity of the sediment are very difficult to measure as the particles generally lie in regions of exceptionally high velocity gradients, and it is difficult to determine the effective boundary location due to irregular roughness elements and the change in the nature of the boundary layer. Liu came to the conclusion that the local velocity and hence the various drag coefficients are all functions of the Particle Reynolds Number, Re_* . Liu went further to find that there is a unique relationship between the ratio of the shear velocity, v_* , to the particle settling velocity, v_{ss} , (what is termed the “Movability Number”) and Re_* . The shear velocity, Movability Number and the Particle Reynolds Number can be expressed as follows (Rooseboom, 1974 and 1992):

$$v_* = \sqrt{gDS_0} \quad (2.20)$$

$$\text{Movability Number} = \frac{v_*}{v_{ss}} \quad (2.21)$$

$$\text{Particle Reynolds Number } Re_* = \frac{v_* d}{\nu} \quad (2.22)$$

where,

- v_* = the shear velocity (m/s)
- v_{ss} = the particle settling velocity (m/s) (see Eq. 2.6)
- d = sediment diameter (d_{50} can be used alternatively) (m)
- D = the flow depth or hydraulic mean depth (m)
- S_0 = longitudinal bed slope (m/m)
- ν = kinematic viscosity of water ($= \mu/\rho \approx 10^{-6} \text{ m}^2/\text{s}$)

An interesting finding about a plot of $\frac{V_*}{V_{ss}}$ against Re_* is that it corresponds to the considerations of stream power.

According to the principle of conservancy of power, and bearing in mind that uniform flow is being dealt with, the areas enclosed by the graphs in Figure 2.3 should be equal. Hence, the available stream power at any cross section of a stream equals the applied stream power at that specific section.

The transfer of stream power within a stream occurs differently in each of the modes (laminar or turbulent) of flow:

- In laminar flow, stream power is transferred from water layers nearer to the surface to water layers deeper down by the exchange of momentum in the process of molecular diffusion (Simpson, 1997). Faster moving layers of water therefore transfer momentum, and thus kinetic energy, to slower moving packets of water nearer to the stream bed. These layers in turn transfer momentum to those layers below them, and the kinetic energy is transferred to the stream bed in this way.
- In turbulent flow, stream power transfer is done by direct transfer of kinetic energy on a macro scale. A fast moving packet of water moving as a turbulent eddy will collide with slower moving packets as it moves towards the stream bed, accelerating the slower moving packets and decelerating itself, thus transferring kinetic energy (Rooseboom, 1974 & 1992). Kinetic energy transferred per second is equivalent to power transferred.

The mode of flow which will prevail, is that mode that requires the least applied power. The equations representing stream power applied, are (Course Notes, 2003 and Rooseboom, 1974 & 1992):

- for laminar flow near the boundary:

$$\text{Stream power applied: } P_{t(l)} = \tau \frac{dv}{dy} = \frac{\tau^2}{\rho\nu} = \frac{(\rho g S_0 D)^2}{\mu} \quad (2.23)$$

$$\text{where, } \tau = \mu \frac{dv}{dy} \text{ (Pa)} \quad (2.24)$$

$$\mu = \text{the dynamic viscosity of water } (= \rho\nu \approx 10^{-3}) \text{ (Pa.s)}$$

- for turbulent flow near the boundary:

$$\text{Stream power applied: } P_{t(t)} = \tau \frac{dv}{dy} = \frac{\rho g S_0 D \sqrt{2\pi g D S_0}}{y_0} \quad (2.25)$$

$$\approx \frac{30 \rho g S_0 D \sqrt{2\pi g D S_0}}{k} \quad (2.26)$$

$$\approx \frac{15 \rho g S_0 D \sqrt{2\pi g D S_0}}{R_0} \quad (2.27)$$

$$\text{where, } y_0 \approx \frac{k}{30} \quad (2.28)$$

k = absolute roughness of the stream bed and which also represents the size of the turbulent eddies, which fit in with the bed forms ($= 2 R_0$) (m)

R_0 = the radius of turbulent eddies next to the stream bed (m)

The level above the bed at which the flow changes from laminar to turbulent can be calculated. Flow will start to change from laminar to turbulent for a constant value of shear stress, τ , where $\frac{dv}{dy}$ is the same for both laminar and turbulent flow (Rooseboom 1974 & 1992). The following will thus apply:

$$\left(\frac{dv}{dy}\right)_{0, \text{turbulent}} = \left(\frac{dv}{dy}\right)_{0, \text{laminar}} \quad (2.29)$$

From equations 2.18, 2.23 and 2.24, near the bed, so $D - y \approx D$:

$$\frac{dv}{dy} = \frac{\sqrt{2\pi g D S_0}}{y} = \frac{\rho g S_0 D}{\mu} \quad (2.30)$$

$$\therefore y_l = \frac{\mu \sqrt{2\pi}}{\rho \sqrt{g D S_0}} = \frac{\nu \sqrt{2\pi}}{\sqrt{g D S_0}} \quad (2.31)$$

where, y_l = the level of the interface between the laminar flow over the bed and the turbulent flow above (m)

A thin layer of laminar flow against a smooth boundary creates the necessary moving platform, which allows turbulent flow to occur in a river or channel.

2.6.4.3 Applied stream power required for sediment motion

The stream power required to suspend the sediment, is known as the “applied stream power required”, P_r . In terms of the concept of minimum applied stream power, the stream will begin to entrain (suspend) particles when the stream power required to suspend the particles becomes less than the stream power applied around them (stream power required to maintain the status quo), thus $P_t \geq P_r$.

The applied stream power required per unit volume to suspend a particle with density, ρ_s , and settling velocity, v_{ss} , in a fluid with density, ρ , is expressed as (Rooseboom, 1974 & 1992):

$$\text{Applied stream power required: } P_r = (\rho_s - \rho) g v_{ss} \quad (2.32)$$

where, the settling velocity, v_{ss} , differs in laminar and turbulent flow.

(a) Laminar boundaries: criteria for sediment motion

A particle wholly contained in the linear layer must be quite small. If $\frac{v_{ss} d}{\nu} < 1$, then Stokes law applies (Armitage, 2002 and Rooseboom, 1974 & 1992), in which case:

$$C_D = \frac{32 \nu}{v_{ss} d} \quad \text{for natural sediment particles} \quad (2.33)$$

Substituting Eq. 2.33 into Eq. 2.6 yields:

$$v_{ss} = \frac{4 (\rho_s - \rho) g d^2}{3 \rho \quad 32 \nu} \quad (2.34)$$

Rooseboom (1974 & 1992) analysed incipient motion data presented by Grass and Yang and found that, in the case of laminar boundaries, the data falls along a curve, for values of the Particle Reynolds Number, $Re_* < 13$, presented by (see Figure 2.4):

$$\text{Movability Number} = \frac{v_*}{v_{ss}} = \frac{1,6}{Re_*} \quad (Re_* < 13) \quad (2.35)$$

$$= \frac{1,6}{\frac{\sqrt{gDS_0} d}{\nu}} \quad (2.36)$$

Armitage (2002), on the other hand found from his study of incipient motion that, in the case of laminar boundaries, the data falls along a curve, but for values of $Re_* < 11,8$, represented by (see Figure 2.5):

$$\text{Movability Number} = \frac{v_*}{v_{ss}} = \frac{2,0}{Re_*} \quad (Re_* < 11,8) \quad (2.37)$$

$$= \frac{2,0}{\frac{\sqrt{gDS_0} d}{v}} \quad (2.38)$$

(b) Turbulent boundaries: criteria for sediment motion

Rooseboom (1974 & 1992) analysed incipient motion data presented by Grass and Yang and found that, in the case of turbulent boundaries, the data falls along a straight line, for values of $Re_* > 13$, presented by (see Figure 2.4):

$$\text{Movability Number} = \frac{v_*}{v_{ss}} = 0,12 \quad (Re_* > 13) \quad (2.39)$$

Armitage (2002), on the other hand found from his study of incipient motion that, in the case of turbulent boundaries, the data also falls along a straight line, but for values of $Re_* > 11,8$, presented by (see Figure 2.5):

$$\text{Movability Number} = \frac{v_*}{v_{ss}} = 0,17 \quad (Re_* > 11,8) \quad (2.40)$$

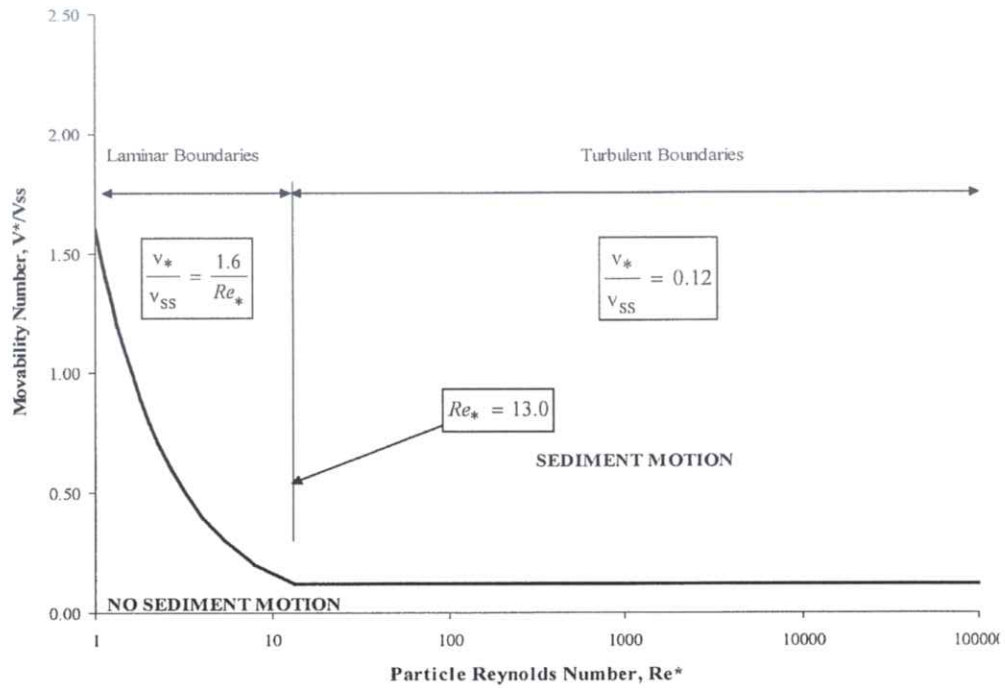


Figure 2.4: The Rooseboom criteria for incipient motion (based on Liu diagram) (Rooseboom, 1974 & 1992)

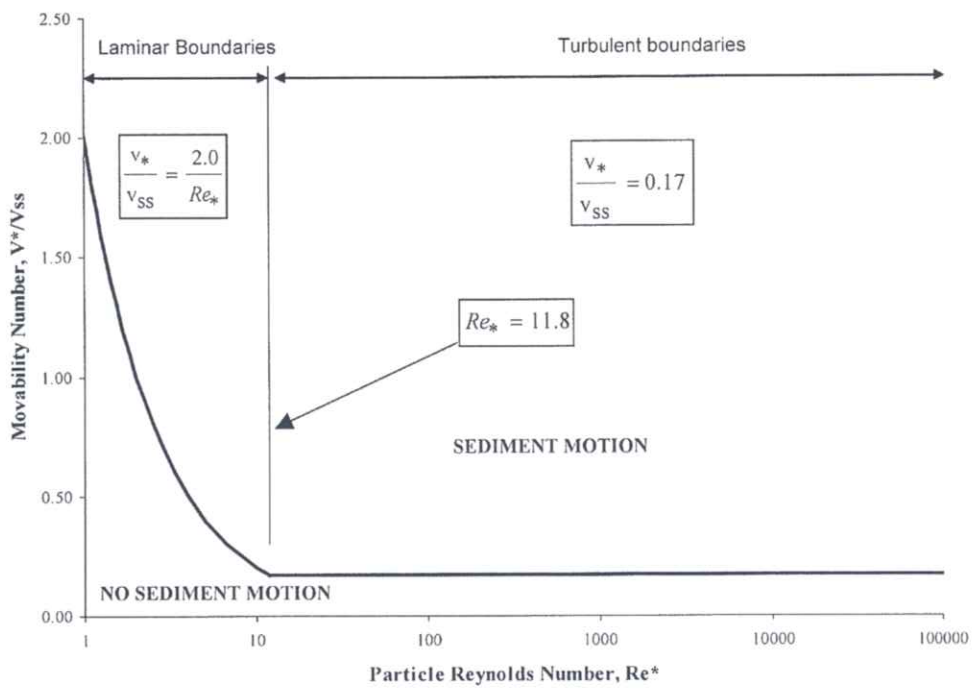


Figure 2.5: The Armitage criteria for incipient scour (based on Liu diagram) (Armitage, 2002)

(c) **Transitional boundaries: criteria for sediment motion**

Rooseboom (1992) did not provide an analytical solution where the transitional region is expected, but instead extrapolated equations 2.36 and 2.39 to a common meeting point, namely where $Re_* \approx 13$.

2.7 Incipient Motion On Sloping Beds

Up to this stage of this literature study, the discussion on incipient motion has been limited to that on horizontal (flat) beds. Normally particles lie on a slope and stream beds are rarely horizontal. Two different types of slopes are generally defined, namely:

- A longitudinal or stream wise slope with a fall (or rise) of the bed in the direction of flow. A fall of bed in the direction of flow is a positive slope and vice versa. The slope is presented by the symbol β (degrees).
- A transverse slope indicates a fall of the bed in either direction normal to the direction of flow. This slope in this case is given by the symbol γ (degrees).

Incipient motion criteria for a slope can be derived in terms of the drag force, F_D , on the particle. The ratio, k_β , of the critical drag force for any given longitudinal slope to the critical drag force for a horizontal bed (or correction factor for a longitudinal slope), can be expressed as follows (Henderson, 1966 and Armitage, 2002):

$$k_\beta = \frac{F_{D,cr}}{F_{D,cr,0}} = \frac{\sin(\phi_r - \beta)}{\sin \phi_r} = \cos \beta \left(1 - \frac{\tan \beta}{\tan \phi_r} \right) \quad (2.41)$$

where, k_β = ratio of the critical drag force for any given longitudinal slope to the critical drag force for a horizontal bed

$F_{D,cr}$ = critical drag force for any given longitudinal slope (N)

- $F_{D,cr,0}$ = critical drag force for a horizontal bed (N)
 ϕ_r = angle of repose of the sediment particle (degrees)
 β = longitudinal slope of bed in the direction of flow (degrees)

Since the bed shear stress is proportional to the drag force, the following also applies:

$$\tau_{0,cr} = k_\beta \tau_{0,cr,0} \quad (2.42)$$

- where,
- $\tau_{0,cr}$ = critical bed shear stress at any given longitudinal slope (Pa)
 $\tau_{0,cr,0}$ = critical bed shear stress on a horizontal bed (Pa)
 k_β = ratio of the critical bed shear stress at any given longitudinal slope to critical bed shear stress on a horizontal bed

The same applies to transverse slopes and sloped channel banks (e.g., trapezoidal channel side slopes), namely:

$$k_\gamma = \frac{F_{D,cr}}{F_{D,cr,0}} = \cos\gamma \sqrt{1 - \frac{\tan^2\gamma}{\tan^2\phi_r}} \quad (2.43)$$

- where,
- k_γ = ratio of the critical drag force for any given transverse slope to the critical drag force for a horizontal bed (or correction factor for a transverse slope)
 $F_{D,cr}$ = critical drag force for any given transverse slope (N)
 $F_{D,cr,0}$ = critical drag force for a horizontal bed (N)
 ϕ_r = angle of repose of the sediment particle (degrees)
 γ = transverse slope of bed normal to the direction of flow (degrees)

and,

$$\tau_{0,cr} = k_\gamma \tau_{0,cr,0} \quad (2.44)$$

For a combination of longitudinal and transverse slopes, the following will apply (Armitage, 2002):

$$\tau_{0,cr} = k_{\beta} k_{\gamma} \tau_{0,cr,0} \quad (2.45)$$

From Armitage (2002), the Movability Number, $\frac{V_{*}}{V_{ss}}$, is proportional to the square root of the drag force, if in the same direction:

$$\frac{V_{*}}{V_{ss}} \propto \sqrt{F_D} \quad (2.46)$$

hence,

$$\left. \frac{V_{*}}{V_{ss}} \right|_{\beta,\gamma} = \psi \left. \frac{V_{*}}{V_{ss}} \right|_0 \quad (2.47)$$

where,

- ψ = the slope correction factor
- β denotes the longitudinal slope of bed in the direction of flow (degrees)
- γ denotes the transverse slope of bed normal to flow (degrees)
- 0 denotes the horizontal bed condition

The slope correction factor, ψ , can be defined as follows (from equations 2.41 and 2.43):

$$\psi = \sqrt{k_{\beta} k_{\gamma}} = \sqrt{\cos \beta \left(1 - \frac{\tan \beta}{\tan \phi_r} \right) \cos \gamma \left(1 - \frac{\tan^2 \gamma}{\tan^2 \phi_r} \right)^{\frac{1}{2}}} \quad (2.48)$$

The slope correction factor, ψ , can thus be used with the unit stream power and bed shear stress equations, as discussed in section 2.6, in the following way:

- If stream power is used as the criterion:

$$P_t = \psi^2 \eta_l P_r \quad (\text{Laminar boundaries}) \quad (2.49)$$

$$P_t = \psi^3 \eta_t P_r \quad (\text{Turbulent boundaries}) \quad (2.50)$$

where, η_l and η_t = the ratios of applied unit stream power to unit stream power required to suspend a particle in a laminar and a turbulent boundary respectively

- If critical bed shear stress is used as the criterion (from equation 2.45 and 2.47):

$$\tau_{0,cr} = \psi^2 \tau_{0,cr,0} \quad (2.51)$$

2.8 Layer Thicknesses Of Rip Rap And Reno Mattress Revetments

The thickness of the rip rap rock layers should be at least two times the diameter of the rock, but never smaller than 200 mm (SANRAL, 1997).

Rooseboom went further and suggested the following with respect to the design of gabions and Reno mattresses (SANRAL, 1997): Designing of the single stones to be used in the Reno mattresses should be done according to equations 2.15 and 2.16, which will then determine the equivalent size of the Reno mattress or gabion to be used. The mass of the individual gabion or Reno mattress must be at least 1,5 to 2 times that of the rock calculated in accordance with equations 2.12 and 2.13.

Simons and Şentürk (1977) made valuable contributions regarding the gradation of rip rap rock:

- The ratio of the maximum size (d_{max}) to d_{50} should be about 2.0, which means that the largest stones would be about 6,5 times the mass of the median size.
- The ratio of d_{50} to d_{20} should also be about 2.0.
- The layer thickness of rip rap should be sufficient to accommodate the largest stones in the rip rap, i.e., 2 times d_{50} . If strong wave action is of concern, the layer thickness should be increased by 50% (Simons and Şentürk, 1977).

Another way to determine the layer thickness of rip rap when placed below water is given by Burcharth and Hughes (2003) in the Coastal Engineering Manual (U.S. Army Corps of Engineers) in the following equation:

$$r = 3,8 \left(\frac{W_{30}}{\gamma_s} \right)^{\frac{1}{3}} = 3,2 \left(\frac{W_{50 \min}}{\gamma_s} \right)^{\frac{1}{3}} \quad (2.52)$$

$$\approx \frac{3,2}{1,25} \left(\frac{\rho_s g \frac{\pi d_{50}^3}{6}}{\rho_s g} \right)^{\frac{1}{3}}$$

$$= \frac{3,2}{1,25} \left(\frac{\pi d_{50}^3}{6} \right)^{\frac{1}{3}} \quad (2.53)$$

where,

r = rip rap layer thickness (m) (0,5m minimum recommended for coastal conditions (Burcharth and Hughes, 2003))

W_{30} = the rock weight for which 30 % of the rock is smaller by weight (N/m³)

W_{50} = the rock weight for which 50 % of the rock is smaller by weight (N/m³)(assume $W_{50 \min} = W_{50}/1,25$ and $W_{50} = (W_{50 \min} + W_{50 \max})/2$, where $W_{50 \max} = 1,5 W_{50 \min}$ (Burcharth and Hughes, 2003))

3. BACKGROUND OF STUDY DONE BY COLORADO STATE UNIVERSITY (CSU)

3.1 Introduction

Maccaferri had the need for further research in order to generate the required data base from which to develop design criteria for Reno mattress applications. Such criteria were required to ensure adequate performance of Reno mattresses under specific hydraulic and geometric conditions.

The CSU study (CSU, 1984) was aimed at evaluating the performance of Maccaferri mattress products when used as river and canal bank and bed revetment. A hydraulic testing program was developed and undertaken to provide experimental data pertaining to the performance of Reno mattresses. Test data was utilized to develop design criteria for Maccaferri Reno (gabion) mattresses.

3.2 Objectives Of The CSU Study

Limited information had been available regarding the performance of mattresses under high flow conditions. The objectives of the CSU study were to address the following aspects with respect to Reno mattresses (CSU, 1984):

- the permissible design flow conditions for various types of mattresses, including the determination of incipient motion conditions of filling rock within the mattresses,
- the changes in mattress performance (deformation) when the flow conditions exceed the incipient motion conditions, and
- filter requirements under high flow conditions.

3.3 Test Program

Only aspects regarding the determination of incipient motion of filling rock within the Reno mattresses, with regard to the CSU study, will be highlighted.

Performance tests on Reno mattresses over a range of conditions were done, which involved full scale (prototype) tests complemented by scale-model tests. In developing the test methodology, velocity was assumed to be the major factor controlling Reno mattress stability. Data obtained from full-scale testing at the required velocity but reduced depth, were supplemented with scale-model testing in order to determine the effect of depth on Reno mattress stability.

3.3.1 Scale-model testing

Hydraulic tests of scale-model mattresses were conducted in a 2,44 m wide, 1,22 m high and 61 m long indoor flume, which could be raised or lowered to produce longitudinal gradients or slopes ranging from 0% to approximately 2%. A maximum flow rate of approximately 2.84 m³/s could be achieved. Valves and orifices were used to control and measure discharges. Two series of scale-model mattress tests were done, namely one utilising the 2,44 m flume and the other utilising a reduced 1,22 m flume. The latter was fabricated by the installation of a 30,5 m long partition wall along the centre of the 2,44 m indoor flume. The reason for this reduction in width, was to test scale-model mattresses under increased unit-width discharge, velocity and depth conditions.

Hydraulic tests of full-scale 150 mm and 230 mm thick Reno mattresses were conducted in a 2,15 m wide, 1,22 m high and 22,86 m long outdoor flume with a slope of 13%. The maximum discharge capacity was 2,84 m³/s. The characteristics of these mattresses are given in Table A-1 in Annexure A (CSU, 1984).

The scale-model wire mesh mattresses were constructed geometrically similar to the prototype Maccaferri Reno mattresses, but reduced by a scale ratio of 1:3. The dimensions and characteristics of the scale-model mattresses are given in Table A-1 in Annexure A (CSU, 1984). Other model-to-prototype scaling ratios are given in Table 3.1.

Table 3.1: Model-to-prototype scaling ratios (CSU, 1984)

| Variable | Model-to-prototype scaling ratios |
|-----------------|--|
| Length | 1:3 |
| Rock size | 1:3 |
| Velocity | $1:\sqrt{3}$ |
| Discharge | $1:3^{2.5}$ |
| Shear stress | 1:3 |
| Pressure | 1:3 |
| Force | $1:3^3$ |

The mattresses, in terms of prototype sizes, tested in the CSU study included 150 mm, 230 mm, 300 mm and 450 mm nominal thick mattresses.

It was difficult to achieve dynamic similarity between the model mesh and prototype mesh. Different sizes of crushed rock were used to fill the different types of model-scale mattresses according to a 1:3 scaling ratio of the specified rock ranges required for the full-scale mattresses, as shown in Table A-1 in Annexure A (CSU, 1984).

To provide some indication of rock movement within the mattress diaphragms, the surface layers of the rock in alternative mattress diaphragm sections were spray painted.

Vertical pressure fluctuations within the Reno mattress sections, associated with turbulence in a moving fluid, could be measured by using calibrated pressure transducers.

Once the desired flow conditions in terms of discharge, depth and velocity had been established, data collection was undertaken. Depth and velocity were measured at three cross sections (stations) in the scale-model mattress test section. The locations of these stations (cross sections) correspond with the positions where the pressure fluctuations were measured by means of the pressure transducers. Depth of flow was measured by means of a steel point gauge, while velocities at the centreline were measured utilising an Ott propeller-type current meter.

Mattress sections were scrutinised to identify any rock movement and photographs were taken before and after testing to monitor any such appreciable movement.

3.3.1.1 Test conditions and data collected in 2,44 m flume

Only the scaled 230 mm thick mattresses were tested in the 2,44 m flume. The range of hydraulic conditions in the 2,44 m flume, to which scale-model revetment mattresses were subjected, are indicated in Table 3.2 (CSU, 1984). The characteristics of these mattress units are described in Table A-1 in Annexure A (CSU, 1984). The station numbers in Table 3.2 (CSU, 1984) indicate the longitudinal positions within the mattress test section where data was collected. Station 1 was located approximately 1,52 m upstream of the downstream end of the test section, Station 2 coincided with the midpoint, and Station 3 was located approximately 1,52 m downstream of the upstream end. These locations coincided with the locations of pressure measurements.

The Manning equation, together with the measured values of velocity and depth, were used to determine the overall Manning roughness coefficient, n , and the Manning roughness coefficient for the bed, n_b . The latter was determined by assuming the wetted perimeter as the bed width. At each run these values were calculated for each station, and average values for n and n_b were determined, as shown in Table 3.3 (CSU, 1984).

Table 3.2: Scale-model mattress test data in the 2,44 m flume (CSU, 1984)

| Run No. | Station | Flow Rate (m ³ /s) | Depth (m) | Flume slope (m/m) | Velocity (m/s) | Froude Number |
|---------|---------|-------------------------------|-----------|-------------------|----------------|---------------|
| 1 | 1 | 0.589 | 0.262 | 0.0172 | 1.006 | 0.62 |
| | 2 | 0.589 | 0.213 | 0.0172 | 1.113 | 0.77 |
| | 3 | 0.589 | 0.149 | 0.0172 | 1.609 | 1.33 |
| 2 | 1 | 1.070 | 0.366 | 0.0069 | 1.250 | 0.66 |
| | 2 | 1.070 | 0.351 | 0.0069 | 1.292 | 0.70 |
| | 3 | 1.070 | 0.338 | 0.0069 | 1.308 | 0.72 |
| 3 | 1 | 1.606 | 0.482 | 0.0040 | 1.356 | 0.62 |
| | 2 | 1.606 | 0.485 | 0.0040 | 1.350 | 0.62 |
| | 3 | 1.606 | 0.488 | 0.0040 | 1.326 | 0.61 |
| 4 | 1 | 2.135 | 0.668 | 0.0015 | 1.454 | 0.57 |
| | 2 | 2.135 | 0.680 | 0.0015 | 1.445 | 0.56 |
| | 3 | 2.135 | 0.689 | 0.0015 | 1.451 | 0.56 |
| 5 | 1 | 2.577 | 0.661 | 0.0040 | 1.768 | 0.69 |
| | 2 | 2.577 | 0.683 | 0.0040 | 1.731 | 0.67 |
| | 3 | 2.577 | 0.689 | 0.0040 | 1.713 | 0.66 |
| 6 | 1 | 1.934 | 0.543 | 0.0059 | 1.704 | 0.74 |
| | 2 | 1.934 | 0.558 | 0.0059 | 1.682 | 0.72 |
| | 3 | 1.934 | 0.555 | 0.0059 | 1.710 | 0.73 |
| 7 | 1 | 1.317 | 0.341 | 0.0102 | 1.628 | 0.89 |
| | 2 | 1.317 | 0.332 | 0.0102 | 1.701 | 0.94 |
| | 3 | 1.317 | 0.305 | 0.0102 | 1.899 | 1.10 |
| 8 | 1 | 0.782 | 0.183 | 0.0201 | 1.570 | 1.17 |
| | 2 | 0.782 | 0.183 | 0.0201 | 1.640 | 1.22 |
| | 3 | 0.782 | 0.189 | 0.0201 | 1.768 | 1.30 |
| 9 | 1 | 2.268 | 0.555 | 0.0079 | 1.923 | 0.82 |
| | 2 | 2.268 | 0.558 | 0.0079 | 1.972 | 0.84 |
| | 3 | 2.268 | 0.558 | 0.0079 | 2.045 | 0.87 |
| 10 | 1 | 1.506 | 0.317 | 0.0135 | 2.082 | 1.18 |
| | 2 | 1.506 | 0.302 | 0.0135 | 2.201 | 1.28 |
| | 3 | 1.506 | 0.308 | 0.0135 | 2.216 | 1.27 |
| 11 | 1 | 2.636 | 0.488 | 0.0118 | 2.454 | 1.12 |
| | 2 | 2.636 | 0.463 | 0.0118 | 2.591 | 1.21 |
| | 3 | 2.636 | 0.475 | 0.0118 | 2.630 | 1.22 |
| 12 | 1 | 1.846 | 0.347 | 0.0203 | 2.783 | 1.51 |
| | 2 | 1.846 | 0.347 | 0.0203 | 2.743 | 1.49 |
| | 3 | 1.846 | 0.354 | 0.0203 | 2.728 | 1.46 |
| 13 | 1 | 2.665 | 0.442 | 0.0159 | 2.603 | 1.25 |
| | 2 | 2.665 | 0.445 | 0.0159 | 2.643 | 1.26 |
| | 3 | 2.665 | 0.445 | 0.0159 | 2.673 | 1.28 |
| 14 | 1 | 2.679 | 0.424 | 0.0199 | 3.005 | 1.47 |
| | 2 | 2.679 | 0.424 | 0.0199 | 2.966 | 1.45 |
| | 3 | 2.679 | 0.430 | 0.0199 | 3.005 | 1.46 |

Meyer-Peter and Müller (Simons and Şentürk, 1977) defined Manning's bed roughness, n_b , in terms of a sediment particle size, d_{90} (in metres), of which 90% of particles are finer by mass.

$$n_b = \frac{d_{90}^{1/6}}{26} \quad (3.1)$$

Table 3.3: Manning's roughness coefficient for the model-scale mattresses tests conducted in the 2,44 m flume (CSU, 1984)

| Run | Manning's roughness coefficients | |
|-----|----------------------------------|---------------------|
| | Overall n | Bed n_b |
| 1 | 0.021 | 0.023 |
| 2 | 0.021 | 0.024 |
| 3 | 0.023 | 0.025 |
| 4 | 0.015 | 0.027 |
| 5 | 0.021 | 0.027 |
| 6 | 0.024 | 0.026 |
| 7 | 0.023 | 0.024 |
| 8 | 0.025 | 0.023 |
| 9 | 0.024 | 0.026 |
| 10 | 0.021 | 0.024 |
| 11 | 0.021 | 0.025 |
| 12 | 0.022 | 0.024 |
| 13 | 0.023 | 0.025 |
| 14 | 0.022 | 0.025 |
| | $\bar{n} = 0.022$ | $\bar{n}_b = 0.025$ |

3.3.1.2 Test conditions and data collected in 1,22 mm flume

The range of hydraulic conditions in the 1,22 m flume, to which scale-model revetment mattresses were subjected, are indicated in Tables 3.4, 3.5, 3.6 and 3.7 (CSU, 1984). The characteristics of the various mattresses tested, are described in Table A-1 in Annexure A (CSU, 1984).

The bed shear stress, τ_0 , and the Shield's parameter, θ , were calculated using the following equations:

$$\theta = \frac{\tau_0}{(\rho_s - \rho)gd_{50}} \quad (2.9)$$

$$\tau_0 = \rho g R_b S_0 = \rho g D S_0 \quad (2.10)$$

Table 3.4: Run sequence for Test A: 150 mm nominal thick mattress (1,22 m flume)

| Total Discharge Q (m ³ /s) | Depth D (m) | Flume Slope S_0 (m/m) | Velocity v (m/s) | Bed Shear Stress τ_0 (Pa) | Shield's Parameter θ | Froude Number F | Bed Roughness n_b |
|---|---------------------|-------------------------------|--------------------------|--------------------------------------|--------------------------------|----------------------|------------------------|
| 1.501 | 0.655 | 0.004 | 2.164 | 25.472 | 0.044 | 0.86 | - |
| 1.982 | 0.789 | 0.004 | 2.246 | 30.931 | 0.053 | 0.81 | - |
| 1.557* | 0.555 | 0.010 | 2.643 | 54.392 | 0.094 | 1.13 | 0.0199 |
| 2.039 | 0.640 | 0.010 | 2.749 | 62.723 | 0.108 | 1.10 | 0.0208 |
| 2.407 | 0.741 | 0.010 | 2.963 | 72.586 | 0.125 | 1.10 | 0.0205 |
| 2.010 | 0.567 | 0.020 | 3.304 | 111.130 | 0.192 | 1.40 | 0.0243 |
| 2.577 | 0.652 | 0.020 | 3.502 | 127.888 | 0.221 | 1.38 | 0.0247 |

*: Flow condition at which movement of filling rocks was first observed.

Table 3.5: Run sequence for Test B: 230 mm nominal thick mattress (1,22 m flume)

| Total Discharge Q (m ³ /s) | Depth D (m) | Flume Slope S_0 (m/m) | Velocity v (m/s) | Bed Shear Stress τ_0 (Pa) | Shield's Parameter θ | Froude Number F | Bed Roughness n_b |
|---|---------------------|-------------------------------|--------------------------|--------------------------------------|--------------------------------|----------------------|------------------------|
| 1.416 | 0.628 | 0.004 | 1.911 | 24.610 | 0.042 | 0.77 | - |
| 1.982 | 0.796 | 0.004 | 2.289 | 31.170 | 0.054 | 0.82 | - |
| 1.586* | 0.576 | 0.010 | 2.615 | 56.451 | 0.097 | 1.10 | 0.0204 |
| 2.010 | 0.664 | 0.010 | 2.688 | 65.117 | 0.112 | 1.05 | 0.0215 |
| 2.322 | 0.698 | 0.010 | 2.920 | 68.421 | 0.118 | 1.12 | 0.0200 |
| 2.435 | 0.658 | 0.015 | 3.246 | 96.814 | 0.167 | 1.28 | 0.0219 |
| 2.095 | 0.567 | 0.020 | 3.554 | 111.130 | 0.192 | 1.51 | 0.0226 |
| 2.605 | 0.664 | 0.020 | 3.581 | 130.282 | 0.225 | 1.40 | 0.0235 |

*: Flow condition at which movement of filling rocks was first observed.

Table 3.6: Run sequence for Test C: 300 mm nominal thick mattress (1,22 m flume)

| Total Discharge Q (m ³ /s) | Depth D (m) | Flume Slope S_0 (m/m) | Velocity v (m/s) | Bed Shear Stress τ_θ (Pa) | Shield's Parameter θ | Froude Number F | Bed Roughness n_b |
|---|---------------------|-------------------------------|--------------------------|---|--------------------------------|----------------------|------------------------|
| 1.416 | 0.640 | 0.004 | 1.804 | 25.089 | 0.035 | 0.72 | - |
| 1.897 | 0.792 | 0.004 | 2.469 | 31.122 | 0.044 | 0.89 | - |
| 1.444 | 0.533 | 0.010 | 2.408 | 52.189 | 0.074 | 1.05 | 0.0218 |
| 1.756 | 0.610 | 0.010 | 2.591 | 59.850 | 0.084 | 1.06 | 0.0217 |
| 2.294* | 0.701 | 0.010 | 3.018 | 71.820 | 0.101 | 1.13 | 0.0205 |
| 0.566 | 0.259 | 0.020 | 2.225 | 50.753 | 0.072 | 1.40 | 0.0234 |
| 1.869 | 0.579 | 0.020 | 3.444 | 107.731 | 0.152 | 1.48 | 0.0227 |
| 2.605 | 0.655 | 0.020 | 3.780 | 131.671 | 0.186 | 1.47 | 0.0223 |

*: Flow condition at which movement of filling rocks was first observed.

Table 3.7: Run sequence for Test D: 450 mm nominal thick mattress (1,22 m flume)

| Total Discharge Q (m ³ /s) | Depth D (m) | Flume Slope S_0 (m/m) | Velocity v (m/s) | Bed Shear Stress τ_θ (Pa) | Shield's Parameter θ | Froude Number F | Bed Roughness n_b |
|---|---------------------|-------------------------------|--------------------------|---|--------------------------------|----------------------|------------------------|
| 2.039 | 0.808 | 0.004 | 2.170 | 31.649 | 0.041 | 0.77 | - |
| 1.586 | 0.591 | 0.010 | 2.368 | 57.935 | 0.075 | 0.98 | 0.0227 |
| 2.379* | 0.716 | 0.010 | 2.914 | 70.192 | 0.091 | 1.10 | 0.0206 |
| 2.492 | 0.668 | 0.015 | 3.316 | 98.155 | 0.127 | 1.30 | 0.0215 |
| 2.633 | 0.640 | 0.020 | 3.655 | 125.494 | 0.163 | 1.46 | 0.0226 |

*: Flow condition at which movement of filling rocks was first observed.

3.3.2 Full-scale testing

Hydraulic tests of full-scale 150 mm and 230 mm thick Reno mattresses were conducted in a 2,15 m wide, 1,22 m high and 22,86 m long outdoor flume with a slope of 13%. The maximum discharge capacity was 2,84 m³/s. The characteristics of these mattresses are given in Table A-1 in Annexure A (CSU, 1984).

The instrumentation for full-scale revetment mattress testing was set up so that similarity between prototype data and model data would be maintained as far as possible. The main focus of the full-scale mattress tests was to determine flow conditions within the mattress, the velocity at the mattress / filter interface, the velocity at the filter / soil interface, as well as the deformation of the mattress.

Velocities immediately above and below mattresses were determined from piezometric tube readings less the hydrostatic pressures. The discharge within the mattress was calculated by assuming that the velocity through rock voids was two-thirds of the velocity immediately below the mattress, and that the porosity of the rock was 0,45.

Although the test results are given in Tables 3.8, 3.9 and 3.10 (CSU, 1984) for the purpose of completeness, the full-scale model tests will not be discussed in further detail, except for some aspects regarding the deformation of mattresses, which will be discussed briefly in Chapter 4. During further discussion in this investigation, more emphasis will be given to incipient motion conditions, which were the main focus of the scale-model test results as discussed in paragraph 3.3.1.

Table 3.8: Test run sequence – discharge, velocity, depth measurements for the 150 mm full-scale mattress tests (CSU, 1984)

| Total Discharge Q_T (m^3/s) | Velocity v_1 (m/s) | Depth D_1 (m) | Velocity V_2 (m/s) | Depth D_2 (m) |
|---|--------------------------------|---------------------------|--------------------------------|---------------------------|
| 0.510 | 2.164 | 0.091 | 2.164 | 0.091 |
| 1.586 | 4.633 | 0.143 | 3.658 | 0.174 |
| 2.605 | 5.852 | 0.183 | 4.450 | 0.265 |
| 2.718 | 6.096 | 0.183 | 4.542 | 0.274 |

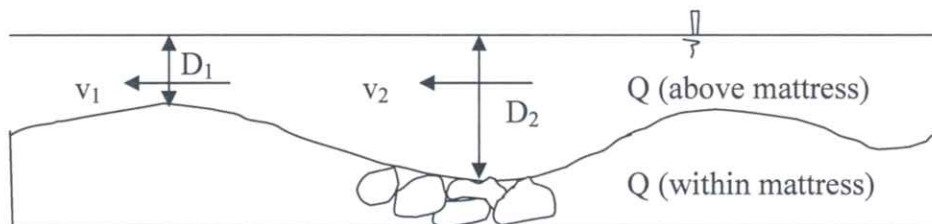


Table 3.9: Test run sequence – discharge, velocity, depth measurements for the 230 mm full-scale mattress tests (CSU, 1984)

| Total Discharge Q_T (m^3/s) | Velocity v_1 (m/s) | Depth D_1 (m) | Velocity v_2 (m/s) | Depth D_2 (m) | Discharge | |
|---|--------------------------------|---------------------------|--------------------------------|---------------------------|-----------------------------------|------------------------------------|
| | | | | | Q (above mattress) (m^3/s) | Q (within mattress) (m^3/s) |
| 0.510 | 2.073 | 0.101 | 2.073 | 0.101 | 0.382 | 0.127 |
| 0.850 | 3.292 | 0.116 | 3.078 | 0.131 | 0.736 | 0.113 |
| 1.133 | 3.780 | 0.128 | 3.231 | 0.171 | 1.008 | 0.125 |
| 1.699 | 4.999 | 0.152 | 4.328 | 0.198 | 1.569 | 0.130 |
| 2.265 | 5.304 | 0.174 | 4.084 | 0.287 | 2.141 | 0.125 |
| 2.549 | 5.913 | 0.174 | 4.450 | 0.299 | 2.430 | 0.119 |

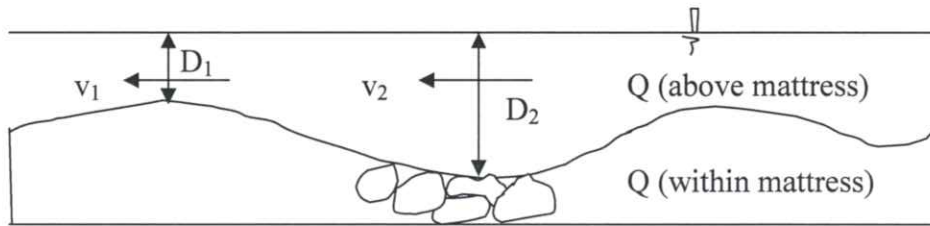


Table 3.10: Determination of 230 mm mattress properties, roughness coefficient, n_b and bed shear stress, τ_0 (CSU, 1984)

| Total Discharge Q_T (m^3/s) | Discharge Q (above mattress) (m^3/s) | Average Velocity v (m/s) | Average Depth D (m) | Hydraulic Radius R (m) | Total Roughness Coefficient n | Bed Roughness Coefficient n_b | Bed Hydraulic Radius R_b (m) | Bed Shear Stress τ_0 (Pa) |
|---|---|---------------------------------------|-------------------------------|-------------------------------------|--|--|--|--|
| 0.850 | 0.736 | 3.200 | 0.125 | 0.110 | 0.026 | 0.028 | 0.123 | 156.568 |
| 1.133 | 1.008 | 3.505 | 0.158 | 0.128 | 0.026 | 0.028 | 0.144 | 182.903 |
| 1.699 | 1.569 | 4.663 | 0.183 | 0.148 | 0.022 | 0.024 | 0.169 | 214.982 |
| 2.265 | 2.141 | 4.694 | 0.250 | 0.185 | 0.025 | 0.028 | 0.219 | 279.142 |
| 2.549 | 2.430 | 5.182 | 0.256 | 0.187 | 0.023 | 0.026 | 0.225 | 286.803 |

3.4 Analysis Of Results

The data collected in the model-scale mattress and full-scale mattress tests were analysed to determine (CSU, 1984):

- the hydraulics of mattress channels,
- incipient motion conditions, and
- deformation of mattresses under high flow conditions

The findings and analysis of the CSU study are subsequently discussed in terms of the above.

3.4.1 Hydraulics of mattress channels

3.4.1.1 Roughness coefficients

Manning's roughness coefficients were calculated for all the test conditions, using the well known Manning's equation. The surface roughness can also be assumed as (CSU, 1984):

$$n_b = \frac{d_{90}^{1/6}}{26} \quad (3.1)$$

where, n_b = Manning's bed roughness
 d_{90} = particle size of which 90% of particles are finer by mass (m)

Figure 3.1 shows the comparison between the measured and the calculated values from Equation 3.1. The relatively good agreement (CSU, 1984) indicates that Equation 3.1 can be utilised to calculate Manning's roughness coefficient for the mattress.

For the 75 mm to 150 mm size filling rock used in the 150 mm and 230 mm mattresses, $d_{90} \approx 140$ mm. Then, from Equation 3.1, $n_b \approx 0,0275$. This agrees well with the measured data (CSU, 1984). For the 450 mm mattresses, the filling rocks would be 100 mm to 200 mm size with a $d_{90} \approx 190$ mm and corresponding $n_b \approx 0,0292$.

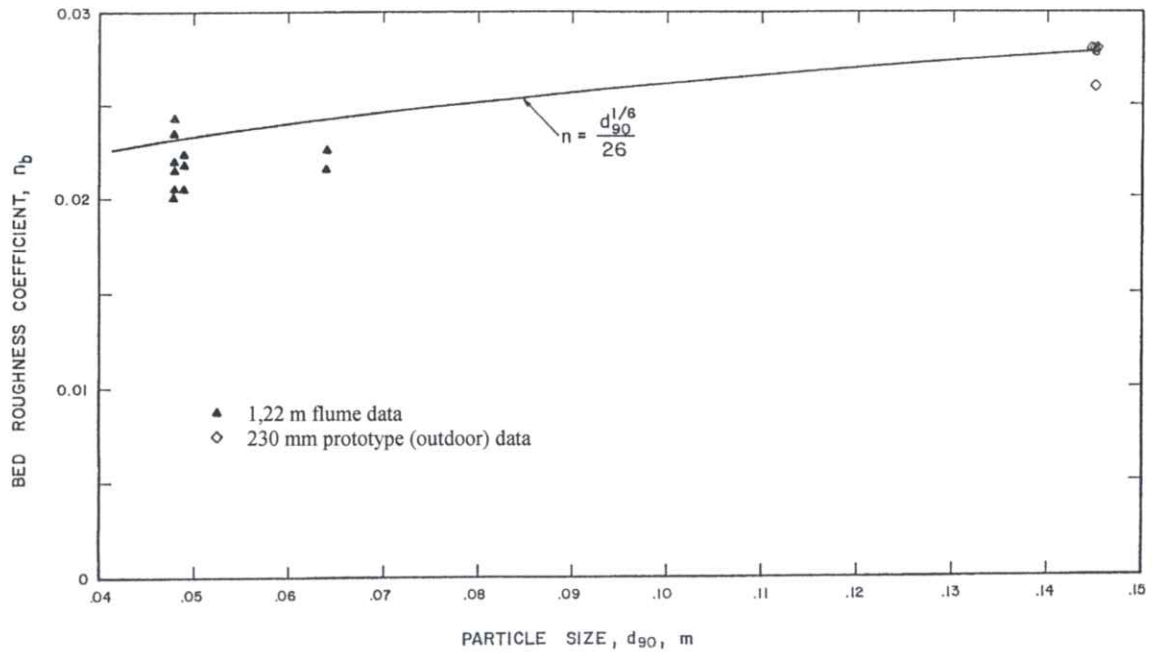


Figure 3.1: Comparison between the measured and calculated Manning's roughness coefficient (CSU, 1984)

With an increase in velocities, rocks within the mattresses would be moved downstream to cause a bed deformation, which would slightly increase n_b .

3.4.1.2 Velocity distribution

For average velocity, velocity distribution can be calculated by means of Equation 3.2 (CSU, 1984):

$$\frac{V}{v_*} = 5.75 \log\left(12.25 \frac{R_b}{k}\right) \quad (3.2)$$

where, v_* = the shear velocity (m/s) (see Equation 2.7)
 R_b = the bed hydraulic radius (m)
 k = absolute roughness of bed, approximated by the median size of the filling rock (m) (CSU, 1984)

Figure 3.2 compares the measured average velocity distribution for the model scale mattress tests with that of the values calculated, using Equation 3.2.

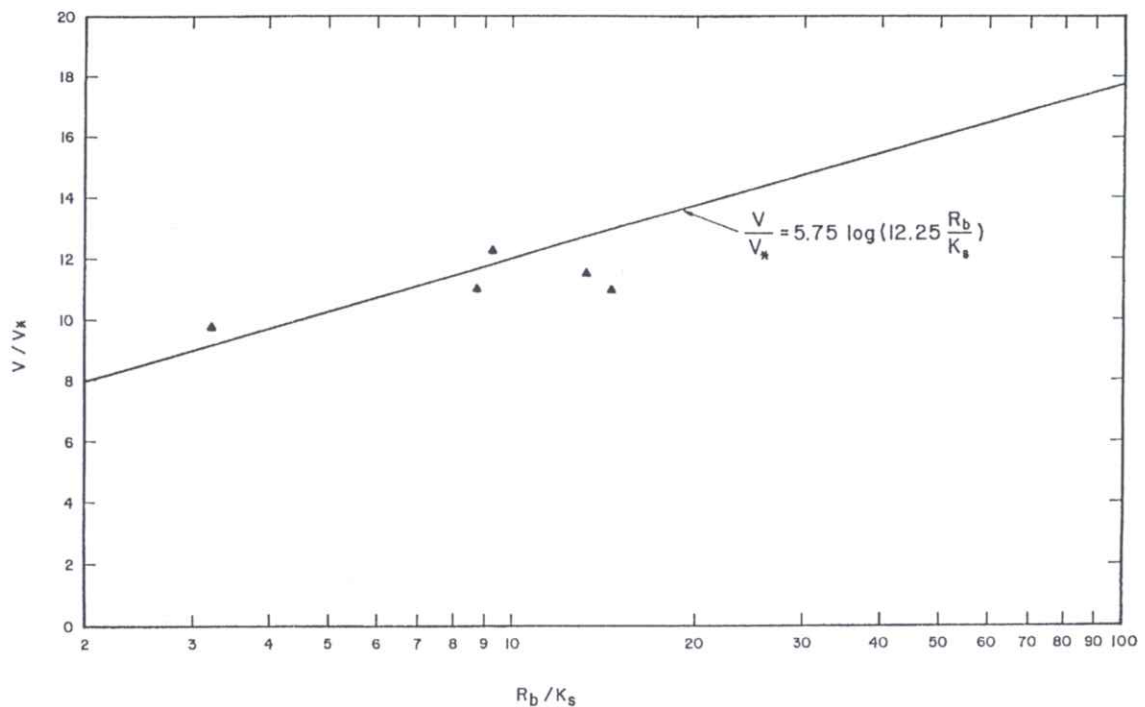


Figure 3.2: Average velocity distribution for selected model-scale mattress tests in the 1,22 m flume (CSU, 1984)

3.4.1.3 Relation between shear stress and velocities

From Manning's equation:

$$S_0 = \frac{v^2 n^2}{R^3} \quad (3.3)$$

and
$$\tau_0 = \rho g R S_0 = \rho g D S_0 \quad (2.10)$$

hence,
$$\tau_0 = \frac{\rho g v^2 n^2}{R^{\frac{1}{3}}} = \frac{\rho g v^2 n^2}{D^{\frac{1}{3}}} \quad (3.4)$$

Equation 3.4 indicates that, for the same velocity, shear stress increases with decrease in hydraulic radius or depth. Shear stress is also strongly dependent on velocity and weakly dependent on depth (CSU, 1984). Shear stress is proportional to the velocity gradient and is the major factor that controls the stability of a Reno mattress or rip rap. Drag acting on a mattress or on rip rap is larger for a shallower depth with the same average velocity, and vice versa, namely as the depth is increased for a given velocity, stability will be increased due to the reduction in shear stress. Figure 3.3 show some results obtained from the model-scale mattress tests in the 1,22 m flume. The line shown was determined by assuming $n_b = 0.025$. A relative good agreement indicates the applicability of Equation 3.4 (CSU, 1984).

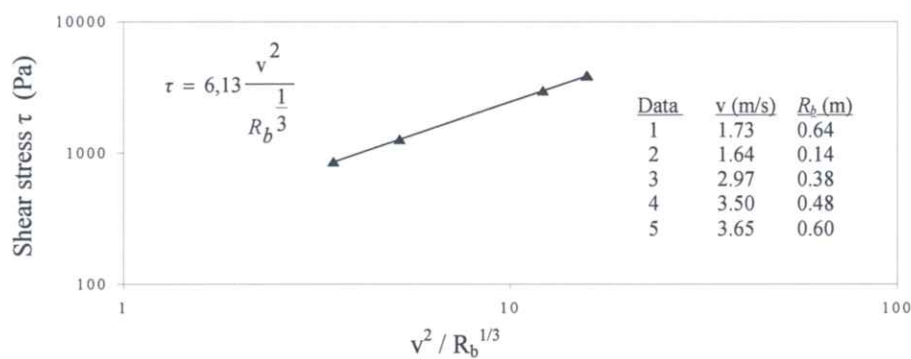


Figure 3.3: Relationship between shear stress, velocity and hydraulic radius (CSU,1984)

3.4.2 Incipient motion conditions

The following statement is made in the CSU study (CSU, 1984): “The ability of the mattress to resist movement by the current relies on its monolithic continuity to resist displacement and not the mass of the mattress. The rocks inside the mattress are retained by the wire netting.”

In general, when the velocity and shear stress reach a critical magnitude (incipient motion condition), the rocks inside the mattress start to move in the direction of the flow. The conditions of incipient motion were determined. Figure 3.4 shows the critical velocity versus mattress thickness (CSU, 1984). All the model-scale mattress data tested in the 1,22 m flume had a Froude number less than 1,5 and the full-scale mattress data tested in the outdoor steep prototype flume had Froude number values larger than 3,0. As mentioned earlier for the same velocity, the size of mattresses should be increased for a shallower depth condition to obtain the same degree of stability in a deeper channel (CSU, 1984). Figure 3.4 shows that a 450 mm mattress unit should be utilised for a highly supercritical flow ($F > 3$) to obtain the same degree of stability as a 230 mm mattress for a nearly critical to sub-critical flow ($F < 1,5$) (CSU, 1984). The critical velocities for various mattress thicknesses determined from the CSU study were compared with the velocities suggested in a study done by Agostini and Papetti (CSU, 1984) in Table 3.11.

Table 3.11: Critical velocities for various mattress thicknesses determined from the CSU study compared with the velocities suggested in a study done by Agostini and Papetti (CSU, 1984)

| Mattress thickness (mm) | Critical velocity determined from the CSU study (CSU,1984) (m/s) | | Velocity suggested by Agostini and Papetti (CSU,1984) (m/s) |
|-------------------------|--|---------|---|
| | $F < 1.5$ | $F > 3$ | |
| 150 | 4.420 | 3.688 | 1.798 |
| 230 | 4.694 | 3.962 | 3.597 |
| 300 | 4.999 | 4.206 | 4.511 |
| 450 | 5.578 | 4.755 | 5.395 |

It was found that the permissible velocities suggested by Agostini and Papetti (CSU, 1984) were all lower than the critical velocities determined from the CSU study for $F < 1,5$, particularly for the 150 mm and 230 mm thick mattresses. This indicated that the mattress linings, using Agostini and Papetti's criteria, were thicker than that required when using the CSU criteria.

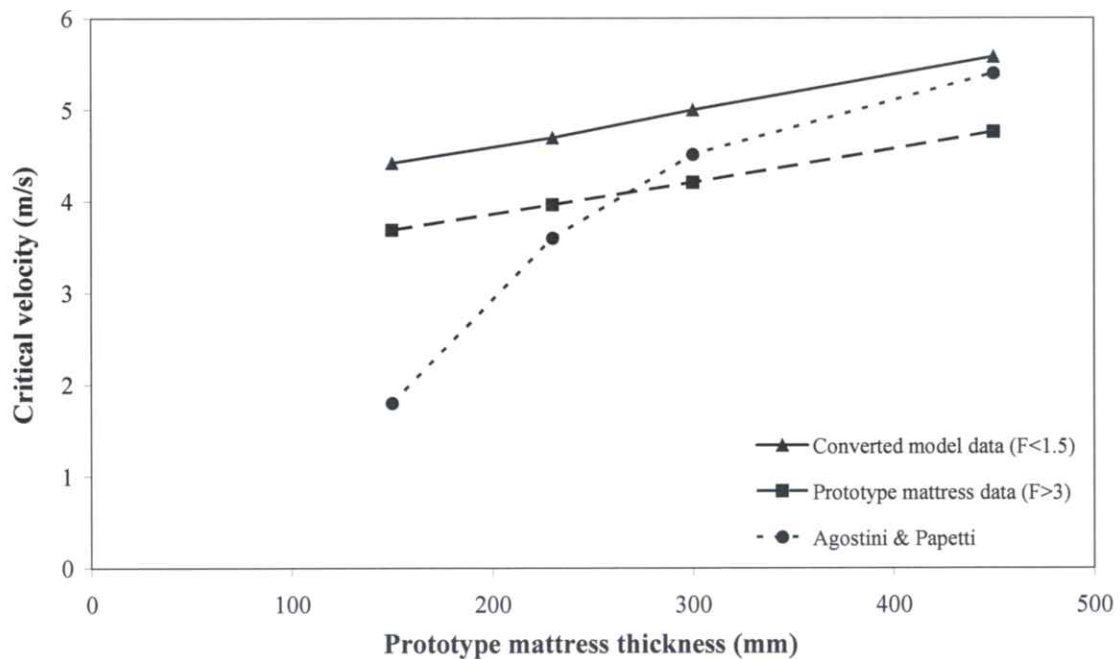


Figure 3.4: Critical velocity that indicates rock movement as a function of mattress thickness (CSU, 1984)

The CSU study further alleged that the mattress mesh would enhance stability of filling rock by doubling the critical shear stress required for movement compared to that for rip rap (CSU, 1984). The required mattress thickness given in Table 3.12, was determined from the CSU laboratory tests and is shown in Figure 3.5. The comparison done in the CSU study alleged that in practical flow range, the required thickness of rip rap could be 1,5 times to 3 times the required mattress thickness, which is an indication that the wire mesh strength is a major factor controlling stability of mattresses. The values of Shield's parameter, θ , used and suggested in the CSU study are $\theta \approx 0,10$ for the mattress and $\theta \approx 0,047$ for the rip rap respectively (CSU, 1984).

Table 3.12: Required mattress thickness as determined from laboratory tests compared to that suggested for rip rap (CSU, 1984)

| Shear Stress (Pa) | Thickness (mm) | |
|----------------------|----------------|---------|
| | Mattress | Rip rap |
| 167.6 | 150 | 432 |
| 191.5 | 230 | 508 |
| 220.2 | 300 | 584 |
| 263.3 | 450 | 711 |

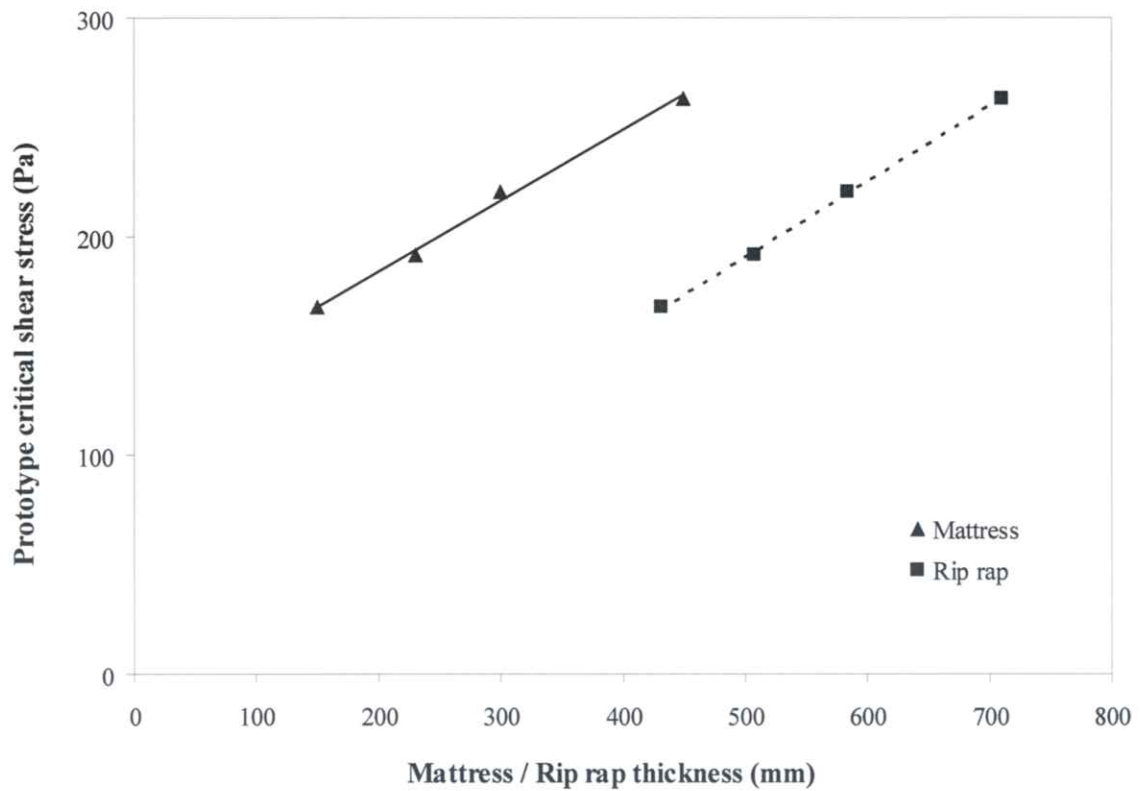


Figure 3.5: Critical shear stress versus mattress / rip rap thickness (CSU, 1984)

3.4.3 Deformation of mattresses under high flow conditions

With further increase in flow velocity and shear stress beyond the critical values for incipient motion, a significant amount of rocks would move from the upstream portion of the mattress compartment to the downstream portion of the compartment.

3.5 Summary And Conclusions Of CSU Study

The tests, described in paragraph 3.3, were analysed to determine incipient motion of mattresses, hydraulic conditions in the mattress channel, velocities at the mattress / filter interface and at the filter / soil interface, pressure variations and the extent of mattress deformation when subjected to very high flow velocities. The analysis results were utilised to develop design criteria.

The major conclusions made by CSU regarding the mattress test program are as follows (CSU, 1984):

- The hydraulic conditions in a mattress channel are the same as those in a gravel channel.
- The roughness of mattresses is mainly caused by filling rocks. The mesh has insignificant effect on mattress roughness.
- The stability of mattress and rip rap structures is highly dependent on the flow velocity and weakly dependent on the flow depth. The relative effect of velocity and depth on mattress and rip rap structure stability is about 6:1.
- Flow velocity and shear stress that cause incipient motion of the filling rock within a mattress compartment, are approximately two times higher than the same size of rock in rip rap (CSU, 1984). The corresponding Shield's parameter is approximately 0,1 for mattresses compared to a value of 0,047 for rip rap (CSU, 1984). Mattress mesh greatly enhances the stability of filling rocks. Test results indicate that stability of a mattress structure is higher than the stability of a rip rap structure of the same thickness. To achieve the same degree of stability, the rock size of a rip rap structure has to be approximately two times larger than the filling rock within the mattress and the rip rap structure has to be thicker. According to the CSU study (1984) this indicates that the mattress structure will be more economical than rip rap. A comparison of the suggested thickness of rip rap shows a saving of 50% to 200% for flow velocities up to approximately 6,1 m/s (CSU, 1984).

- When mattresses are subjected to very high flow velocities, rock within mattress compartments will move downstream and cause a rippling deformation surface. If the reduced thickness of rocks is larger than the median rock size, then the mattresses are still effective in channel protection (CSU, 1984). This phenomenon was based on observing the specific head variation at the mattress / filter interface, which showed that the specific head remained fairly constant despite the mattress deformation. Additional tests are required to confirm this finding.
- The velocity at the mattress / filter interface was found to be quite significant for steep channel flow. The interface velocity is highly dependent on the mattress slope and the interface spacing, and can be determined by Manning's equation. The velocity immediately underneath the filter fabric is about 0,25 to 0,50 of this interface velocity (CSU,1984). This indicates that even if mattresses remain stable, there is a possibility of failure due to high underlying velocity that erodes the base materials. A suitable (graded) filter can be used to mitigate this problem. For low interface velocities, a filter fabric (geotextile) is recommended because it is effective and easy to install. For large interface velocities, a graded gravel filter or a combined geotextile / gravel filter can be utilised to assist in stabilising the base soils, even under very high flow currents far beyond the incipient conditions.
- A design procedure, based on test results obtained from the CSU study and theories regarding mattress bank protection and filter effects, has been developed (CSU, 1984).
- All mattresses tested had prototype compartment lengths of 1 m, which is a significant factor affecting mattress stability. Different compartment lengths should be tested through model-scale tests to evaluate their effect.

4. COMPARISON OF CSU STUDY RESULTS WITH STREAM POWER THEORY, BASED ON THE LIU DIAGRAM, AND SHIELD'S THEORY AS FORECASTERS FOR INCIPIENT MOTION OF ROCK IN RIP RAP

4.1 Introduction

The CSU test results given in Tables 3.4, 3.5, 3.6 and 3.7 have been used to compare the laboratory test results with the theoretical results obtained by applying the stream power principles, based on the Liu diagram, using the criteria of Rooseboom (1974 and 1992) and Armitage (2002), as well as in terms of shear stress, by comparing the values of Shield's parameter for incipient motion conditions.

Firstly, the points of incipient motion observed in the CSU tests, are compared with those obtained by applying the Rooseboom and Armitage criteria of stream power.

Secondly, the values of Shield's parameter, as assumed in the CSU study for Reno mattresses and rip rap for incipient motion conditions, are also compared with those obtained when using the incipient motion conditions in terms of shear stress.

Thirdly, the thicknesses of Reno mattresses and rip rap proposed by the CSU study (CSU 1984), Papetti (1985) and Maccaferri (2004) are compared with those proposed by Rooseboom (SANRAL, 1997), Burcharth & Hughes (2003) in the Coastal Engineering Manual (U.S. Army Corps of Engineers), and those in this thesis.

This chapter of this thesis, as well as the CSU study only deals with motion incipency of bed material and not that on side slopes of channels or around bends.

4.2 Assumptions

This thesis will focus exclusively on non-cohesive particles, that are of concern, as rock is used in Reno mattresses and for rip rap. The following assumptions have been made in the analysis of results:

- The density of the rock or stone is 2650 kg/m³.
- The angle of repose for the rock is 41⁰.
- The drag coefficient used for determining drag forces or settling velocities is 0,4.
- Porosity of the rock matrix, used for gabions mattresses and rip rap, is 0,45.

4.3 Comparison Of Results

4.3.1 Comparison of results in terms of stream power

The model-scale test results and observations given in Tables 3.4, 3.5, 3.6 and 3.7 for 150 mm, 230 mm, 300 mm and 450 mm nominal thick Reno mattresses in the 1,22 m flume, are used to determine the model median rock size, d_{50} . The values for bed shear stress and Shield's parameter were substituted in the following equation to determine the model median rock size for each test run (see Tables 4.1 to 4.4):

$$\theta = \frac{\tau_0}{(\rho_s - \rho)gd_{50}} \quad (2.7)$$

$$\therefore d_{50} = \frac{\tau_0}{(\rho_s - \rho)g\theta}$$

An average median rock size has been calculated for each mattress thickness, converted to prototype median rock size, and used for further calculations.

The data of the model-scale tests are then converted to that of the prototype as shown in Tables 4.1 to 4.4, by applying the model-to-prototype scaling ratios, given in Table 3.1. Thereafter, the settling velocities and shear velocities are calculated by means of the following equations (Armitage, 2002 and Rooseboom, 1974 & 1992):

$$v_{ss} = \sqrt{\frac{4}{3} \left(\frac{\rho_s - \rho}{\rho} \right) \frac{g d_{50}}{C_D}} \quad \text{with } C_D = 0,4 \quad (2.6)$$

and

$$v_* = \sqrt{gDS_0} \quad (2.20)$$

Next, the Movability numbers, and particle Reynolds numbers are calculated, by using equations 2.21 and 2.22. These values are plotted on the Liu diagram and compared to the criteria of Rooseboom (1974 and 1992) and Armitage (2002) (see Figure 4.1).

$$\text{Movability Number} = \frac{v_*}{v_{ss}} \quad (2.21)$$

$$\text{Particle Reynolds Number } Re_* = \frac{v_* d}{\nu} \quad (2.22)$$

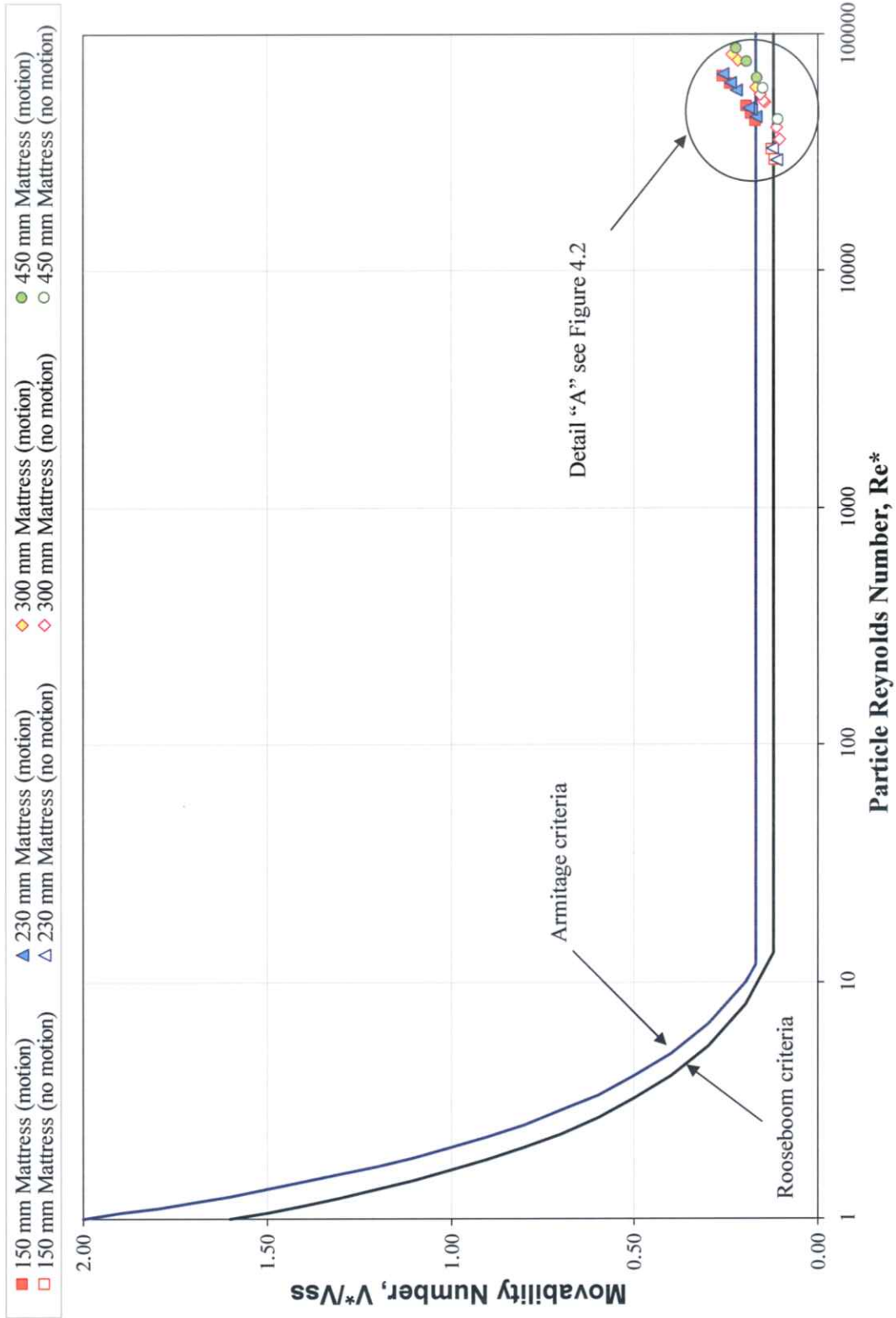
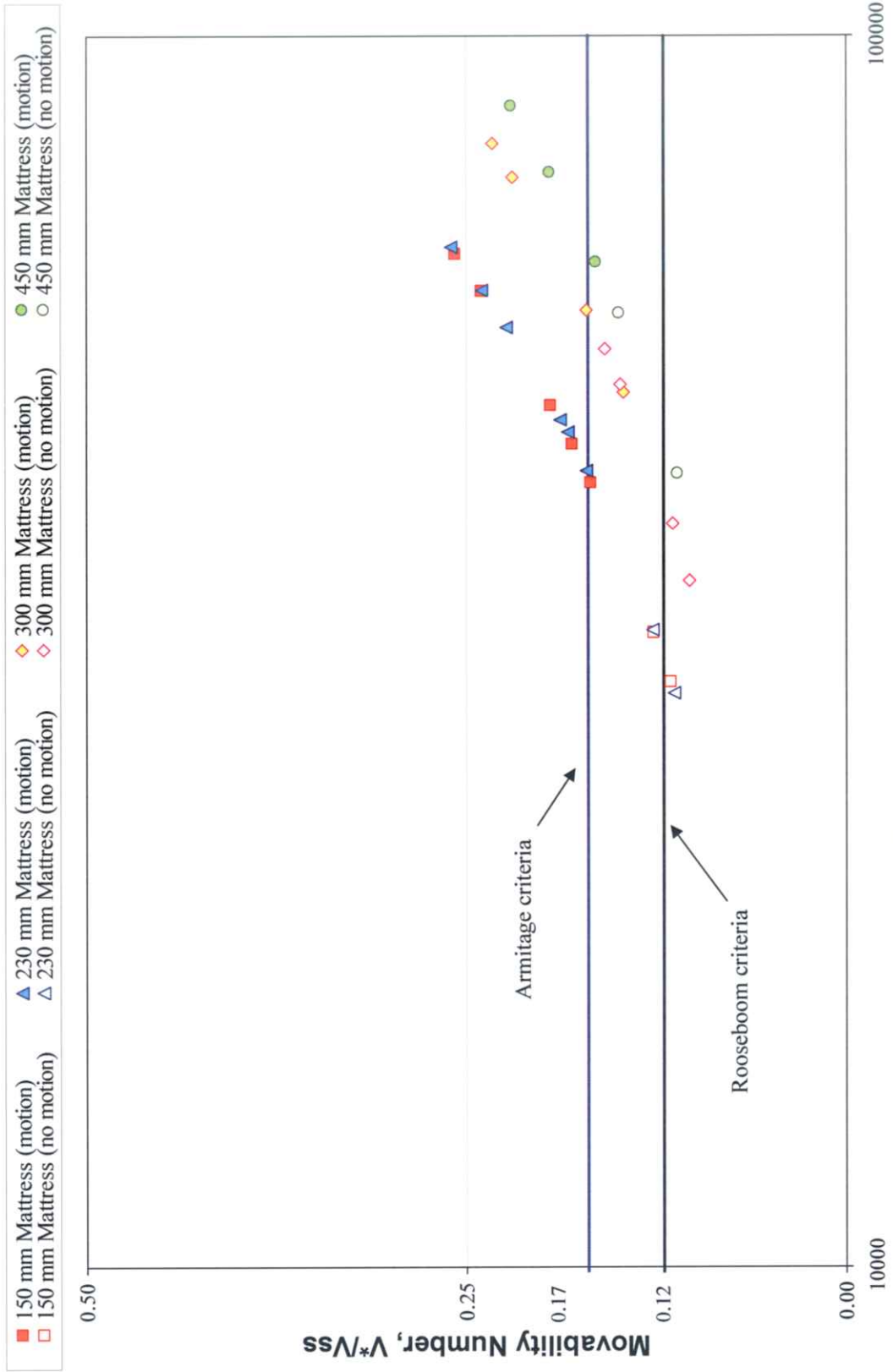


Figure 4.1: Values of movability numbers and particle Reynolds numbers for the 150 mm, 230 mm, 300 mm and 450 mm mattresses plotted on the Liu diagram together with the criteria of Rooseboom (1974, 1992) and Armitage (2002)



Particle Reynolds Number, Re^*

Figure 4.2: Detail "A": see Figure 4.1

Table 4.1: Comparison between CSU Study, Shields & Stream Power based on the Liu Diagram for 150 mm Mattress (Test A)

| Determination of Median Rock Size Used in Run Sequence for Test A - 150 mm Mattress | | | | | | | | | |
|---|--------------|-------------------|------------------|----------------------|---------------------|------------------|------------------------------|---|---|
| Total Discharge Q (m³/s) | Depth D (m) | Flume Slope (m/m) | Velocity v (m/s) | Shear Stress τ₀ (Pa) | Shields Parameter θ | Froude Number F' | Bed Roughness n _b | Model Median Rock Size d ₅₀ (model) (mm) | Model Median Rock Size d ₅₀ (mm) |
| 1.501 | 0.655 | 0.004 | 2.164 | 25.472 | 0.044 | 0.86 | - | 35.8 | |
| 1.982 | 0.789 | 0.004 | 2.246 | 30.931 | 0.053 | 0.81 | - | 36.1 | |
| 1.557 | 0.555 | 0.010 | 2.643 | 54.392 | 0.094 | 1.13 | 0.0199 | 35.7 | |
| 2.039 | 0.640 | 0.010 | 2.749 | 62.723 | 0.108 | 1.10 | 0.0208 | 35.9 | |
| 2.407 | 0.741 | 0.010 | 2.963 | 72.586 | 0.125 | 1.10 | 0.0205 | 35.9 | |
| 2.010 | 0.567 | 0.020 | 3.304 | 111.130 | 0.192 | 1.40 | 0.0243 | 35.8 | |
| 2.577 | 0.652 | 0.020 | 3.502 | 127.888 | 0.221 | 1.38 | 0.0247 | 35.8 | |
| Bold: Flow condition at which movement of filling rocks was first observed. | | | | | | | | | 35.8 |

with $C_D = 0.4$

$$v_{ss} = \sqrt{\frac{2.2 g d_{50}}{C_D}}$$

$$v^* = \sqrt{g D S_0}$$

Shields parameter $\theta = \frac{\tau_0}{(\gamma_s - \gamma) d_{50}}$ with $\rho_s = 2650 \text{ kg/m}^3$

$$\tau_0 = \rho g k S_0 = \rho g D S_0$$

Data converted to that of proto type

| Stream Power based on Liu Diagram | | | | | | | | | | | | | |
|--|--------------|-------------------|------------------|----------------------|---------------------|------------------|------------------------------|--|-----------------|--------|-----------------------------|---|-------|
| Total Discharge Q (m³/s) | Depth D (m) | Flume Slope (m/m) | Velocity v (m/s) | Shear Stress τ₀ (Pa) | Shields Parameter θ | Froude Number F' | Bed Roughness n _b | Proto Type Median Rock Size d ₅₀ (mm) | V _{ss} | V* | $\frac{v^*}{v_{ss}} = \psi$ | $\frac{v^*}{v_{ss} \beta} = \psi \beta$ | Re* |
| 23.395 | 1.966 | 0.004 | 3.748 | 76.417 | 0.044 | 0.85 | - | 107.5 | 2.4083 | 0.2777 | 0.115 | 0.115 | 29858 |
| 30.899 | 2.368 | 0.004 | 3.891 | 92.792 | 0.053 | 0.81 | - | 107.5 | 2.4083 | 0.3048 | 0.127 | 0.126 | 32771 |
| 24.278 | 1.664 | 0.010 | 4.577 | 163.176 | 0.094 | 1.13 | 0.0199 | 107.5 | 2.4083 | 0.4041 | 0.168 | 0.167 | 43435 |
| 31.782 | 1.920 | 0.010 | 4.762 | 188.169 | 0.108 | 1.10 | 0.0208 | 107.5 | 2.4083 | 0.4340 | 0.180 | 0.179 | 46657 |
| 37.520 | 2.222 | 0.010 | 5.131 | 217.759 | 0.125 | 1.10 | 0.0205 | 107.5 | 2.4083 | 0.4669 | 0.194 | 0.193 | 50189 |
| 31.341 | 1.701 | 0.020 | 5.723 | 333.390 | 0.192 | 1.40 | 0.0243 | 107.5 | 2.4083 | 0.5777 | 0.240 | 0.237 | 62098 |
| 40.169 | 1.957 | 0.020 | 6.066 | 383.665 | 0.221 | 1.38 | 0.0247 | 107.5 | 2.4083 | 0.6196 | 0.257 | 0.254 | 66609 |
| Bold: Flow condition at which movement of filling rocks was first observed (assumed motion incipency). | | | | | | | | | | | | | |

| Theoretically calculated values of shear stress and Shield's parameter | | | |
|--|--|------------------------------------|----------------------------------|
| Shear Stress τ _{0,0} (Pa) | k _β (see Eq.'s 2.41 & 2.42) | Shields Parameter θ _{0,0} | Shields Parameter θ ₀ |
| 77.144 | 0.995391 | 0.044 | 0.044 |
| 92.932 | 0.995391 | 0.053 | 0.053 |
| 163.259 | 0.988447 | 0.094 | 0.093 |
| 188.376 | 0.988447 | 0.108 | 0.107 |
| 217.977 | 0.988447 | 0.125 | 0.124 |
| 333.694 | 0.976797 | 0.192 | 0.187 |
| 383.927 | 0.976797 | 0.221 | 0.216 |

37.520 Observed particle motion according to CSU testing

24.278 Flow condition at which particle motion was first observed (CSU, 1984)

0.194 Sediment motion according to Liu diagram

0.168 Mobility number corresponding to the flow condition at which particle motion was first observed

0.127 Mobility number closest to the flow condition at which particle motion would have commenced according to the Liu Diagram, based on the criteria of Rooseboom (1974 & 1992)

Table 4.2: Comparison between CSU Study, Shields & Stream Power based on the Liu Diagram for 230 mm Mattress (Test B)

| Determination of Median Rock Size Used in Run Sequence for Test B - 230 mm Mattress | | | | | | | | |
|---|-------------|-------------------|------------------|----------------------|---------------------|-----------------|-------------------|---|
| Total Discharge Q (m³/s) | Depth D (m) | Flume Slope (m/m) | Velocity v (m/s) | Shear Stress τ₀ (Pa) | Shields Parameter θ | Froude Number F | Bed Roughness n_b | Model Median Rock Size d₅₀ (model) (mm) |
| 1.416 | 0.628 | 0.004 | 1.911 | 24.610 | 0.042 | 0.77 | - | 36.2 |
| 1.982 | 0.796 | 0.004 | 2.289 | 31.170 | 0.054 | 0.82 | - | 35.7 |
| 1.586 | 0.576 | 0.010 | 2.615 | 56.451 | 0.097 | 1.10 | 0.0204 | 36.0 |
| 2.010 | 0.664 | 0.010 | 2.688 | 65.117 | 0.112 | 1.05 | 0.0215 | 35.9 |
| 2.322 | 0.698 | 0.010 | 2.920 | 68.421 | 0.118 | 1.12 | 0.0200 | 35.8 |
| 2.435 | 0.658 | 0.015 | 3.246 | 96.814 | 0.167 | 1.28 | 0.0219 | 35.8 |
| 2.095 | 0.567 | 0.020 | 3.554 | 111.130 | 0.192 | 1.51 | 0.0226 | 35.8 |
| 2.605 | 0.664 | 0.020 | 3.581 | 130.282 | 0.225 | 1.40 | 0.0235 | 35.8 |
| Bold: Flow condition at which movement of filling rocks was first observed. | | | | | | | | Ave d₅₀ (model) = 35.8 |

with C_D=0.4

$$v_{ss} = \sqrt{\frac{2.2 g d_{50}}{C_D}}$$

$$v^* = \sqrt{g D S_0}$$

$$\text{Shields parameter } \theta = \frac{\tau_0}{(\gamma_s - \gamma) d_{50}}$$

with ρ_s = 2650 kg/m³

$$\tau_0 = \rho g k S_0 = \rho g D S_0$$

| Stream Power based on Liu Diagram | | | | | | | | | | | | | | | |
|---|-------------|-------------------|------------------|----------------------|---------------------|-----------------|-------------------|--------------------------------------|-----------------|--------|----------------------|-------------------------------|---|--|-------|
| Data converted to that of proto type | | | | | | | | | | | | | | | |
| Total Discharge Q (m³/s) | Depth D (m) | Flume Slope (m/m) | Velocity v (m/s) | Shear Stress τ₀ (Pa) | Shields Parameter θ | Froude Number F | Bed Roughness n_b | Proto Type Median Rock Size d₅₀ (mm) | V _{ss} | V* | $\frac{v^*}{v_{ss}}$ | k _β (see Eq. 2.41) | Slope correction Factor ψ = √k _β | $\frac{v^*}{v_{ss, \beta}} = \psi \frac{v^*}{v_{ss, 0}}$ | Re* |
| 22.071 | 1.884 | 0.004 | 3.310 | 73.831 | 0.042 | 0.77 | - | 107.5 | 2.4083 | 0.2719 | 0.113 | 0.995391 | 0.997693 | 0.113 | 29226 |
| 30.899 | 2.387 | 0.004 | 3.965 | 93.510 | 0.054 | 0.82 | - | 107.5 | 2.4083 | 0.3060 | 0.127 | 0.995391 | 0.997693 | 0.127 | 32897 |
| 24.719 | 1.728 | 0.010 | 4.530 | 169.352 | 0.097 | 1.10 | 0.0204 | 107.5 | 2.4083 | 0.4117 | 0.171 | 0.988447 | 0.994207 | 0.170 | 44263 |
| 31.341 | 1.993 | 0.010 | 4.656 | 195.351 | 0.112 | 1.05 | 0.0215 | 107.5 | 2.4083 | 0.4422 | 0.184 | 0.988447 | 0.994207 | 0.183 | 47538 |
| 36.196 | 2.094 | 0.010 | 5.058 | 205.263 | 0.118 | 1.12 | 0.0200 | 107.5 | 2.4083 | 0.4532 | 0.188 | 0.988447 | 0.994207 | 0.187 | 48722 |
| 37.962 | 1.975 | 0.015 | 5.622 | 290.442 | 0.167 | 1.28 | 0.0219 | 107.5 | 2.4083 | 0.5391 | 0.224 | 0.982634 | 0.991279 | 0.222 | 57954 |
| 32.665 | 1.701 | 0.020 | 6.156 | 333.390 | 0.192 | 1.51 | 0.0226 | 107.5 | 2.4083 | 0.5777 | 0.240 | 0.976797 | 0.988331 | 0.237 | 62098 |
| 40.610 | 1.993 | 0.020 | 6.203 | 390.847 | 0.225 | 1.40 | 0.0235 | 107.5 | 2.4083 | 0.6254 | 0.260 | 0.976797 | 0.988331 | 0.257 | 67228 |
| Bold: Flow condition at which movement of filling rocks was first observed (assumed motion incipency). | | | | | | | | | | | | | | | |

31.341 Observed particle motion according to CSU testing
 24.719 Flow condition at which particle motion was first observed (CSU, 1984)

0.188 Sediment motion according to Liu diagram
 0.171 Movability number corresponding to the flow condition at which particle motion was first observed
 0.127 Movability number closest to the flow condition at which particle motion would have commenced according to the Liu Diagram, based on the criteria of Rouseboom (1974 & 1992)

| Theoretically calculated values of shear stress and Shield's parameter | | | |
|--|--|-----------------------------------|----------------------------------|
| Shear Stress τ₀θ (Pa) | k _β (see Eq.'s 2.41 & 2.42) | Shields Parameter θ _{0θ} | Shields Parameter θ ₀ |
| 73.915 | 0.995391 | 0.042 | 0.042 |
| 93.650 | 0.995391 | 0.054 | 0.054 |
| 169.538 | 0.988447 | 0.097 | 0.096 |
| 195.552 | 0.988447 | 0.112 | 0.111 |
| 205.419 | 0.988447 | 0.118 | 0.117 |
| 290.637 | 0.982634 | 0.167 | 0.164 |
| 333.694 | 0.976797 | 0.192 | 0.187 |
| 391.104 | 0.976797 | 0.225 | 0.220 |

Table 4.3: Comparison between CSU Study, Shields & Stream Power based on the Liu Diagram for 300 mm Mattress (Test C)

| Determination of Median Rock Size Used in Run Sequence for Test C - 300 mm Mattress | | | | | | | |
|---|-------------|-------------------|------------------|----------------------|---------------------|-----------------|---|
| Total Discharge Q (m³/s) | Depth D (m) | Flume Slope (m/m) | Velocity v (m/s) | Shear Stress τ₀ (Pa) | Shields Parameter θ | Froude Number F | Model Median Rock Size d₅₀ (model) (mm) |
| 1.416 | 0.640 | 0.004 | 1.804 | 25.089 | 0.035 | 0.72 | 44.3 |
| 1.897 | 0.792 | 0.004 | 2.469 | 31.122 | 0.044 | 0.89 | 43.7 |
| 1.444 | 0.533 | 0.010 | 2.408 | 52.189 | 0.074 | 1.05 | 43.6 |
| 1.756 | 0.610 | 0.010 | 2.591 | 59.850 | 0.084 | 1.06 | 44.0 |
| 2.294 | 0.701 | 0.010 | 3.018 | 71.820 | 0.101 | 1.13 | 43.9 |
| 0.566 | 0.259 | 0.020 | 2.225 | 50.753 | 0.072 | 1.40 | 43.5 |
| 1.869 | 0.579 | 0.020 | 3.444 | 107.731 | 0.152 | 1.48 | 43.8 |
| 2.605 | 0.655 | 0.020 | 3.780 | 131.671 | 0.186 | 1.47 | 43.7 |
| Bold: Flow condition at which movement of filling rocks was first observed. | | | | | | | 43.8 |

with C_D=0.4

$$v_{ss} = \sqrt{\frac{2.2 g d_{50}}{C_D}}$$

$$v^* = \sqrt{g D S_0}$$

$$\text{Shields parameter } \theta = \frac{\tau_0}{(\gamma_s - \gamma) d_{50}}$$

with ρ_s = 2650 kg/m³

$$\tau_0 = \rho g k S_0 = \rho g D S_0$$

| Stream Power based on Liu Diagram | | | | | | | | | | | | | | | |
|---|-------------|-------------------|------------------|----------------------|---------------------|-----------------|------------------------------|--|-----------------|--------|----------------------|-------------------------------|---|--|-------|
| Data converted to that of proto type | | | | | | | | | | | | | | | |
| Total Discharge Q (m³/s) | Depth D (m) | Flume Slope (m/m) | Velocity v (m/s) | Shear Stress τ₀ (Pa) | Shields Parameter θ | Froude Number F | Bed Roughness n _b | Proto Type Median Rock Size d ₅₀ (mm) | V _{ss} | V* | $\frac{v^*}{v_{ss}}$ | k _β (see Eq. 2.41) | Slope correction Factor ψ = √k _β | $\frac{v^*}{v_{ss,0}} = \psi \frac{v^*}{v_{ss,0}}$ | Re* |
| 22.071 | 1.920 | 0.004 | 3.125 | 75.268 | 0.035 | 0.72 | - | 131.5 | 2.6633 | 0.2745 | 0.103 | 0.995391 | 0.997693 | 0.103 | 36087 |
| 29.575 | 2.377 | 0.004 | 4.276 | 93.367 | 0.044 | 0.89 | - | 131.5 | 2.6633 | 0.3054 | 0.115 | 0.995391 | 0.997693 | 0.114 | 40154 |
| 22.512 | 1.600 | 0.010 | 4.171 | 156.568 | 0.074 | 1.05 | 0.0218 | 131.5 | 2.6633 | 0.3962 | 0.149 | 0.988447 | 0.994207 | 0.148 | 52088 |
| 27.368 | 1.829 | 0.010 | 4.487 | 179.551 | 0.084 | 1.06 | 0.0217 | 131.5 | 2.6633 | 0.4236 | 0.159 | 0.988447 | 0.994207 | 0.158 | 55684 |
| 35.755 | 2.103 | 0.010 | 5.226 | 215.461 | 0.101 | 1.15 | 0.0205 | 131.5 | 2.6633 | 0.4542 | 0.171 | 0.988447 | 0.994207 | 0.170 | 59714 |
| 8.828 | 0.777 | 0.020 | 3.854 | 152.259 | 0.072 | 1.40 | 0.0234 | 131.5 | 2.6633 | 0.3905 | 0.147 | 0.976797 | 0.988331 | 0.145 | 51338 |
| 29.133 | 1.737 | 0.020 | 5.966 | 323.192 | 0.152 | 1.45 | 0.0227 | 131.5 | 2.6633 | 0.5838 | 0.219 | 0.976797 | 0.988331 | 0.217 | 76755 |
| 40.610 | 1.966 | 0.020 | 6.546 | 395.012 | 0.186 | 1.49 | 0.0223 | 131.5 | 2.6633 | 0.6211 | 0.233 | 0.976797 | 0.988331 | 0.230 | 81649 |
| Bold: Flow condition at which movement of filling rocks was first observed (assumed motion incipency). | | | | | | | | | | | | | | | |

| Theoretically calculated values of shear stress and Shield's parameter | | | |
|--|--|------------------------------------|----------------------------------|
| Shear Stress τ _{0,θ} (Pa) | k _β (see Eq.'s 2.41 & 2.42) | Shields Parameter θ _{6,0} | Shields Parameter θ ₀ |
| 75.350 | 0.995391 | 0.035 | 0.035 |
| 93.291 | 0.995391 | 0.044 | 0.044 |
| 156.980 | 0.988447 | 0.074 | 0.073 |
| 179.405 | 0.988447 | 0.084 | 0.083 |
| 206.316 | 0.988447 | 0.097 | 0.096 |
| 152.494 | 0.976797 | 0.072 | 0.070 |
| 340.870 | 0.976797 | 0.160 | 0.156 |
| 385.721 | 0.976797 | 0.181 | 0.177 |

29.133 Observed particle motion according to CSU testing
 35.755 Flow condition at which particle motion was first observed (CSU, 1984)

0.219 Sediment motion according to Liu diagram
 0.171 Movability number corresponding to the flow condition at which particle motion was first observed
 0.149 Movability number closest to the flow condition at which particle motion would have commenced according to the Liu Diagram, based on the criteria of Rooseboom (1974 & 1992)

Table 4.4: Comparison between CSU Study, Shields & Stream Power based on the Liu Diagram for 450 mm Mattress (Test D)

| Determination of Median Rock Size Used in Run Sequence for Test D - 450 mm Mattress | | | | | | | |
|---|-------------|-------------------|------------------|----------------------------------|---------------------|-----------------|---|
| Total Discharge Q (m³/s) | Depth D (m) | Fiume Slope (m/m) | Velocity v (m/s) | Shear Stress τ _o (Pa) | Shields Parameter θ | Froude Number F | Model Median Rock Size d ₅₀ (model) (mm) |
| 2.039 | 0.808 | 0.004 | 2.170 | 31.649 | 0.041 | 0.77 | 47.7 |
| 1.586 | 0.591 | 0.010 | 2.368 | 57.935 | 0.075 | 0.98 | 47.7 |
| 2.379 | 0.716 | 0.010 | 2.914 | 70.192 | 0.091 | 1.10 | 47.7 |
| 2.492 | 0.668 | 0.015 | 3.316 | 98.155 | 0.127 | 1.30 | 47.7 |
| 2.633 | 0.640 | 0.020 | 3.655 | 125.494 | 0.163 | 1.46 | 47.6 |
| Bold: Flow condition at which movement of filling rocks was first observed. Ave d ₅₀ (model) = | | | | | | | 47.7 |

with C_D = 0.4

$$v_{st} = \sqrt{\frac{2.2 \cdot g \cdot d_{50}}{C_D}}$$

$$v^* = \sqrt{g \cdot D \cdot S_0}$$

$$\text{Shields parameter } \theta = \frac{\tau_o}{(\gamma_s - \gamma) d_{50}} \text{ with } \rho_s = 2650 \text{ kg/m}^3$$

$$\tau_o = \rho g D S_0 = \rho g D S_0$$

| Stream Power based on Liu Diagram | | | | | | | | | | | | | | | |
|--|-------------|-------------------|------------------|----------------------------------|---------------------|-----------------|------------------------------|--|-----------------|--------|-------------------------|-------------------------------|---|--|-------|
| Total Discharge Q (m³/s) | Depth D (m) | Fiume Slope (m/m) | Velocity v (m/s) | Shear Stress τ _o (Pa) | Shields Parameter θ | Froude Number F | Bed Roughness n _b | Proto Type Median Rock Size d ₅₀ (mm) | V _{ss} | V* | $\frac{v_*'}{v_{*s,0}}$ | k _p (see Eq. 2.41) | Slope correction Factor ψ = √k _p | $\frac{v_*'}{v_{*s,0}} = \frac{\psi \cdot v_*'}{v_{*s,0}}$ | Re* |
| 31.782 | 2.423 | 0.004 | 3.759 | 94.947 | 0.041 | 0.77 | - | 143.0 | 2.7780 | 0.3084 | 0.111 | 0.995391 | 0.997693 | 0.111 | 44104 |
| 24.719 | 1.774 | 0.010 | 4.102 | 173.805 | 0.075 | 0.98 | 0.0227 | 143.0 | 2.7780 | 0.4172 | 0.150 | 0.988447 | 0.994207 | 0.149 | 59665 |
| 37.079 | 2.149 | 0.010 | 5.047 | 210.577 | 0.091 | 1.10 | 0.0206 | 143.0 | 2.7780 | 0.4591 | 0.165 | 0.988447 | 0.994207 | 0.164 | 65668 |
| 38.845 | 2.003 | 0.015 | 5.744 | 294.464 | 0.127 | 1.30 | 0.0215 | 143.0 | 2.7780 | 0.5428 | 0.195 | 0.982634 | 0.991279 | 0.194 | 77640 |
| 41.052 | 1.920 | 0.020 | 6.330 | 376.482 | 0.163 | 1.46 | 0.0226 | 143.0 | 2.7780 | 0.6138 | 0.221 | 0.976797 | 0.988331 | 0.218 | 87790 |
| Bold: Flow condition at which movement of filling rocks was first observed (assumed motion incipency). | | | | | | | | | | | | | | | |

41.052 Observed particle motion according to CSU testing

37.079 Flow condition at which particle motion was first observed (CSU, 1984)

| Theoretically calculated values of shear stress and Shield's parameter | | | |
|--|--|------------------------------------|----------------------------------|
| Shear Stress τ _{o,0} (Pa) | k _p (see Eq.'s 2.41 & 2.42) | Shields Parameter θ _{0,0} | Shields Parameter θ ₀ |
| 95.085 | 0.995391 | 0.041 | 0.041 |
| 174.023 | 0.988447 | 0.075 | 0.074 |
| 210.801 | 0.988447 | 0.091 | 0.090 |
| 294.673 | 0.982634 | 0.127 | 0.125 |
| 376.751 | 0.976797 | 0.163 | 0.159 |

0.221 Sediment motion according to Liu diagram

0.165 Movability number corresponding to the flow condition at which particle motion was first observed

0.150 Movability number closest to the flow condition at which particle motion would have commenced according to the Liu Diagram, based on the criteria of Rooseboom (1974 & 1992)

From Figures 4.1 and 4.2, as well as Tables 4.1 to 4.4, it can be seen that the values of Re_* indicate that they fall well within the turbulent zone (the particle Reynolds number, $Re_* > 13$ with the movability number, v^*/v_{ss} constant at 0,12 in the case of Rooseboom's criteria, and $Re_* > 11,8$ with $v^*/v_{ss} = 0,17$ in the case of Armitage's criteria, as given in equations 2.39 and 2.40 respectively).

Movability numbers were calculated for horizontal bed conditions and adapted by means of a slope correction factor (see equations 2.41, 2.47 and 2.48) to obtain the Movability numbers along the actual slopes, which were used in the CSU tests. It can be seen from Tables 4.1 to 4.4 that slopes up to 2% have very little influence on the Movability number. Bigger influences can be expected at very steep gradients.

The flow conditions at which motion of the filling rocks in the Reno mattresses were first observed, are highlighted in Tables 4.1 to 4.4. It can be seen that the calculated Movability numbers for these conditions correspond fairly well with the criteria of Armitage (2002), and that the values of the calculated Movability numbers for these conditions vary between 0.165 and 0.171, with most of the v^*/v_{ss} -values close to 0.17, which is the constant value suggested by Armitage (2002) for incipient motion in the turbulent zone. It must be kept in mind that the rock was enclosed in a wire mesh mattress.

The values of Movability numbers, that nearly correspond to v^*/v_{ss} -values close to 0.12, which is the constant value suggested by Rooseboom (1974 and 1992) for incipient motion in the turbulent zone, are also highlighted in Tables 4.1 to 4.4.

The intervals of the test runs done in the CSU study (CSU, 1984) were fairly rough and should have been done at smaller intervals in order to make finer and thus better comparisons with regard to the criteria suggested by Rooseboom (1974 and 1992) and Armitage (2002).

In view of the rough intervals used for test runs in the CSU study, it can be safely concluded that the general point where incipient motion for rock in mattresses was observed, falls between Movability number values 0,165 to 0,171.

Another disadvantage of the rough intervals used, is the fact that it is difficult to determine the effect of the wire mesh with respect to incipient motion conditions. From the Movability number values given in Tables 4.1 to 4.4, it appears that the effect of the wire mesh is small, and it can be assumed that the incipient motion conditions for Reno mattresses and those for rip rap do not vary by much. The stabilisation effect of the mattress wire mesh is thus not as significant as concluded in the CSU study (CSU, 1984).

The calculated movability numbers, v^*/v_{ss} , which correspond to the flow conditions at which motion of filling rocks in the Reno mattresses for CSU Tests A to D were first observed, are summarised in Table 4.5. The calculated movability numbers for CSU Tests A to D that nearly correspond to the constant value of 0,12 for rip rap, as suggested by Rooseboom (1974 and 1992), are also shown in Table 4.5.

Table 4.5: Movability Numbers for motion incipency, using the Stream Power theory

| Test | Reno mattress | Rip rap |
|--|---------------|--------------|
| A (150 mm thick mattress) | 0,168 | 0,127 |
| B (230 mm thick mattress) | 0,171 | 0,127 |
| C (300 mm thick mattress) | 0,171 | 0,149 |
| D (450 mm thick mattress) | 0,165 | 0,150 |
| Average value of Movability number, v^*/v_{ss} | 0,169 | 0,138 |
| Recommended value of Movability number, v^*/v_{ss} | 0,165 | 0,130 |

Movability numbers close to the minimum values obtained from the CSU test data for Tests A to D (CSU, 1984) are recommended for the design of Reno mattresses and rip rap.

For design purposes it is suggested that a v^*/v_{ss} -value of 0,165 be used as a guideline for incipient motion condition for rock in a mattress, and that a v^*/v_{ss} -value of 0,130 be used as a guideline for incipient motion condition for rock in rip rap, when dealing with flows in the turbulent zone (with C_D assumed as 0,40).

It must be stressed that more accurate values than those given in Table 4.5 could most probably have been obtained if finer intervals for testing had been used in the CSU tests.

4.3.2 Comparison of results in terms of Shield's parameter (shear stress)

Tables 4.1 to 4.4 show the observed points of motion incipency for rock in mattress tests and the corresponding values of the Shield's parameter for the respective mattress thickness tests. The average value of the Shield's parameter for incipient motion of rock in mattresses according to the CSU study (Tests A to D in Tables 4.1 to 4.4), and as shown in Table 4.6, is approximately $0,096 \approx 0,100$, which is in approximate agreement with that concluded in the CSU study (1984). In this thesis it is recommended that the value of Shield's parameter, $\theta = 0,090$ for Reno mattresses be used for design purposes. This value is regarded as safe, as it corresponds well with the minimum values of Shield's parameter for Reno mattresses given in Table 4.6.

If the stream power criteria of Rooseboom (1974 & 1992) for incipient motion for rock in rip rap are applied to the corresponding θ -values obtained in the CSU study (highlighted values for Tests A to D in Tables 4.1 to 4.4), it is found that the corresponding average value of the Shield's parameter is approximately $0,064 \approx 0,060$, as shown in Table 4.6. This differs from the value of 0,047, which was suggested in the CSU study.

It is recommended in this thesis that the value of Shield's parameter, $\theta = 0,056$ for rip rap be used for design purposes. This is regarded as a safe design value for rip rap, as it corresponds well with the minimum values of Shield's parameter for rip rap given in Table 4.6. This value is also the same as proposed by Henderson (1966) and Rooseboom (SANRAL, 1997).

It must be stressed that more accurate values than those given in Table 4.6 could most probably have been obtained if finer intervals for testing had been used in the CSU tests.

Table 4.6: Shield's parameter for motion incipency, using Shield's theory

| Test | Reno mattress | Rip rap |
|---|---------------|--------------|
| A (150 mm thick mattress) | 0,094 | 0,053 |
| B (230 mm thick mattress) | 0,097 | 0,054 |
| C (300 mm thick mattress) | 0,101 | 0,074 |
| D (450 mm thick mattress) | 0,091 | 0,075 |
| Average value of Shield's parameter | 0,096 | 0,064 |
| Recommended value of Shield's parameter, θ | 0,090 | 0,056 |

The values used in the CSU study (CSU, 1984) for shear stress and Shield's parameter are compared to those obtained from calculations by applying the theoretical equations given in Chapter 2 of this thesis, and are summarised in Table 4.7.

It can be seen that the values used in the CSU study correspond to those calculated for a horizontal bed. The values in general compare very well. At steeper slopes bigger differences between the values for a horizontal bed and a sloped bed can be expected.

Table 4.7: Comparative values of shear stress and Shield's parameter obtained from the CSU tests done (CSU, 1984) and those calculated theoretically

| 150 mm nominal thick Reno mattress (see Table 4.1) | | | | | |
|--|---------------------|--------------------------|---------------------------|---------------|-----------------------|
| CSU Test A (CSU, 1984) | | Theoretical calculations | | | |
| Shear stress | Shield's | Shear stress | Shield's | Shear stress | Shield's |
| τ_0 (Pa) | Parameter, θ | $\tau_{0,0}$ (Pa) | Parameter, $\theta_{0,0}$ | τ_0 (Pa) | Parameter, θ_0 |
| 76.417 | 0.044 | 77.144 | 0.044 | 76.789 | 0.044 |
| 92.792 | 0.053 | 92.932 | 0.053 | 92.504 | 0.053 |
| 163.176 | 0.094 | 163.259 | 0.094 | 161.373 | 0.093 |
| 188.169 | 0.108 | 188.376 | 0.108 | 186.199 | 0.107 |
| 217.759 | 0.125 | 217.977 | 0.125 | 215.459 | 0.124 |
| 333.390 | 0.192 | 333.694 | 0.192 | 325.951 | 0.187 |
| 383.665 | 0.221 | 383.927 | 0.221 | 375.019 | 0.216 |
| 230 mm nominal thick Reno mattress (see Table 4.2) | | | | | |
| CSU Test B (CSU, 1984) | | Theoretical calculations | | | |
| Shear stress | Shield's | Shear stress | Shield's | Shear stress | Shield's |
| τ_0 (Pa) | Parameter, θ | $\tau_{0,0}$ (Pa) | Parameter, $\theta_{0,0}$ | τ_0 (Pa) | Parameter, θ_0 |
| 73.831 | 0.042 | 73.915 | 0.042 | 73.574 | 0.042 |
| 93.510 | 0.054 | 93.650 | 0.054 | 93.218 | 0.054 |
| 169.352 | 0.097 | 169.538 | 0.097 | 167.579 | 0.096 |
| 195.351 | 0.112 | 195.552 | 0.112 | 193.293 | 0.111 |
| 205.263 | 0.118 | 205.419 | 0.118 | 203.046 | 0.117 |
| 290.442 | 0.167 | 290.637 | 0.167 | 285.589 | 0.164 |
| 333.390 | 0.192 | 333.694 | 0.192 | 325.951 | 0.187 |
| 390.847 | 0.225 | 391.104 | 0.225 | 382.029 | 0.220 |
| 300 mm nominal thick Reno mattress (see Table 4.3) | | | | | |
| CSU Test C (CSU, 1984) | | Theoretical calculations | | | |
| Shear stress | Shield's | Shear stress | Shield's | Shear stress | Shield's |
| τ_0 (Pa) | Parameter, θ | $\tau_{0,0}$ (Pa) | Parameter, $\theta_{0,0}$ | τ_0 (Pa) | Parameter, θ_0 |
| 75.268 | 0.035 | 75.350 | 0.035 | 75.003 | 0.035 |
| 93.367 | 0.044 | 93.291 | 0.044 | 92.861 | 0.044 |
| 156.568 | 0.074 | 156.980 | 0.074 | 155.166 | 0.073 |
| 179.551 | 0.084 | 179.405 | 0.084 | 177.333 | 0.083 |
| 215.461 | 0.101 | 206.316 | 0.097 | 203.932 | 0.096 |
| 152.259 | 0.072 | 152.494 | 0.072 | 148.956 | 0.070 |
| 323.192 | 0.152 | 340.870 | 0.160 | 332.961 | 0.156 |
| 395.012 | 0.186 | 385.721 | 0.181 | 376.772 | 0.177 |
| 450 mm nominal thick Reno mattress (see Table 4.4) | | | | | |
| CSU Test D (CSU, 1984) | | Theoretical calculations | | | |
| Shear stress | Shield's | Shear stress | Shield's | Shear stress | Shield's |
| τ_0 (Pa) | Parameter, θ | $\tau_{0,0}$ (Pa) | Parameter, $\theta_{0,0}$ | τ_0 (Pa) | Parameter, θ_0 |
| 94.947 | 0.041 | 95.085 | 0.041 | 94.647 | 0.041 |
| 173.805 | 0.075 | 174.023 | 0.075 | 172.013 | 0.074 |
| 210.577 | 0.091 | 210.801 | 0.091 | 208.366 | 0.090 |
| 294.464 | 0.127 | 294.673 | 0.127 | 289.556 | 0.125 |
| 376.482 | 0.163 | 376.751 | 0.163 | 368.009 | 0.159 |

4.4 Comparison Of Proposed Rip Rap Layer And Reno Mattress Thicknesses

Different methodologies and various suggested values for Shield's parameter (θ) and movability numbers (v^*/v_{ss}) with respect to particle sizes and thicknesses to be used for rip rap and Reno mattresses have been investigated and are discussed below.

The information of the test data, in particular the flow depth, bed slope and the bed shear stress of the CSU study, as given in Tables 4.1 to 4.4, have been used to compare the particle sizes and thicknesses required for rip rap layers and Reno mattresses that will just resist motion, i.e., at the point of motion incipency.

4.4.1 Rip rap

The median diameter sizes for rock in rip rap, as proposed by the Rooseboom method (SANRAL, 1997), in this thesis, as well as in the CSU study, have been determined by using Shield's theory and the stream power theory. The median rock diameter size used for determining the rip rap layer thickness, as proposed by Burcharth and Hughes (2003) for coastal conditions, has been assumed as the same size, as determined by the Rooseboom method (SANRAL, 1997).

Rooseboom (SANRAL, 1997) suggested that rip rap layer thicknesses should be 2 to 3 times the designed mean rock diameter. In this thesis the different rock diameter sizes, obtained by using different methodologies, have been multiplied by 2 to obtain the proposed rip rap layer thicknesses, except for the method proposed by Burcharth and Hughes (2003). The reason for using the minimum rip rap layer thickness of 2 times the designed mean rock diameter, is that it corresponds well with the rip rap layer thickness suggested by Burcharth and Hughes (2003).

The different methodologies and various suggested values with respect to particle sizes and thicknesses for rip rap are as follows:

- The methodology proposed by Rooseboom for the design of rip rap and Reno mattresses in the SANRAL Drainage Manual (SANRAL, 1997) are given by equations 2.11, 2.12 and 2.13 in section 2.6.3 of this thesis,
- Shield's theory (equation 2.7) with the Shield's parameter taken as $\theta = 0,056$ as derived in this thesis from the data obtained in the CSU study, and proposed by Henderson (1966) and Rooseboom (SANRAL, 1997), for the determination of rip rap size and layer thickness.

Stream power theory (equation 2.21) with the movability number taken as $v^*/v_{ss} = 0.130$ as derived in this thesis from data obtained in the CSU study, for the determination of rip rap size and layer thickness.

The relation of rip rap layer thicknesses using Shield's theory with $\theta = 0,056$ versus that using stream power theory with $v^*/v_{ss} = 0,130$ for motion incipency, based on CSU Tests A to D, is shown in Figure 4.3.

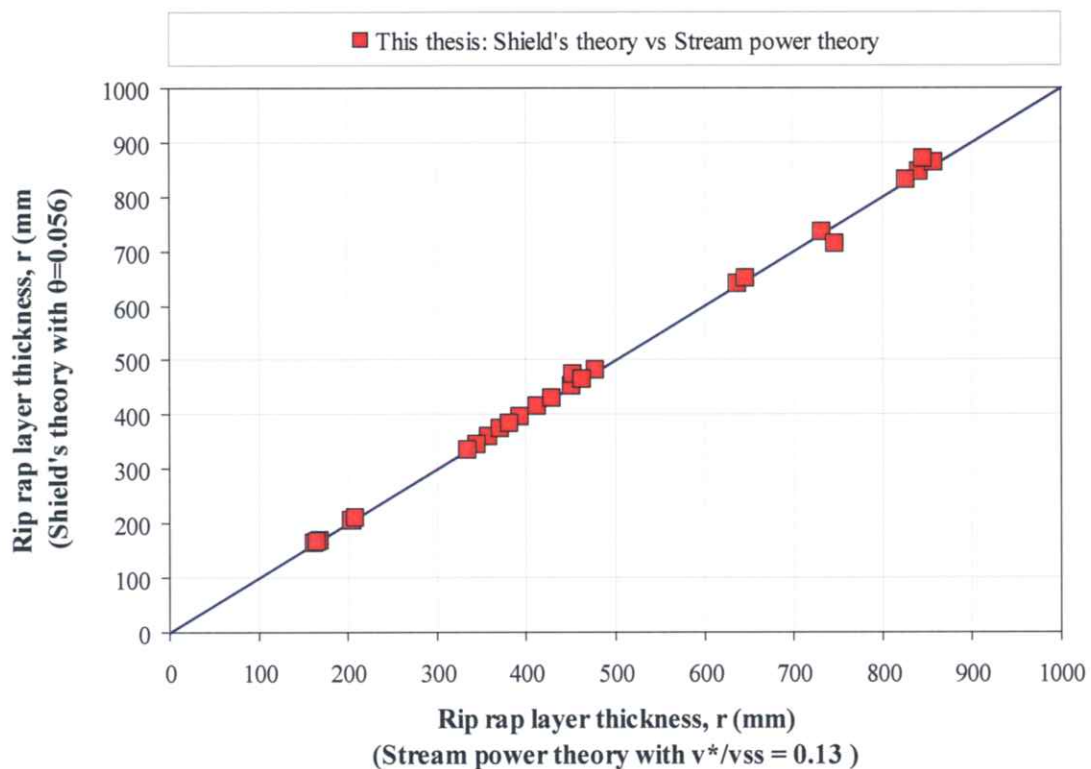


Figure 4.3: Rip rap layer thicknesses as proposed in this thesis using Shield's theory versus that using stream power theory

Figure 4.3 shows a very good correlation between Shield's theory and stream power theory by using the design values of $\theta = 0,056$ and $v^*/v_{ss} = 0,130$ as proposed in this thesis.

- The Shield's equation (equation 2.7) with the Shield's parameter taken as $\theta = 0,047$ as recommended in the CSU study for the determination of rip rap size and layer thickness,
- The recommended rip rap layer thicknesses proposed by Burcharth and Hughes (2003) for coastal conditions (see equations 2.52 and 2.53 in section 2.8 of this thesis), by using the average rock size determined by applying equation 2.11 (Rooseboom methodology in SANRAL (1997)),
- Rip rap layer thicknesses are based on 2 times the required or designed mean rock diameter, except for the Burcharth and Hughes method for coastal conditions (Burcharth and Hughes, 2003), but never less than 200 mm.

The results of the methods, mentioned above, are given in Tables 4.8 to 4.11, and shown in Figures 4.4 to 4.7, and are based on the minimum required rock sizes and layer thicknesses for rip rap that will just resist motion, i.e., at the point of motion incipency.

The x-axes of the comparative graphs, shown in Figures 4.4 to 4.7, have been chosen to represent the bed shear stress, as shear stress is a function of both the flow depth and bed slope parameters used.

It can be seen from Figures 4.4 to 4.7 that the rip rap layer thicknesses as proposed by Rooseboom (SANRAL, 1997) and proposed in this thesis are the same, while those proposed by Burcharth and Hughes (2003) are very close for the same shear stress. This indicates that the results obtained by using the design values of $\theta = 0,056$ and $v^*/v_{ss} = 0,130$ as proposed in this thesis, based on CSU Tests A to D, correspond very well with those of Rooseboom (SANRAL, 1997).

The values of layer thickness as proposed by the CSU study are constantly larger than the other proposals. The main reason is that the Shield's parameter value of 0,047, as assumed by the CSU study, is regarded as too low.

TABLE 4.8: RIP RAP: REQUIRED ROCK SIZE AND LAYER THICKNESS THAT WILL JUST RESIST MOTION (AT POINT OF MOTION INCIPIENCY) USING THE SLOPES AND FLOW DEPTHS AS PER CSU TEST A

| Data converted to that of proto type 150 mm Mattress (Test A) | | Rooseboom Methodology (SANRAL, 1997) Rip Rap | | Shield's Theory with $\theta = 0.047$ (CSU study - Rip rap) | | Shield's Theory with $\theta = 0.056$ (This thesis - Rip rap) | | Stream Power Theory with $v^3/vss = 0.13$ (This thesis - Rip rap) | | CEM (US Army Corps - Rip rap) (Burcharth & Hughes, 2003) | |
|--|-------------------|--|------------------------|--|---------------------------|--|--|--|--|--|-------------------------|
| Total Discharge Q (m ³ /s) | Depth D (m) | Fiume Slope S ₀ (m/m) | Velocity V (m/s) | Shear Stress τ (Pa) | $d_{50} = 11DS_0$ (mm) | Layer thickness (mm) | $d_{50} = \frac{\tau_0}{(\rho_s - \rho)g\theta}$ (mm) | Layer thickness (mm) | $d_{50} = \frac{D S_0}{5.5 (v^3 / vss)^{1/3}}$ (mm) | Layer thickness (mm) | Layer thickness (mm) |
| 23.395 | 1.966 | 0.004 | 3.748 | 76.417 | 85 | 200 | 84 | 200 | 85 | 200 | 200 |
| 30.899 | 2.368 | 0.004 | 3.891 | 92.792 | 103 | 205 | 102 | 205 | 102 | 204 | 212 |
| 24.278 | 1.664 | 0.010 | 4.577 | 163.176 | 180 | 360 | 180 | 360 | 179 | 358 | 372 |
| 31.782 | 1.920 | 0.010 | 4.762 | 188.169 | 208 | 416 | 208 | 415 | 207 | 413 | 429 |
| 37.520 | 2.222 | 0.010 | 5.131 | 217.759 | 240 | 481 | 240 | 480 | 239 | 478 | 496 |
| 31.341 | 1.701 | 0.020 | 5.723 | 333.390 | 368 | 736 | 368 | 736 | 366 | 732 | 760 |
| 40.169 | 1.957 | 0.020 | 6.066 | 383.665 | 424 | 847 | 423 | 847 | 421 | 842 | 874 |

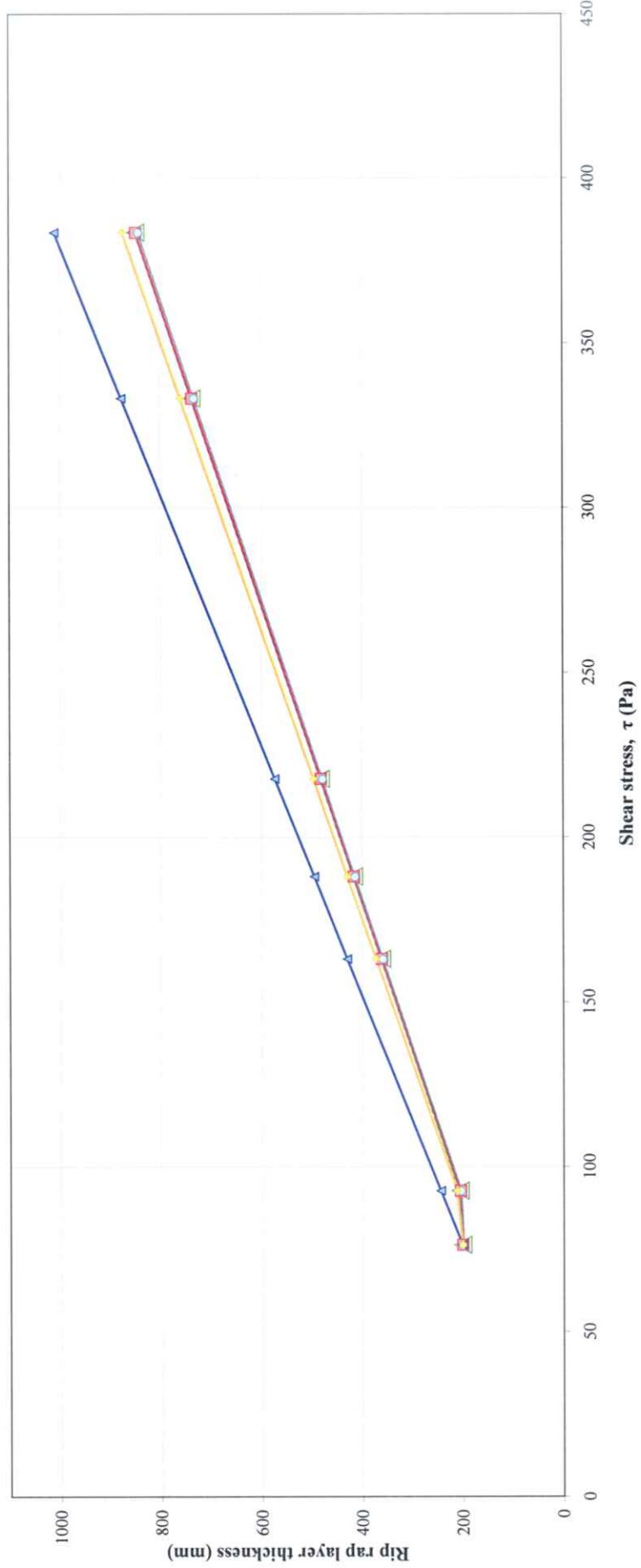


FIGURE 4.4: REQUIRED RIP RAP LAYER THICKNESSES FOR TEST A

TABLE 4.9: RIP RAP: REQUIRED ROCK SIZE AND LAYER THICKNESS THAT WILL JUST RESIST MOTION (AT POINT OF MOTION INCIPIENCY) USING THE SLOPES AND FLOW DEPTHS AS PER CSU TEST B

| Data converted to that of proto type 230 mm Mattress (Test B) | | Rooseboom Methodology (SANRAL, 1997) Rip Rap | | Shield's Theory with $\theta = 0.047$ (CSU study - Rip rap) | | Shield's Theory with $\theta = 0.056$ (This thesis - Rip rap) | | Stream Power Theory with $v^*/v_{sc} = 0.13$ (This thesis - Rip rap) | | CEM (US Army Corps - Rip rap) (Burcharth & Hughes, 2003) | |
|--|-------------------|--|------------------------|--|---------------------------|--|--|---|---|--|-------------------------|
| Total Discharge Q (m ³ /s) | Depth D (m) | Flume Slope S ₀ (m/m) | Velocity V (m/s) | Shear Stress τ (Pa) | $d_{50} = 11DS_0$ (mm) | Layer thickness (mm) | $d_{50} = \frac{\tau_0}{(\rho_s - \rho)g\theta}$ (mm) | Layer thickness (mm) | $d_{50} = \frac{D S_0}{5.5 (v^*/v_{sc})^2}$ (mm) | Layer thickness (mm) | Layer thickness (mm) |
| 22.071 | 1.884 | 0.004 | 3.310 | 73.831 | 82 | 200 | 81 | 200 | 81 | 82 | 200 |
| 30.899 | 2.387 | 0.004 | 3.965 | 93.510 | 103 | 207 | 123 | 246 | 103 | 103 | 213 |
| 24.719 | 1.728 | 0.010 | 4.530 | 169.352 | 187 | 374 | 223 | 445 | 186 | 187 | 386 |
| 31.341 | 1.993 | 0.010 | 4.656 | 195.351 | 216 | 431 | 216 | 431 | 214 | 216 | 445 |
| 36.196 | 2.094 | 0.010 | 5.058 | 205.263 | 227 | 453 | 270 | 540 | 225 | 227 | 468 |
| 37.962 | 1.975 | 0.015 | 5.622 | 290.442 | 321 | 641 | 382 | 764 | 319 | 321 | 662 |
| 32.665 | 1.701 | 0.020 | 6.156 | 333.390 | 368 | 756 | 438 | 876 | 366 | 368 | 760 |
| 40.610 | 1.993 | 0.020 | 6.203 | 390.847 | 431 | 863 | 514 | 1028 | 429 | 431 | 890 |

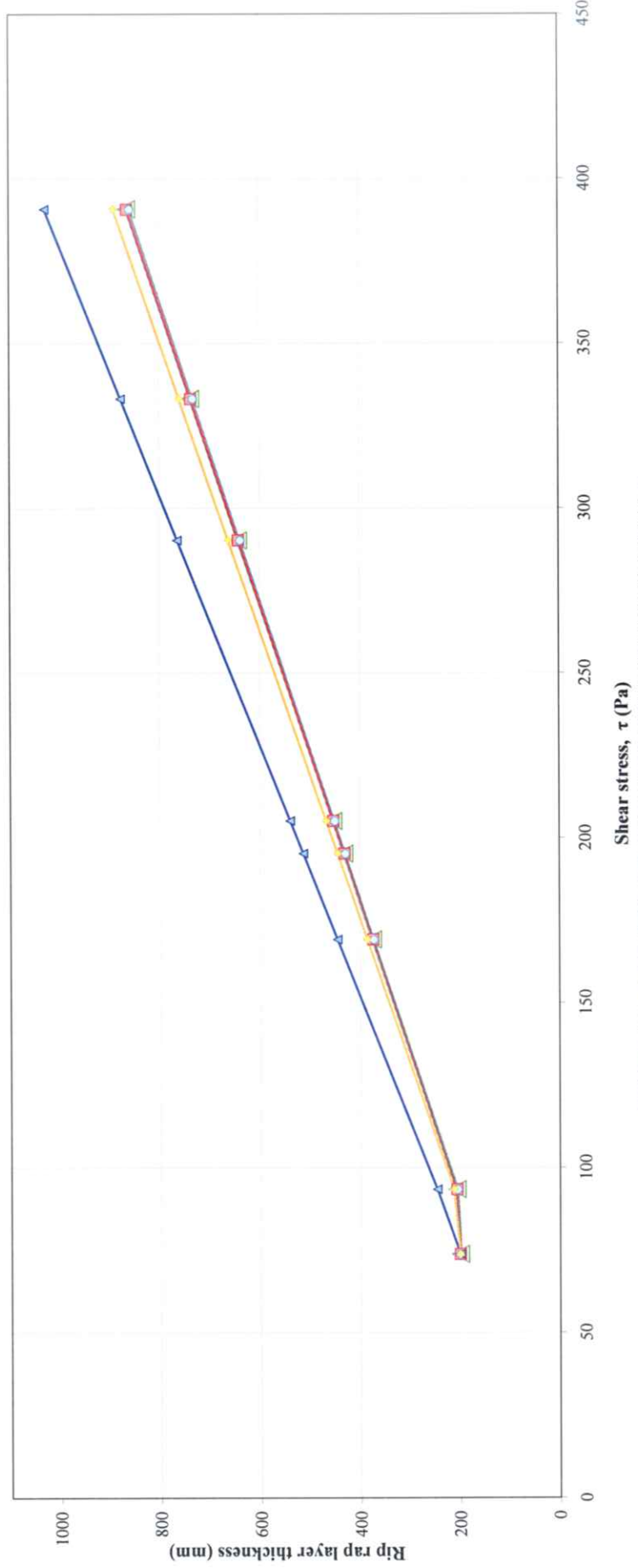


FIGURE 4.5: REQUIRED RIP RAP LAYER THICKNESSES FOR TEST B

TABLE 4.10: RIP RAP: REQUIRED ROCK SIZE AND LAYER THICKNESS THAT WILL JUST RESIST MOTION (AT POINT OF MOTION INCIPIENCY) USING THE SLOPES AND FLOW DEPTHS AS PER CSU TEST C

| Data converted to that of proto type 300 mm Mattress (Test C) | | | Rooseboom Methodology (SANRAL, 1997) | | Shield's Theory with $\theta = 0.047$ (CSU study - Rip rap) | | Shield's Theory with $\theta = 0.056$ (This thesis - Rip rap) | | Stream Power Theory with $v^4/vss = 0.13$ (This thesis - Rip rap) | | CEM (US Army Corps - Rip rap) (Burcharth & Hughes, 2003) | |
|--|-------------------|---|---|-----------------------------------|--|-------------------------|--|-------------------------|--|-------------------------|--|-------------------------|
| Total Discharge Q (m ³ /s) | Depth D (m) | Flume Slope S ₀ (m/m) | Velocity V (m/s) | Shear Stress τ (Pa) | Rip Rap | | $d_{50} = \frac{\tau_0}{(\rho_s - \rho)g\theta}$ (mm) | Layer thickness (mm) | $d_{50} = \frac{D S_0}{5.5 (v^4 / vss)^2}$ (mm) | Layer thickness (mm) | d ₅₀ (mm) | Layer thickness (mm) |
| | | | | | d ₅₀ = 11DS ₀ (mm) | Layer thickness (mm) | | | | | | |
| 22.071 | 1.920 | 0.004 | 3.125 | 75.268 | 83 | 200 | 83 | 200 | 83 | 200 | 83 | 200 |
| 29.575 | 2.377 | 0.004 | 4.276 | 93.367 | 103 | 206 | 103 | 206 | 102 | 205 | 103 | 212 |
| 22.512 | 1.600 | 0.010 | 4.171 | 156.568 | 173 | 346 | 173 | 345 | 172 | 344 | 173 | 357 |
| 27.368 | 1.829 | 0.010 | 4.487 | 179.551 | 198 | 396 | 198 | 396 | 197 | 394 | 198 | 408 |
| 35.755 | 2.103 | 0.010 | 5.226 | 215.461 | 228 | 455 | 228 | 475 | 226 | 453 | 228 | 470 |
| 8.828 | 0.777 | 0.020 | 3.854 | 152.259 | 168 | 336 | 168 | 336 | 167 | 334 | 168 | 347 |
| 29.133 | 1.737 | 0.020 | 5.966 | 323.192 | 376 | 752 | 376 | 713 | 374 | 748 | 376 | 776 |
| 40.610 | 1.966 | 0.020 | 6.546 | 395.012 | 426 | 851 | 426 | 872 | 423 | 846 | 426 | 878 |

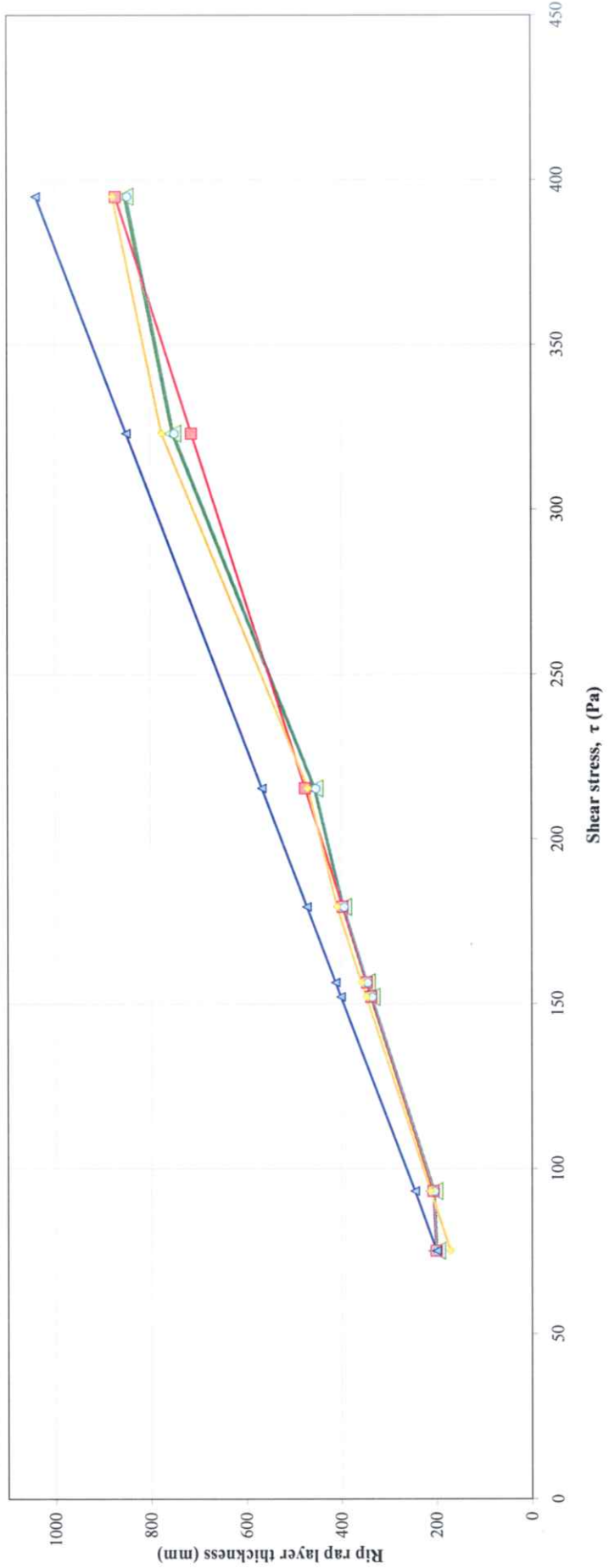


FIGURE 4.6: REQUIRED RIP RAP LAYER THICKNESSES FOR TEST C

TABLE 4.11: RIP RAP: REQUIRED ROCK SIZE AND LAYER THICKNESS THAT WILL JUST RESIST MOTION (AT POINT OF MOTION INCIPIENCY) USING THE SLOPES AND FLOW DEPTHS AS PER CSU TEST D

| Data converted to that of proto type 450 mm Mattress (Test D) | | Rooseboom Methodology (SANRAL, 1997) Rip Rap | | Shield's Theory with $\theta = 0.047$ (CSU study - Rip rap) | | Shield's Theory with $\theta = 0.056$ (This thesis - Rip rap) | | Stream Power Theory with $v^*/v_{cs} = 0.13$ (This thesis - Rip rap) | | CEM (US Army Corps - Rip rap) (Burcharth & Hughes, 2003) | |
|--|-------------------|--|------------------------|--|---------------------------|--|--|---|--|--|-------------------------|
| Total Discharge Q (m ³ /s) | Depth D (m) | Flume Slope S ₀ (m/m) | Velocity V (m/s) | Shear Stress τ (Pa) | $d_{50} = 11DS_0$ (mm) | Layer thickness (mm) | $d_{50} = \frac{\tau_0}{(\rho_s - \rho)g\theta}$ (mm) | Layer thickness (mm) | $d_{50} = \frac{D S_0}{5.75 (v^* / v_{cs})^2}$ (mm) | Layer thickness (mm) | Layer thickness (mm) |
| 31.782 | 2.423 | 0.004 | 3.759 | 94.947 | 105 | 210 | 105 | 104 | 105 | 216 | 216 |
| 24.719 | 1.774 | 0.010 | 4.102 | 173.805 | 192 | 384 | 192 | 191 | 192 | 396 | 396 |
| 37.079 | 2.149 | 0.010 | 5.047 | 210.577 | 233 | 465 | 232 | 231 | 233 | 480 | 480 |
| 38.845 | 2.003 | 0.015 | 5.744 | 294.464 | 325 | 650 | 325 | 323 | 325 | 671 | 671 |
| 41.052 | 1.920 | 0.020 | 6.330 | 376.482 | 416 | 831 | 415 | 413 | 416 | 858 | 858 |

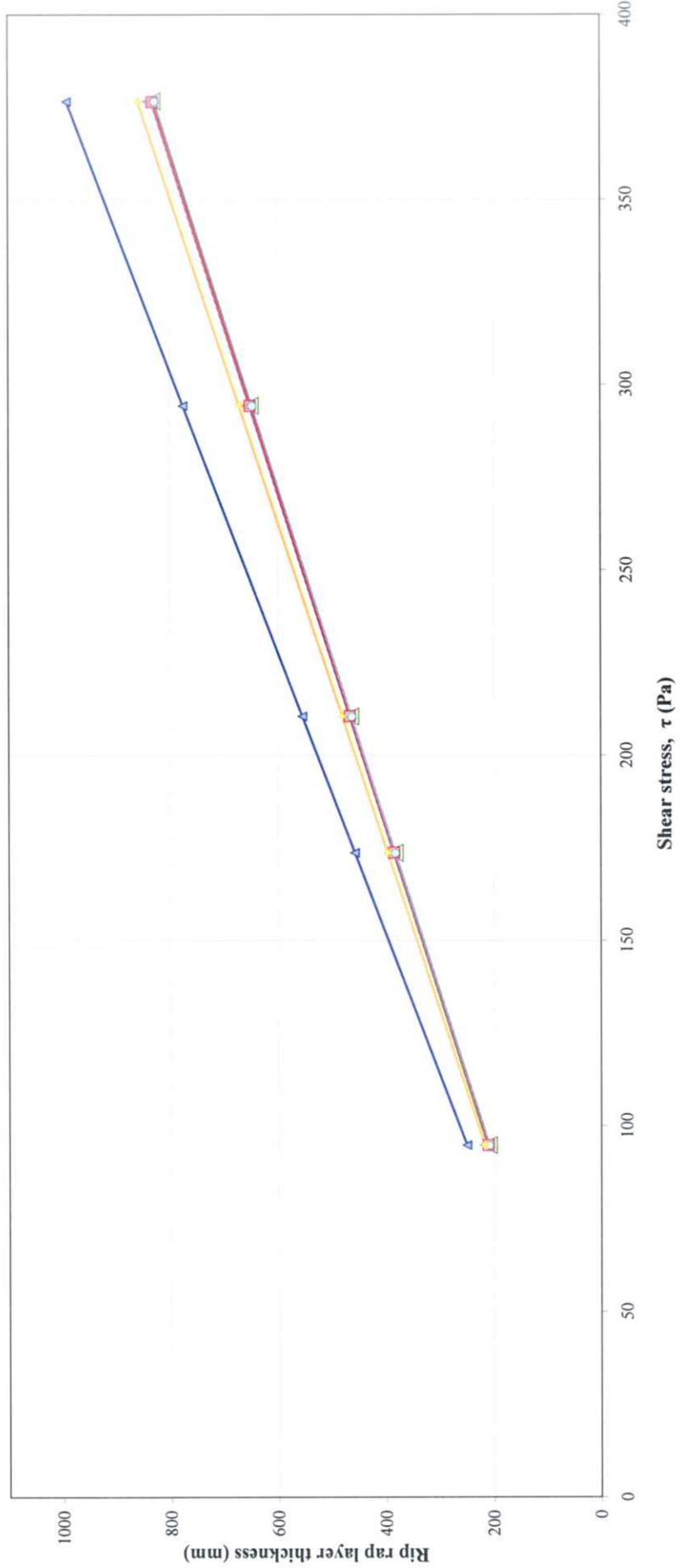


FIGURE 4.7: REQUIRED RIP RAP LAYER THICKNESSES FOR TEST D

The median rock diameter size, as proposed by the Rooseboom method (SANRAL, 1997), this thesis and the CSU study can also be expressed graphically as shown in Figure 4.8, with both the x-axis and y-axis being represented by dimensionless variables.

The x-axis is represented by the Froude number, which is a function of flow depth, slope and velocity, while the y-axis is represented by the ratio of mean particle diameter divided by the flow depth. The corresponding values for Tests A to D, as executed in the CSU study, have been plotted and a linear trend line for each rock size proposal drawn. Figure 4.7 shows a fairly good correspondence between results for the proposals in this thesis and those for the Rooseboom method (SANRAL, 1997).

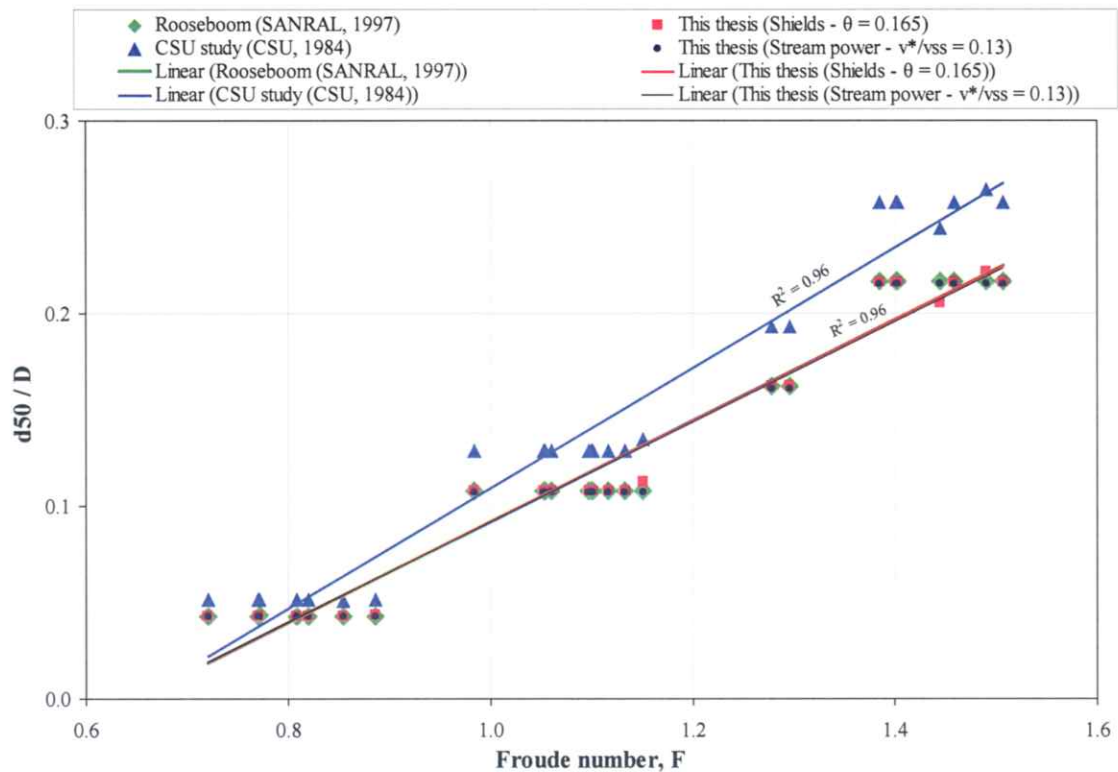


Figure 4.8: Recommended rip rap size for different methods applied to CSU test data Tests A to D (CSU, 1984)

4.4.2 Reno mattresses

The median diameter sizes for rock in Reno mattresses, as proposed in this thesis, as well as in the CSU study, were determined by using Shield's theory and the stream power theory, while those proposed by Maccaferri were obtained graphically (Maccaferri, 2004).

Rooseboom (SANRAL, 1997) suggested that the mass per unit area of an individual gabion or Reno mattress should be at least 1,5 to 2 times that of the calculated median rock particle diameter. In this thesis layer thicknesses of 2 times the median rock particle diameter are used, which is the same principle used to determine the layer thicknesses in the case of rip rap. These layer thicknesses obtained, were rounded up to the standard Reno mattress thicknesses available, namely 170 mm, 230 mm, 300 mm and 500 mm respectively. A detailed explanation, proving that the mass of a rock layer with thickness equal to 2 times the mean rock particle diameter falls within the range of at least 1,5 to 2 times the mass per unit area of a layer with thickness equal to the median rock particle diameter, is given in Annexure B (see equation B.7).

It must be kept in mind that the minimum rock size to be used in Reno mattresses or gabions should not be less than the largest mesh aperture dimension (100 mm).

The different methodologies / various suggested values with respect to particle sizes and Reno mattress thicknesses are as follows:

- The Shield's equation (equation 2.7) with the Shield's parameter taken as $\theta = 0,090$ as recommended in this thesis and based on data obtained in the CSU study (CSU, 1984) for determination of required rock sizes and thicknesses for Reno mattresses.

Stream power theory (equation 2.21) with the movability number taken as $v^*/v_{ss} = 0.165$ as derived in this thesis from data obtained in the CSU study, for the determination of required rock sizes and thicknesses for Reno mattresses.

The relation of median rock diameter sizes required for Reno mattresses using Shield's theory with $\theta = 0,090$ versus that using stream power theory with $v^*/v_{ss} = 0,165$ at the point of motion incipency, based on CSU Tests A to D, is shown in Figure 4.9.

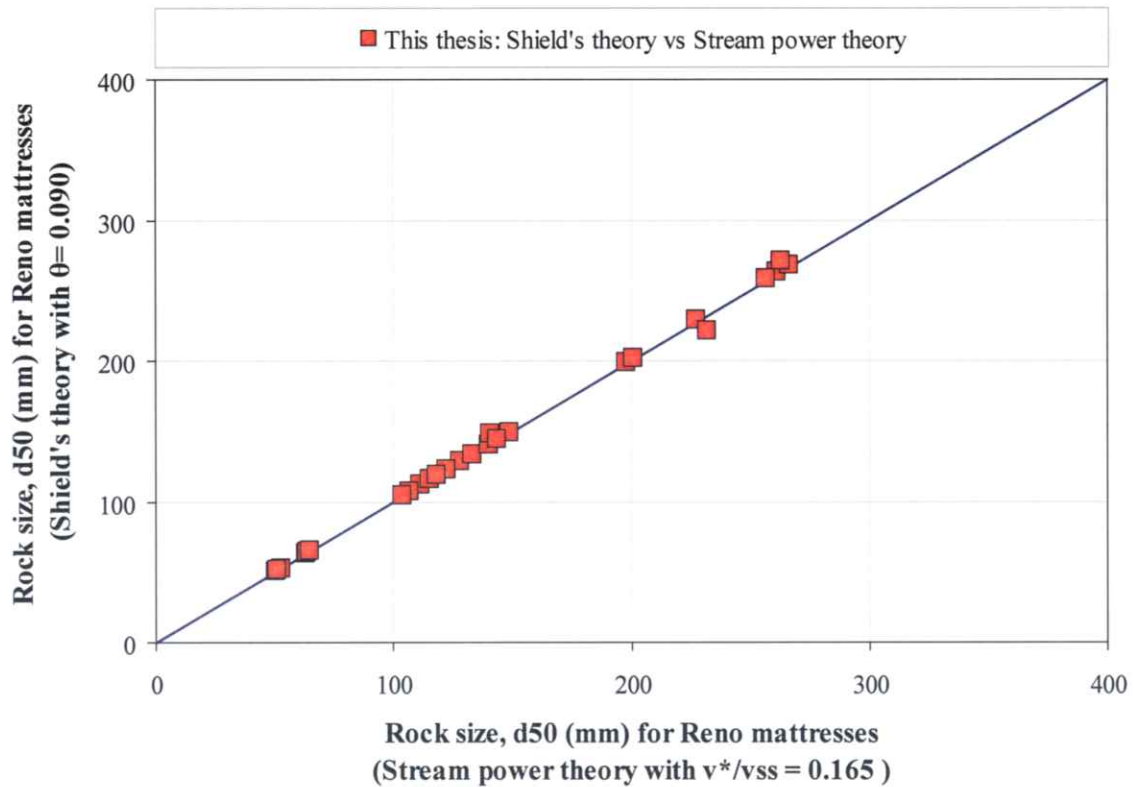


Figure 4.9: Median rock diameter sizes required for Reno mattresses as proposed in this thesis using Shield's theory versus that using stream power theory

The relation of Reno mattress thicknesses using Shield's theory with $\theta = 0,090$ versus that using stream power theory with $v^*/v_{ss} = 0,165$ at the point of motion incipency, based on CSU Tests A to D, is shown in Figure 4.10.

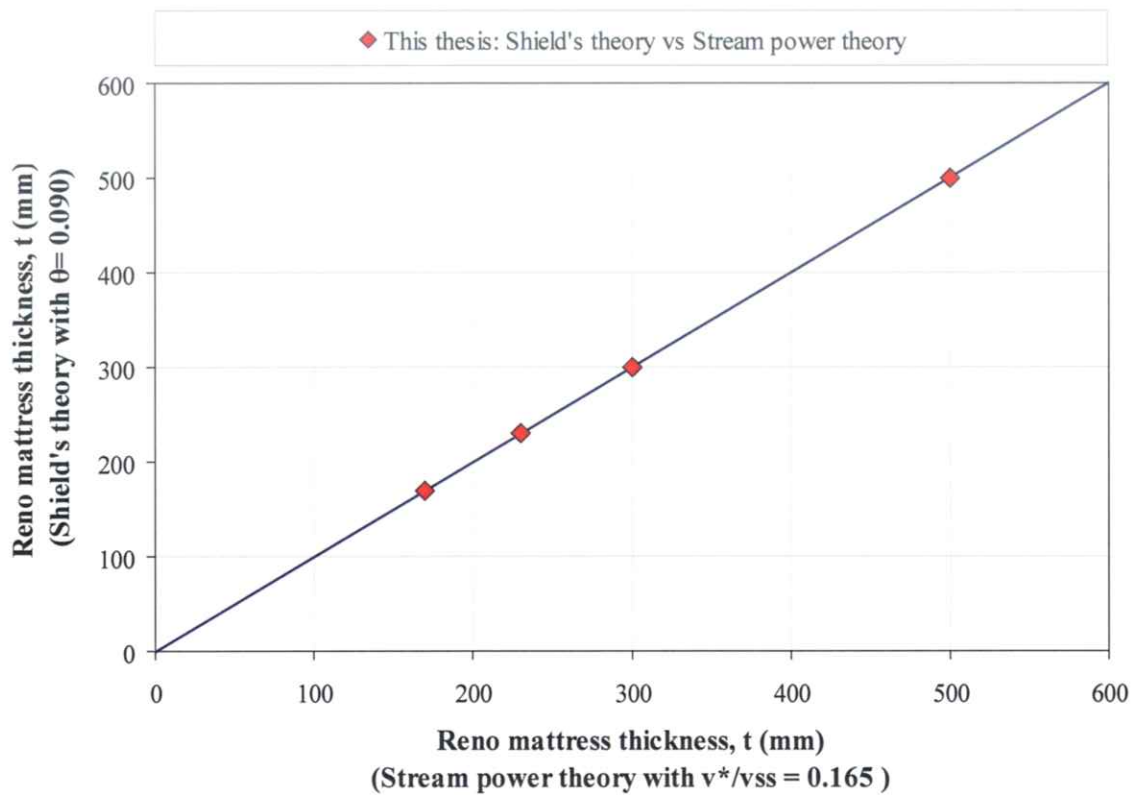


Figure 4.10: Reno mattress thicknesses as proposed in this thesis using Shield's theory versus that using stream power theory

Figures 4.9 and 4.10 show very good correlation between Shield's theory and stream power theory by using values of $\theta = 0,090$ and $v^*/v_{ss} = 0,165$ as proposed in this thesis.

- The Shield's equation (equation 2.7) with the Shield's parameter taken as $\theta = 0,100$ as recommended in the CSU study for determination of required rock sizes and thicknesses for Reno mattresses,
- The design criteria proposed by Maccaferri have been obtained graphically from Figures C-1 and C-2, as well as Table C-1 in Annexure C (Maccaferri, 2004). The critical velocity is used to read off the required rock size and thickness for Reno mattresses.

- Reno mattress thicknesses are based on 2 times the required or designed mean rock diameter, rounded up to the standard Reno mattress thicknesses available, namely 170 mm, 230 mm, 300 mm and 500 mm respectively, but never less than 170 mm.

The results of the methods, mentioned above, are given in Tables 4.12 to 4.15, and shown in Figures 4.11 to 4.14. These results are based on the minimum required rock sizes and thicknesses for Reno mattresses that will just resist motion, i.e., at the point of motion incipency.

The x-axes of the comparative graphs, shown in Figures 4.11 to 4.14, have been chosen to represent the bed shear stress, as shear stress is a function of both the flow depth and bed slope parameters used.

Figures 4.11 to 4.14 indicate that, for Reno mattresses with thicknesses in the 300 mm to 500 mm thick range, larger thicknesses are generally required in the case of Maccaferri's design criteria than in the case of proposals by CSU and this thesis for the same shear stress.

Except for the latter, the results obtained by using the design values of $\theta = 0,090$ and $v^*/v_{ss} = 0,165$, as proposed in this thesis, based on CSU Tests A to D (CSU, 1984), correspond fairly well with the other methodologies used.

TABLE 4.12: RENO MATTRESSES: REQUIRED ROCK SIZE AND MATTRESS THICKNESS THAT WILL JUST RESIST MOTION (AT POINT OF MOTION INCIPIENCY) USING THE SLOPES, FLOW DEPTHS, VELOCITIES AND SHEAR STRESSES AS PER CSU TEST A

| Data converted to that of prototype 150 mm Mattress (Test A) | | Shield's Theory with $\theta = 0.100$ (CSU study - Reno mattresses) | | Shield's Theory with $\theta = 0.090$ (This thesis - Reno mattresses) | | Stream Power Theory with $v^*/v_{*s} = 0.165$ (This thesis - Reno mattresses) | | Maccaferri's design criteria (Values obtained graphically from Maccaferri (2004) and Papetti (1985)) | |
|--|-------------------------|---|--------------------------|---|------------------------------|---|------------------------------|--|------------------------------|
| Depth D (m) | Flume Slope S_0 (m/m) | Velocity V (m/s) | Shear Stress τ (Pa) | $d_{50} = \frac{\tau_0}{(\rho_s - \rho)g\theta}$ (mm) | Reno mattress thickness (mm) | $d_{50} = \frac{\tau_0}{(\rho_s - \rho)g\theta}$ (mm) | Reno mattress thickness (mm) | $d_{50} = \frac{D S_0}{5.5 (v^*/v_{*s})^2}$ (mm) | Reno mattress thickness (mm) |
| 1.966 | 0.004 | 3.748 | 76.42 | 47 | 170 | 52 | 170 | 53 | 170 |
| 2.368 | 0.004 | 3.891 | 92.79 | 57 | 170 | 64 | 170 | 63 | 170 |
| 1.664 | 0.010 | 4.577 | 163.18 | 101 | 230 | 112 | 230 | 111 | 230 |
| 1.920 | 0.010 | 4.762 | 188.17 | 116 | 300 | 129 | 300 | 128 | 300 |
| 2.222 | 0.010 | 5.131 | 217.76 | 135 | 300 | 149 | 300 | 148 | 300 |
| 1.701 | 0.020 | 5.723 | 333.39 | 206 | 500 | 229 | 500 | 227 | 500 |
| 1.957 | 0.020 | 6.066 | 383.66 | 237 | 500 | 263 | 600 | 261 | 600 |

These are assumed extrapolated values and could not be read off directly from the Maccaferri design graphs (see Annexure C, Figures C-1 and C-2)

- △ CSU study - Reno mattresses (CSU, 1984)
- This thesis - Reno mattresses (Stream Power theory)
- ◇ This thesis - Reno mattresses (Shield's theory)
- Maccaferri Reno mattresses (Maccaferri, 2004 & Papetti, 1985)

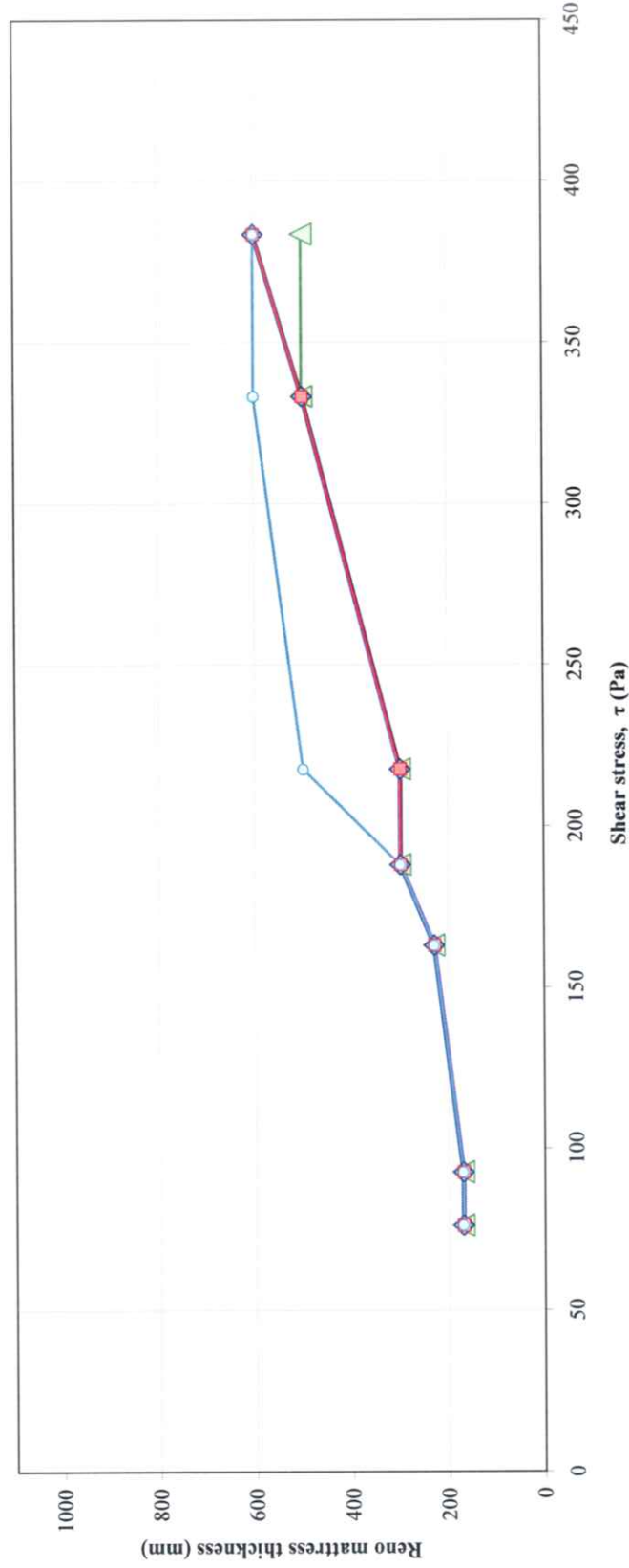


FIGURE 4.11: REQUIRED RENO MATTRESS THICKNESSES FOR TEST A

TABLE 4.13: RENO MATTRESSES: REQUIRED ROCK SIZE AND MATTRESS THICKNESS THAT WILL JUST RESIST MOTION (AT POINT OF MOTION INCIPIENCY) USING THE SLOPES, FLOW DEPTHS, VELOCITIES AND SHEAR STRESSES AS PER CSU TEST B

| Depth D (m) | Flume Slope S ₀ (m/m) | Velocity V (m/s) | Shear Stress τ (Pa) | Shield's Theory with θ = 0.100 (CSU study - Reno mattresses) | | Shield's Theory with θ = 0.090 (This thesis - Reno mattresses) | | Stream Power Theory with v*/v _{cs} = 0.165 (This thesis - Reno mattresses) | | Maccaferri's design criteria (Values obtained graphically from Maccaferri (2004) and Papetti (1985)) | |
|-------------------|---|------------------------|------------------------------|---|------------------------------------|---|------------------------------------|--|------------------------------------|---|------------------------------------|
| | | | | $d_{50} = \frac{\tau_0}{(\rho_s - \rho)g\theta}$ (mm) | Reno mattress thickness (mm) | $d_{50} = \frac{\tau_0}{(\rho_s - \rho)g\theta}$ (mm) | Reno mattress thickness (mm) | $d_{50} = \frac{D S_0}{5.75 (v^* / v_{cs})^2}$ (mm) | Reno mattress thickness (mm) | d_{50} (mm) | Reno mattress thickness (mm) |
| 1.884 | 0.004 | 3.310 | 73.831 | 46 | 170 | 51 | 170 | 50 | 170 | 59 | 170 |
| 2.387 | 0.004 | 3.965 | 93.510 | 58 | 170 | 64 | 170 | 64 | 170 | 81 | 170 |
| 1.728 | 0.010 | 4.530 | 169.352 | 105 | 230 | 116 | 230 | 115 | 230 | 102 | 230 |
| 1.993 | 0.010 | 4.656 | 195.351 | 121 | 300 | 134 | 300 | 133 | 300 | 106 | 300 |
| 2.094 | 0.010 | 5.058 | 205.263 | 127 | 300 | 141 | 300 | 140 | 300 | 120 | 300 |
| 1.975 | 0.015 | 5.622 | 290.442 | 179 | 500 | 199 | 500 | 198 | 500 | 140 | 500 |
| 1.701 | 0.020 | 6.156 | 333.390 | 206 | 500 | 229 | 500 | 227 | 500 | 159 | 600 |
| 1.993 | 0.020 | 6.203 | 390.847 | 241 | 500 | 268 | 600 | 266 | 600 | 161 | 600 |

These are assumed extrapolated values and could not be read off directly from the Maccaferri design graphs (see Annexure C, Figures C-1 and C-2)

- △ CSU study - Reno mattresses (CSU, 1984)
- ◇ This thesis - Reno mattresses (Shield's theory)
- This thesis - Reno mattresses (Stream Power theory)
- △ Maccaferri Reno mattresses (Maccaferri, 2004 & Papetti, 1985)

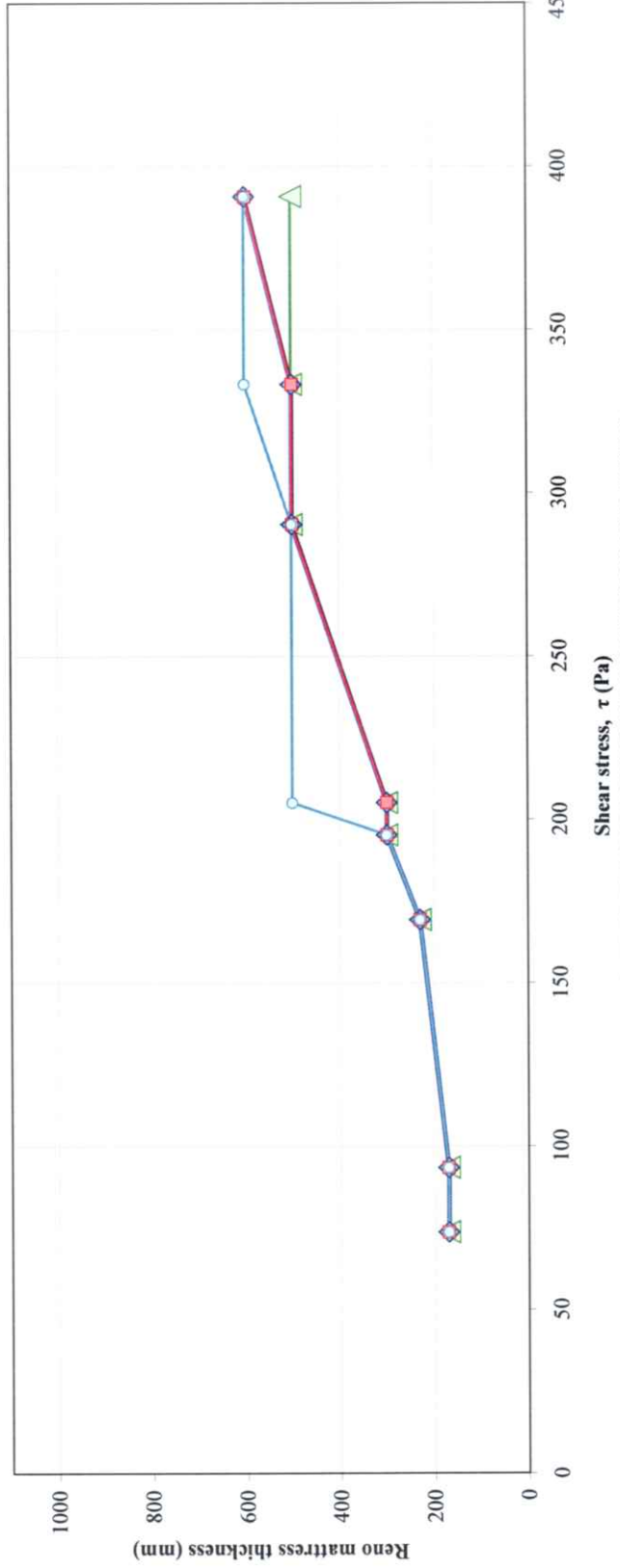


FIGURE 4.12: REQUIRED RENO MATTRESS THICKNESSES FOR TEST B

TABLE 4.14: RENO MATTRESSES: REQUIRED ROCK SIZE AND MATTRESS THICKNESS THAT WILL JUST REST MOTION (AT POINT OF MOTION INCIPIENCY) USING THE SLOPES, FLOW DEPTHS, VELOCITIES AND SHEAR STRESSES AS PER CSU TEST C

| Data converted to that of prototype 300 mm Mattress (Test C) | | Shield's Theory with $\theta = 0.100$ (CSU study - Reno mattresses) | | Shield's Theory with $\theta = 0.090$ (This thesis - Reno mattresses) | | Stream Power Theory with $v^*/v_{ss} = 0.165$ (This thesis - Reno mattresses) | | Maccaferri's design criteria (Values obtained graphically from Maccaferri (2004) and Papetti (1985)) | | | |
|--|-------------------------|---|--------------------------|---|------------------------------|---|------------------------------|--|------------------------------|---------------|------------------------------|
| Depth (m) | Flume Slope S_0 (m/m) | Velocity V (m/s) | Shear Stress τ (Pa) | $d_{50} = \frac{\tau_0}{(\rho_s - \rho)g\theta}$ (mm) | Reno mattress thickness (mm) | $d_{50} = \frac{\tau_0}{(\rho_s - \rho)g\theta}$ (mm) | Reno mattress thickness (mm) | $d_{50} = \frac{D S_0}{5.5 (v^*/v_{ss})^2}$ (mm) | Reno mattress thickness (mm) | d_{50} (mm) | Reno mattress thickness (mm) |
| 1.920 | 0.004 | 3.125 | 75.268 | 47 | 170 | 52 | 170 | 51 | 170 | 52 | 170 |
| 2.377 | 0.004 | 4.276 | 93.367 | 58 | 170 | 64 | 170 | 64 | 170 | 92 | 170 |
| 1.600 | 0.010 | 4.171 | 156.568 | 97 | 230 | 107 | 230 | 107 | 230 | 88 | 170 |
| 1.829 | 0.010 | 4.487 | 179.551 | 111 | 230 | 123 | 300 | 122 | 300 | 101 | 230 |
| 2.103 | 0.010 | 5.226 | 215.461 | 133 | 300 | 148 | 300 | 140 | 300 | 126 | 500 |
| 0.777 | 0.020 | 3.854 | 152.259 | 94 | 230 | 105 | 230 | 104 | 230 | 77 | 170 |
| 1.737 | 0.020 | 5.966 | 323.192 | 200 | 500 | 222 | 500 | 232 | 500 | 152 | 600 |
| 1.966 | 0.020 | 6.546 | 395.012 | 244 | 500 | 271 | 600 | 263 | 600 | 172 | 800 |
| xxxx | | | | | | | | | | | |

These are assumed extrapolated values and could not be read off directly from the Maccaferri design graphs (see Annexure C, Figures C-1 and C-2)

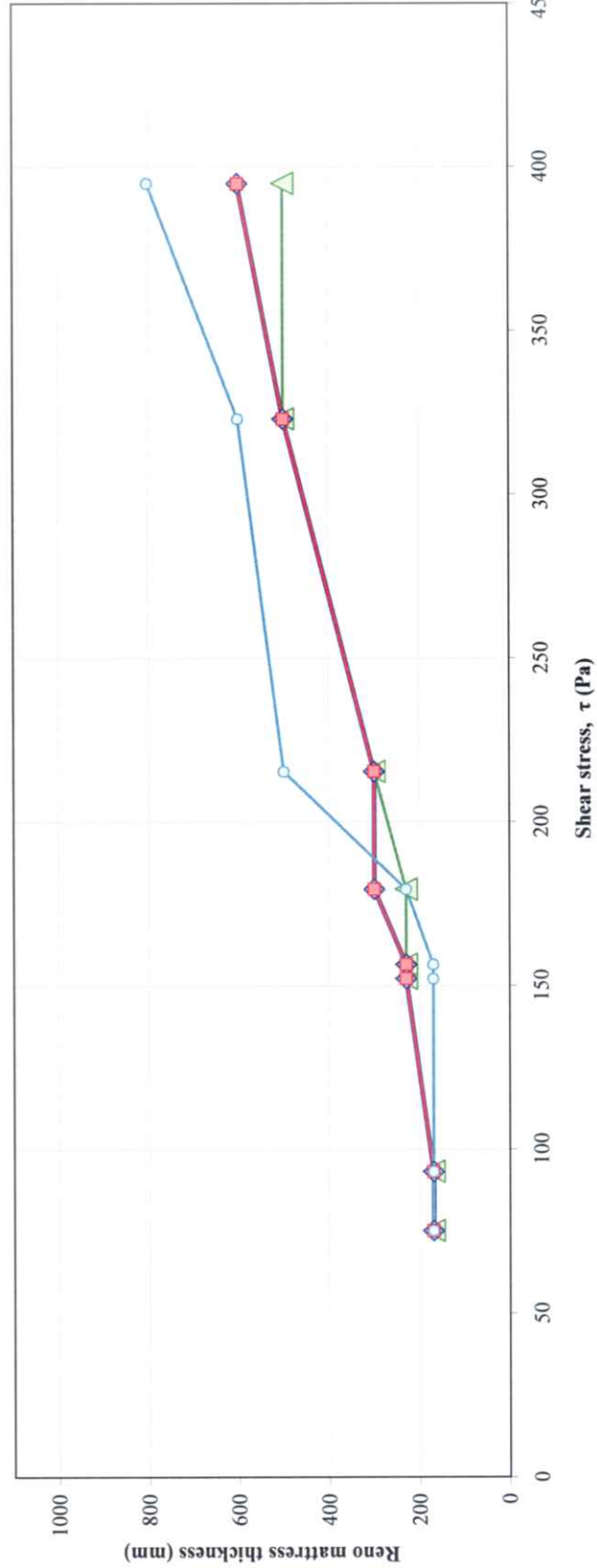


FIGURE 4.13: REQUIRED RENO MATTRESS THICKNESSES FOR TEST C

TABLE 4.15: RENO MATTRESSES: REQUIRED ROCK SIZE AND MATTRESS THICKNESS THAT WILL JUST RESIST MOTION (AT POINT OF MOTION INCIPENCY) USING THE SLOPES, FLOW DEPTHS, VELOCITIES AND SHEAR STRESSES AS PER CSU TEST D

| Data converted to that of prototype 450 mm Mattress (Test D) | | Shield's Theory with $\theta = 0.100$ (CSU study - Reno mattresses) | | Shield's Theory with $\theta = 0.090$ (This thesis - Reno mattresses) | | Stream Power Theory with $v^*/v_{ss} = 0.165$ (This thesis - Reno mattresses) | | Maccaferri's design criteria (Values obtained graphically from Maccaferri (2004) and Papetti (1985)) | | | |
|--|-------------------------|---|--------------------------|---|------------------------------|---|------------------------------|--|------------------------------|---------------|------------------------------|
| Depth D (m) | Flume Slope S_0 (m/m) | Velocity V (m/s) | Shear Stress τ (Pa) | $d_{50} = \frac{\tau_0}{(\rho_s - \rho)g\theta}$ (mm) | Reno mattress thickness (mm) | $d_{50} = \frac{\tau_0}{(\rho_s - \rho)g\theta}$ (mm) | Reno mattress thickness (mm) | $d_{50} = \frac{D S_0}{5.5 (v^*/v_{ss})^2}$ (mm) | Reno mattress thickness (mm) | d_{50} (mm) | Reno mattress thickness (mm) |
| 2.423 | 0.004 | 3.759 | 94.947 | 59 | 170 | 65 | 170 | 65 | 170 | 74 | 170 |
| 1.774 | 0.010 | 4.102 | 173.805 | 107 | 230 | 119 | 300 | 118 | 300 | 86 | 170 |
| 2.149 | 0.010 | 5.047 | 210.577 | 130 | 300 | 145 | 300 | 144 | 300 | 116 | 500 |
| 2.003 | 0.015 | 5.744 | 294.464 | 182 | 500 | 202 | 500 | 201 | 500 | 144 | 500 |
| 1.920 | 0.020 | 6.330 | 376.482 | 233 | 500 | 258 | 600 | 256 | 600 | 165 | 800 |
| xxx | | | | | | | | | | | |

These are assumed extrapolated values and could not be read off directly from the Maccaferri design graphs (see Annexure C, Figures C-1 and C-2)

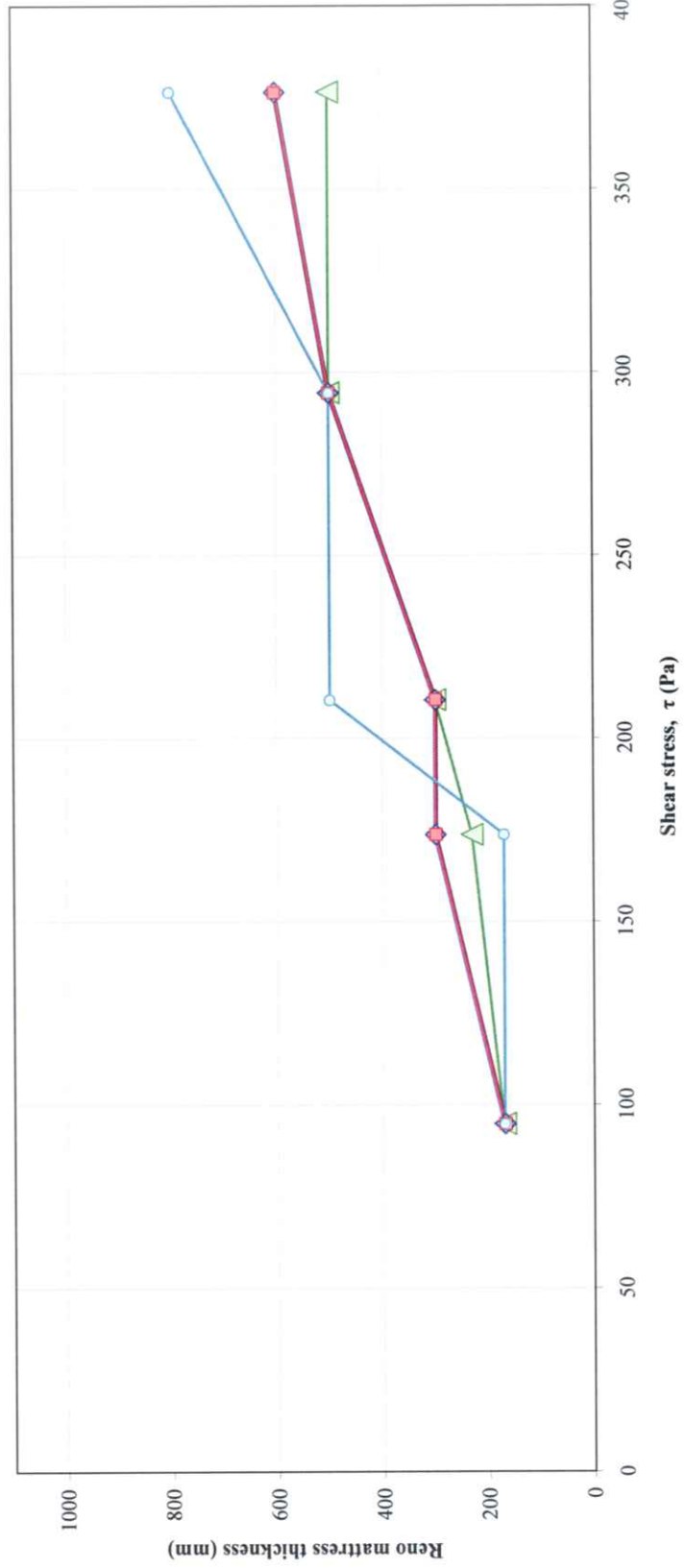


FIGURE 4.14: REQUIRED RENO MATTRESS THICKNESSES FOR TEST D

4.5 Reno Mattresses: Proposals Of This Thesis Versus Proposals By Maccaferri

The CSU study (CSU, 1984) used the Shield's theory, while this thesis used both the Shield's and stream power theories as mathematical background for determining rock sizes and Reno mattress thicknesses.

Maccaferri's design criteria are based on velocities and Froude numbers that are used to graphically determine rock sizes and Reno mattress thicknesses. The graphs and table utilised to determine these values are included as Figures C-1 and C-2 and Table C-1 in Annexure C (Maccaferri, 2004 and Papetti, 1985). In Figure C-1 velocities are used to read off applicable rock sizes to be used in Reno mattresses according to the value of the particular Froude number. In Figure C-2 velocities are also used to read off applicable Reno mattress thicknesses according to the value of the particular Froude number. Table C-1 gives indicative Reno mattress and gabion thicknesses in relation to flow velocities.

Comparative rock sizes to be used in Reno mattresses and Reno mattress thicknesses proposed in this thesis, by the CSU study and Maccaferri (2004), based on the test data used in CSU Tests A to D (CSU, 1984), are subsequently discussed.

- **Comparative proposed rock sizes to be used in Reno mattresses**

The comparative rock sizes proposed by the different methodologies, based on the test data used in CSU Tests A to D (CSU, 1984), are summarised in Table 4.16.

The relation of the rock sizes proposed for Reno mattresses by Maccaferri, obtained graphically (Maccaferri, 2004), to that proposed in this thesis, based on the Shield's and stream power theories, is shown in Figure 4.15.

Table 4.16: Comparative rock sizes for Reno mattresses obtained by applying Shield's theory, Stream Power theory and from Maccaferri's design graphs

| Flow velocity v (m/s) | Froude Number | Rock sizes for Reno mattresses: d_{50} (mm) | | | |
|-------------------------------|---------------|---|---|---|--|
| | | CSU Tests (CSU, 1984) | Shield's theory ($\theta = 0.090$) | Stream Power theory ($v^*/v_{ss} = 0.165$) | Maccaferri (values obtained graphically – see Annexure C) |
| Test A | | | | | |
| 3.748 | 0.85 | 47 | 52 | 53 | 70 * |
| 3.891 | 0.81 | 57 | 64 | 63 | 78 * |
| 4.577 | 1.13 | 101 | 112 | 111 | 103 |
| 4.762 | 1.10 | 116 | 129 | 128 | 110 |
| 5.131 | 1.10 | 135 | 149 | 148 | 124 |
| 5.723 | 1.40 | 206 | 229 | 227 | 145 |
| 6.066 | 1.38 | 237 | 263 | 261 | 156 |
| Test B | | | | | |
| 3.310 | 0.77 | 46 | 51 | 50 | 59 * |
| 3.965 | 0.82 | 58 | 64 | 64 | 81 |
| 4.530 | 1.10 | 105 | 116 | 115 | 102 |
| 4.656 | 1.05 | 121 | 134 | 133 | 106 |
| 5.058 | 1.12 | 127 | 141 | 140 | 120 |
| 5.622 | 1.28 | 179 | 199 | 198 | 140 |
| 6.156 | 1.51 | 206 | 229 | 227 | 159 |
| 6.203 | 1.40 | 241 | 268 | 266 | 161 |
| Test C | | | | | |
| 3.125 | 0.72 | 47 | 52 | 51 | 52 * |
| 4.276 | 0.89 | 58 | 64 | 64 | 92 |
| 3.854 | 1.05 | 94 | 105 | 104 | 88 |
| 4.171 | 1.06 | 97 | 107 | 107 | 101 |
| 4.487 | 1.15 | 111 | 123 | 122 | 126 |
| 5.226 | 1.40 | 133 | 148 | 140 | 77 |
| 5.966 | 1.45 | 200 | 222 | 232 | 152 |
| 6.546 | 1.49 | 244 | 271 | 263 | 172 |
| Test D | | | | | |
| 3.759 | 0.77 | 59 | 65 | 65 | 74 * |
| 4.102 | 0.98 | 107 | 119 | 118 | 86 |
| 5.047 | 1.10 | 130 | 145 | 144 | 116 |
| 5.744 | 1.30 | 182 | 202 | 201 | 144 |
| 6.330 | 1.46 | 233 | 258 | 256 | 165 |

* These are assumed extrapolated values and could not be read off directly from the design graphs (see Annexure C, Figure C-1)

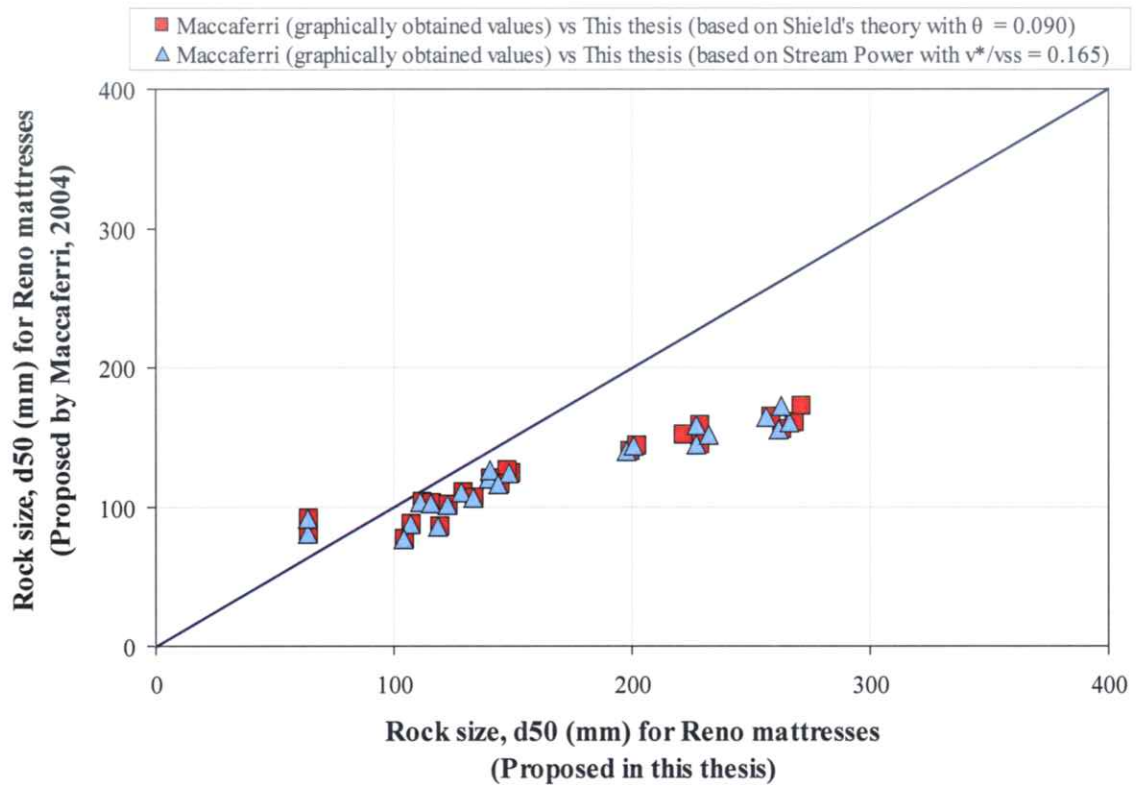


Figure 4.15: Rock sizes for Reno mattresses as proposed by Maccaferri, obtained graphically (Maccaferri, 2004), versus that proposed in this thesis, based on Shield's theory and Stream Power theory, for CSU Tests A to D (CSU, 1984)

From Table 4.16 and Figure 4.15 it can be seen that the rock sizes proposed for Reno mattresses in this thesis are more conservative than those proposed by Maccaferri (2004).

- **Comparative proposed Reno mattress thicknesses**

The comparative Reno mattress thicknesses proposed by the different methodologies, based on the test data used in CSU Tests A to D (CSU, 1984), are given in Table 4.17.

The relation of the Reno mattress thicknesses proposed by Maccaferri, obtained graphically (Maccaferri, 2004), to that proposed in this thesis, based on the Shield's and stream power theories, is shown in Figure 4.16.

Table 4.17: Comparative Reno mattress thicknesses obtained by applying Shield's theory, Stream Power theory and from Maccaferri's design graphs

| Flow velocity v (m/s) | Froude Number | Reno mattress thickness: t (mm) | | | |
|-------------------------------|---------------|-----------------------------------|---|---|--|
| | | CSU Tests (CSU, 1984) | Shield's theory ($\theta = 0.090$) | Stream Power theory ($v^*/v_{ss} = 0.165$) | Maccaferri (values obtained graphically – see Annexure C) |
| Test A | | | | | |
| 3.748 | 0.85 | 170 | 170 | 170 | 170 |
| 3.891 | 0.81 | 170 | 170 | 170 | 170 |
| 4.577 | 1.13 | 230 | 230 | 230 | 230 |
| 4.762 | 1.10 | 300 | 300 | 300 | 300 |
| 5.131 | 1.10 | 300 | 300 | 300 | 500 |
| 5.723 | 1.40 | 500 | 500 | 500 | 600 * |
| 6.066 | 1.38 | 500 | 600 | 600 | 600 * |
| Test B | | | | | |
| 3.310 | 0.77 | 170 | 170 | 170 | 170 |
| 3.965 | 0.82 | 170 | 170 | 170 | 170 |
| 4.530 | 1.10 | 230 | 230 | 230 | 230 |
| 4.656 | 1.05 | 300 | 300 | 300 | 300 |
| 5.058 | 1.12 | 300 | 300 | 300 | 500 |
| 5.622 | 1.28 | 500 | 500 | 500 | 500 |
| 6.156 | 1.51 | 500 | 500 | 500 | 600 * |
| 6.203 | 1.40 | 500 | 600 | 600 | 600 * |
| Test C | | | | | |
| 3.125 | 0.72 | 170 | 170 | 170 | 170 |
| 4.276 | 0.89 | 170 | 170 | 170 | 170 |
| 3.854 | 1.05 | 230 | 230 | 230 | 170 |
| 4.171 | 1.06 | 230 | 230 | 230 | 170 |
| 4.487 | 1.15 | 230 | 300 | 300 | 230 |
| 5.226 | 1.40 | 300 | 300 | 300 | 500 |
| 5.966 | 1.45 | 500 | 500 | 500 | 600 * |
| 6.546 | 1.49 | 500 | 600 | 600 | 800 * |
| Test D | | | | | |
| 3.759 | 0.77 | 170 | 170 | 170 | 170 |
| 4.102 | 0.98 | 230 | 300 | 300 | 170 |
| 5.047 | 1.10 | 300 | 300 | 300 | 500 |
| 5.744 | 1.30 | 500 | 500 | 500 | 500 |
| 6.330 | 1.46 | 500 | 600 | 600 | 800 * |

* These are assumed extrapolated values and could not be read off directly from the design graphs (see Annexure C, Figure C-2)

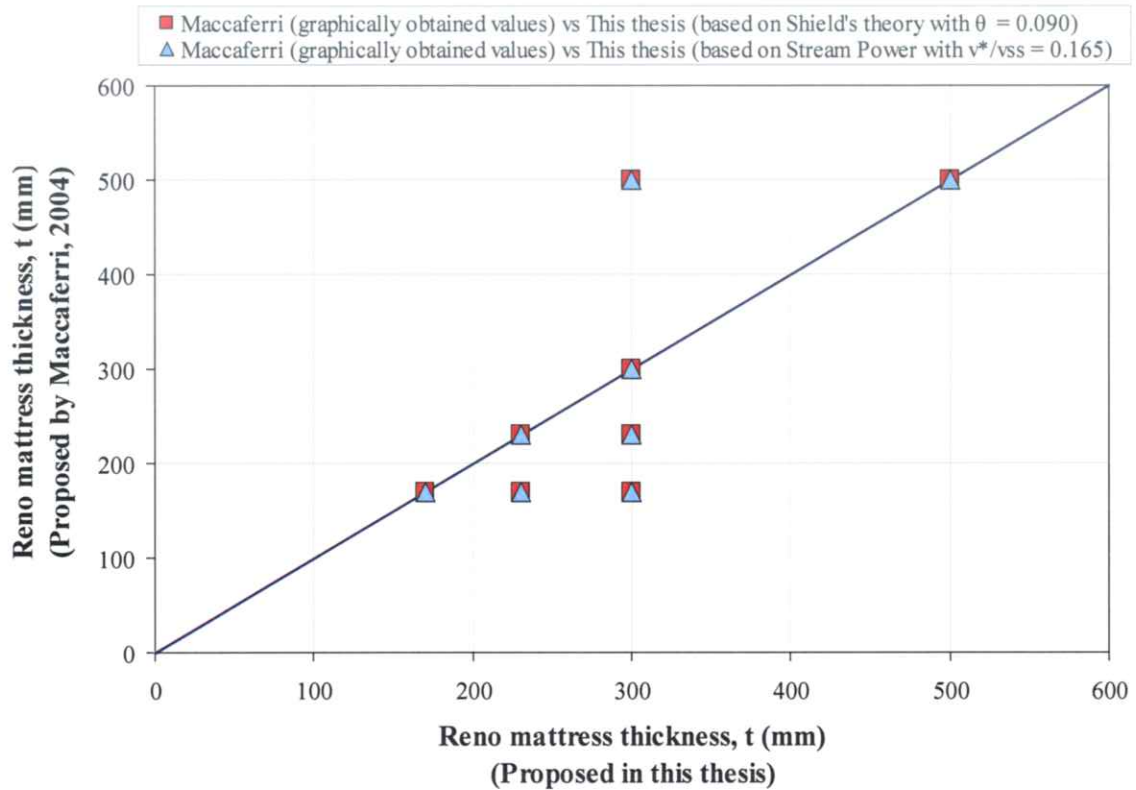


Figure 4.16: Reno mattress thicknesses as proposed by Maccaferri, obtained graphically (Maccaferri, 2004), versus that proposed in this thesis, based on Shield's theory and Stream Power theory, for CSU Tests A to D (CSU, 1984)

Table 4.17 and Figure 4.16 show a fairly good correlation between the proposed Reno mattresses in this thesis and that proposed by Maccaferri (2004).

4.6 Combination Of Results

A combination of results of all the methodologies used in this thesis for both the determination of required rip rap and Reno mattresses to just resist motion (at the point of motion incipency), based on the CSU test data of Tests A to D (CSU, 1984), is graphically shown in Figures D-1 to D-4 in Annexure D.

5. PARAMETER SENSITIVITY

Generally speaking, parameter sensitivity is defined as the rate of change of a selected variable with respect to change of a particular parameter. For a proper parameter sensitivity analysis, one variable needs to be varied at a time in order to evaluate its effect on a particular parameter, of which it is a function. Also, the parameter, which is a function of a few (more than one) variables, will be very sensitive to any possible changes of these variables.

Taking the above into account, the most critical variables in this research have been identified as the bed roughness, n or k (absolute roughness), the bed slope S_0 and the flow depth, D . The shape and size of the rock, d_{50} , used in rip rap and Reno mattresses and hydraulic radius determine the roughness of the channel. Parameters such as velocity, v , shear stress, τ , and Froude number, F , are specific parameters, which are functions of the variables n or k , S_0 and D .

From Manning's equation:

$$S_0 = \frac{v^2 n^2}{R^{\frac{4}{3}}} \quad (3.3)$$

and

$$\tau_0 = \rho g R S_0 = \rho g D S_0 \quad (2.10)$$

hence,

$$\tau_0 = \frac{\rho g v^2 n^2}{R^{\frac{1}{3}}} = \frac{\rho g v^2 n^2}{D^{\frac{1}{3}}} \quad (3.4)$$

Equation 3.4 indicates that, theoretically, for the same velocity, shear stress increases with decrease in hydraulic radius or depth. Shear stress is proportional to the velocity gradient and is the major factor that controls the stability of a Reno mattress or rip rap. Drag acting on a mattress or on rip rap is larger for a shallower depth with the same

average velocity, and vice versa, namely as the depth is increased for a given velocity, stability will be increased due to the reduction in shear stress.

The relations of parameters d_{50} / D , v , τ and F to one another, with respect to the CSU test data for Tests A to D, are shown in Figures 4.8, 5.1, 5.2 and 5.3 respectively. Figures E-1 to E-4 in Annexure E show additional relationships between different parameters applicable to the same CSU test data.

The test data are plotted and trend lines are drawn to give a linear relationship between the particular parameters. The R^2 value for each trend line is given. The R^2 value is an indication of the accuracy of the trend line, for the purpose it is intended. The closer the value is to 1, the more accurate the values that will be obtained by utilising the trend line. From the above and the given figures, it can be concluded that the R^2 values are such that the trend lines are considered to be accurate enough to read off the required parameter values.

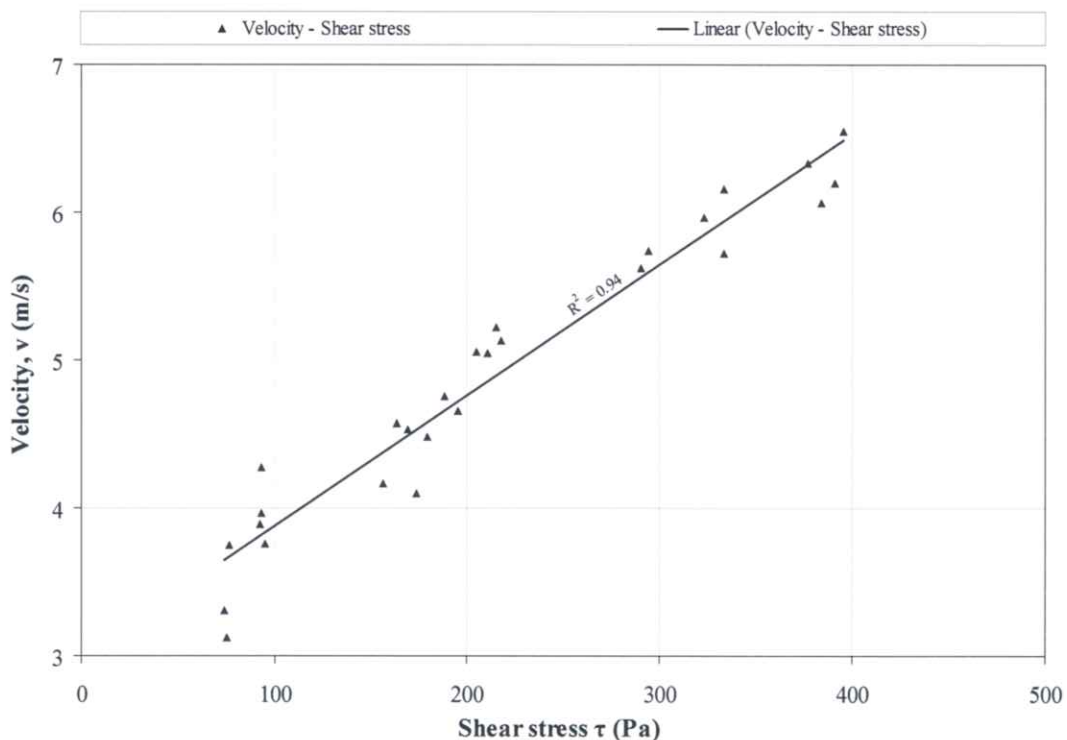


Figure 5.1: The relationship of flow velocity to bed shear stress for minimum conditions to just resist particle motion (at point of motion incipency) based on data of CSU tests A to D (see Tables 4.8 to 4.15 and Figures 4.4 to 4.7 & 4.11 to 4.14)

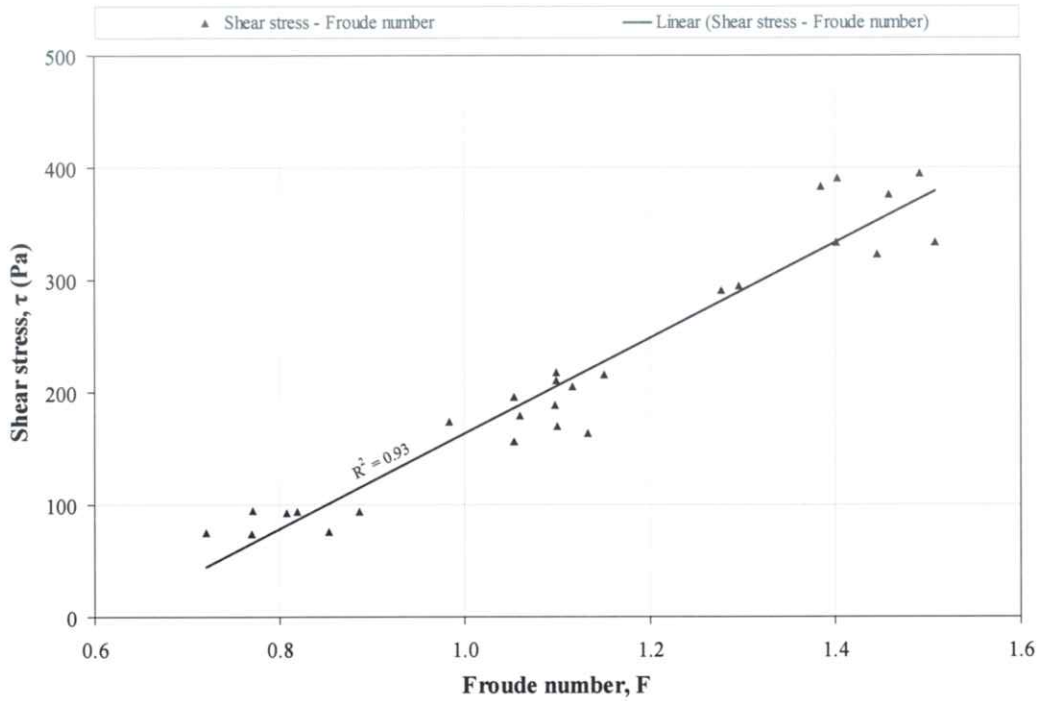


Figure 5.2: The relationship of bed shear stress to Froude number for minimum conditions to just resist particle motion (at point of motion incipency) based on data of CSU tests A to D (see Tables 4.8 to 4.15 and Figures 4.4 to 4.7 & 4.11 to 4.14)

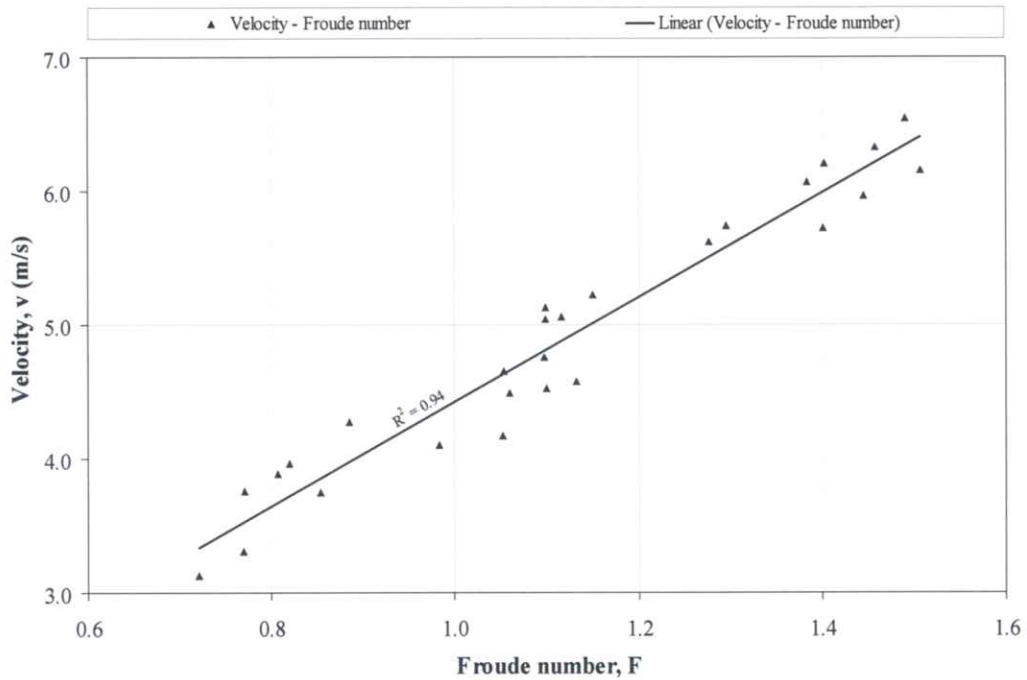


Figure 5.3: The relationship of flow velocity to Froude number for minimum conditions to just resist particle motion (at point of motion incipency) based on data of CSU tests A to D (see Tables 4.8 to 4.15 and Figures 4.4 to 4.7 & 4.11 to 4.14)

Although incipient motion can be described in terms of flow velocity, v , bed shear stress, τ_0 , and stream power, P , these parameters are related. Flow velocity and stream power can both be expressed in terms of the Movability number, v^*/v_{ss} .

From Equations 2.7, 2.10 and 2.20:

$$\begin{aligned} v_* &= \sqrt{gDS_0} \\ &= \sqrt{\frac{\tau_0}{\rho}} \end{aligned} \quad (5.1)$$

The Movability number is thus also proportional to the square root of the bed shear stress.

Up to this stage parameter sensitivity has been discussed and shown graphically on a theoretical basis. It is suggested that parameter sensitivity be investigated as part of laboratory testing to show the implications of changing one variable at a time and its effect on the particular parameter under investigation. Further studies and testing, over and above the theoretical discussion above, will thus be required. For example, it is difficult to predict the flow depth for a certain discharge and bed slope for a specific porosity of rock matrix used, as flow within the rock matrix will occur, and the flow depth has to be physically measured.

It must be kept in mind that the results and conclusions of this thesis are based on the CSU study data being used. The accuracy and calibration thereof thus depend on the accuracy of the CSU tests being done. The frame of reference of this thesis is set by the CSU study testing. The calibration achieved, proposals made and accuracy of conclusions can thus only be examined within those limits.

6. COST ANALYSIS

In this chapter a comparison is made between the costs of rip rap and Reno mattresses. Comparisons of costs are made between the various methodologies investigated, including this thesis, for the minimum required rip rap and Reno mattresses to just resist motion (at point of motion incipency), based on the CSU tests A to D (see Tables 4.8 to 4.15).

The rates used in the cost analysis are based on average tendered rates for rip rap and Reno mattresses by contractors in the Western Cape at the time of this thesis. The following assumptions have been made:

- It has been assumed that the underlying filter for Reno mattresses and rip rap are the same and are thus excluded from the unit costs.
- The unit cost of rock per cubic metre from the particular sources is the same for rip rap and Reno mattresses, irrespective of the gradation thereof, and is based on the cost per m³. It has been assumed that although larger rock sizes have greater voids, the number of voids are less than in the case of smaller rock with a greater number of voids, but which are smaller, resulting in the same percentage of voids in the respective rock matrixes.
- The source of the rock used in Reno mattresses and rip rap is the same and the transport cost per cubic metre will thus be the same. Transport costs have therefore been omitted from the unit rates.
- The main difference in unit cost between a Reno mattress and rip rap will be the wire mesh cages required for the Reno mattresses, and the way the rock is placed.
- The placing of the rock in the case of Reno mattresses is based on hand-packed labour methods. The rip rap can either be hand-packed or machine-placed. For the purpose of this study, rip rap is assumed to be placed by hand as in the case of Reno mattresses, wherever possible. Larger diameter rock will be placed by machine, as it is impractical to place it by hand.

The unit costs for Reno mattresses and rip rap are based on the cost per square metre (R/m²). The thickness of the respective layers, which are determined by the most sensitive factors as discussed in Chapter 5, will then mainly determine the actual cost per square metre. The unit costs, used in this thesis, are made up as follows:

- **Reno mattresses / gabions**

| | |
|---------------------------------------|---------------------------|
| Cost of rock hand-packed: | R 400.00 / m ³ |
| Wire mesh cage 1000 x 1000 x 170 mm: | R 530.00 / m ³ |
| Wire mesh cage 1000 x 1000 x 230 mm: | R 400.00 / m ³ |
| Wire mesh cage 1000 x 1000 x 300 mm: | R 380.00 / m ³ |
| Wire mesh cage 1000 x 1000 x 500 mm: | R 350.00 / m ³ |
| Wire mesh cage 1000 x 1000 x 1000 mm: | R 300.00 / m ³ |

- **Rip rap**

| | |
|-------------------------------------|---------------------------|
| Cost of rock hand-/ machine-packed: | R 425.00 / m ³ |
|-------------------------------------|---------------------------|

The unit costs used for comparison of costs are summarised in Table 6.1.

Table 6.1: Unit costs used in cost analysis

| Item description | Unit cost per m³ (excluding VAT) |
|---|--|
| Reno mattresses (filled with rock) | |
| 1000 x 1000 x 170 mm | R 930.00 |
| 1000 x 1000 x 230 mm | R800.00 |
| 1000 x 1000 x 300 mm | R780.00 |
| 1000 x 1000 x 500 mm | R750.00 |
| 1000 x 1000 x 1000 mm | R700.00 |
| Rip rap | |
| Rock hand-/ machine-packed | R425.00 |

The comparative costs for rip rap and Reno mattresses between the different methods used in Tables 4.8 to 4.15 and Figures 4.4 to 4.7 and 4.11 to 4.14, have been calculated for the minimum required layer thicknesses required to just resist motion (at point of motion incipency), based on the data as per CSU tests A to D. These comparative costs are shown in Figures F-1 to F-4 in Annexure F, and reflect the difference in cost for each option.

The comparative costs per m² between Reno mattresses and rip rap, based on layer thicknesses obtained from Tables 4.8 to 4.15 and Figures 4.4 to 4.7 and 4.11 to 4.14 as per data used in tests A to D in the CSU study, are shown in Figure 6.1.

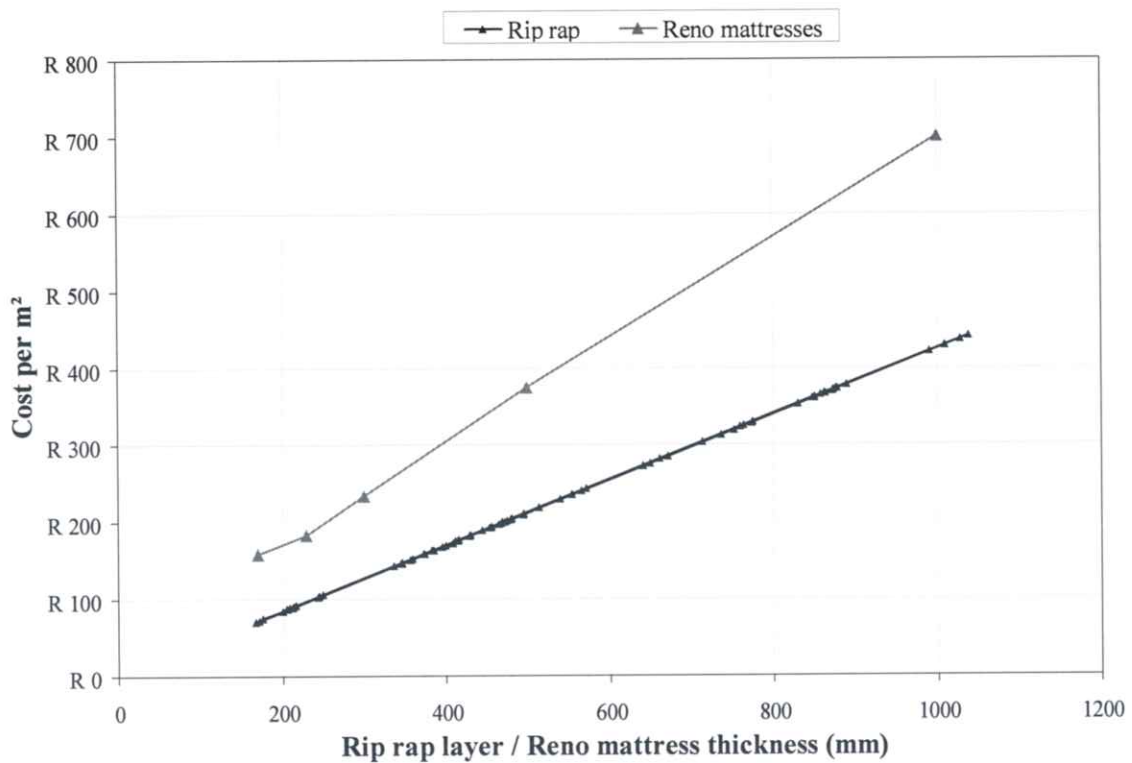


Figure 6.1: Cost comparison between rip rap and Reno mattresses, based on the layer thicknesses proposed in Tables 4.8 to 4.15 and Figures 4.4 to 4.7 and 4.11 to 4.14

Figure 6.1, as well as Figures F-1 to F-4 (see Annexure F), indicate that rip rap generally appears to be the more economical viable option for erosion protection of channel or river beds, based on the data used from the CSU study.

7. SUMMARY OF RESULTS

In this thesis the results of the CSU study, with respect to motion incipency of rock in Reno mattresses and rip rap, have been evaluated mainly in terms of the stream power theory and in terms of Shield's theory (shear stress). The results and suggestions of this thesis can be summarised as follows:

- In terms of stream power, the Movability number, v^*/v_{ss} , suggested for design of Reno mattresses = 0,165 and that for rip rap = 0,130 (within the reference framework of this thesis).
- In terms of shear stress, the Shield's parameter, θ , recommended for the design of Reno mattresses = 0,090 and that for rip rap = 0,056 (within the reference framework of this thesis). This thesis is in agreement with the Shield's parameter value of 0,056 as recommended for design purposes by Rooseboom (SANRAL, 1997) and Henderson (1966), but not with the value of 0,047 recommended by the CSU study for the design of rip rap.
- Finer testing intervals in the CSU study could have resulted in more accurate values recommended above for the Movability number, v^*/v_{ss} , and Shield's parameter, θ .
- In the case of rip rap, layer thicknesses are based on 2 times the required or designed mean rock diameter, but never less than 200 mm (see paragraph 4.4.1).
- In the case of Reno mattresses, mattress or layer thicknesses are based on 2 times the designed or required mean rock diameter, complying with at least 1,5 to 2 times the mass of the designed or required mean rock diameter per unit area (SANRAL, 1997), with the mattress thicknesses then rounded up to the applicable standard mattress thicknesses, namely 170 mm, 230 mm, 300 mm or 500 mm.
- The wire mesh cages used in Reno mattresses contribute to the stability of rock in mattresses, as can be seen from the recommended design values for the Movability numbers in terms of stream power and Shield's parameters in terms of shear stress. The effect thereof is however considered not to be as significant as suggested by the CSU study.

- From a cost point of view, rip rap (according to all the different methods investigated) appears to be more economical than Reno mattresses, especially for smaller rock sizes ($d_{50} < 100$ mm) and where larger layer thicknesses (Reno mattresses > 300 mm) are required, namely at higher flow conditions (see Figures 6.1 and 7.1, Tables 7.1 and 7.2, as well as Figures F-1 to F-4 in Annexure F). For proposed layer thicknesses in excess of 300 mm, Reno mattresses pose a high risk in the sense that, should the wire mesh fail as a result of fire, erosion or impact, etc., the rock will be moved or even removed from the mattress and the mattress could fail with the result of possible erosion and further damage.

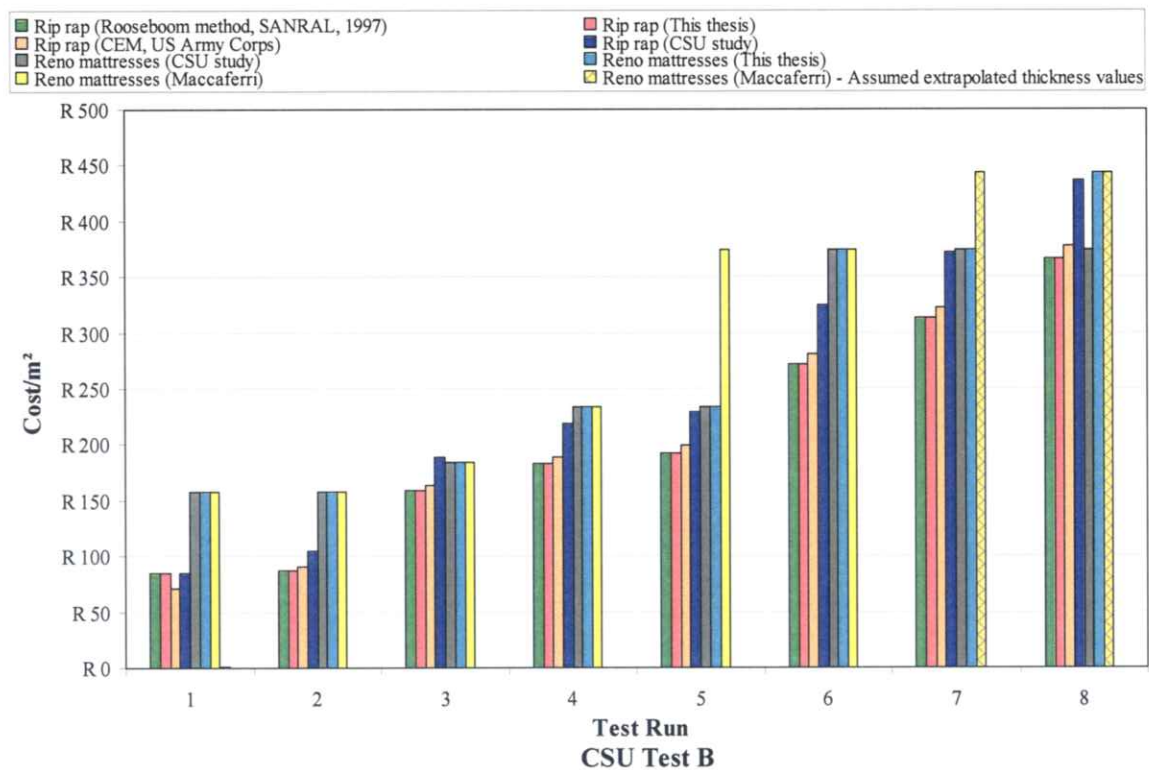


Figure 7.1: Comparative costs for rip rap and Reno mattresses for minimum required layer thicknesses to just resist motion (at incipient motion condition) as per CSU Test B (see Tables 3.5, 4.2, 4.9 and 4.13, as well as Figures 4.5 and 4.12)

Table 7.1: Comparative minimum required layer thickness, r , and cost per m^2 for rip rap to just resist motion (at incipient motion condition) as per CSU Test B

| Test run no. | Flow velocity v (m/s) | Rooseboom method (SANRAL, 1997) | | CSU study (CSU, 1984) | | This thesis | | CEM (Burcharth & Hughes, 2003) | |
|--------------|-------------------------|---------------------------------|-----------------|-----------------------|-----------------|-------------|-----------------|--------------------------------|-----------------|
| | | r (mm) | Cost/ m^2 (R) | r (mm) | Cost/ m^2 (R) | r (mm) | Cost/ m^2 (R) | r (mm) | Cost/ m^2 (R) |
| 1 | 3.310 | 200 | 85.00 | 20 | 85.00 | 200 | 85.00 | 200 | 85.00 |
| 2 | 3.965 | 207 | 87.98 | 246 | 104.55 | 206 | 87.55 | 213 | 90.53 |
| 3 | 4.530 | 374 | 158.95 | 445 | 189.13 | 374 | 158.95 | 386 | 164.05 |
| 4 | 4.656 | 431 | 183.18 | 514 | 218.45 | 431 | 183.18 | 445 | 189.13 |
| 5 | 5.058 | 453 | 192.53 | 540 | 229.50 | 453 | 192.53 | 468 | 198.90 |
| 6 | 5.622 | 641 | 272.43 | 764 | 324.70 | 641 | 272.43 | 662 | 281.35 |
| 7 | 6.156 | 736 | 312.80 | 876 | 372.30 | 736 | 312.80 | 760 | 323.00 |
| 8 | 6.203 | 863 | 366.78 | 1028 | 436.90 | 862 | 366.78 | 890 | 378.25 |

Table 7.2: Comparative minimum required thicknesses, t , and cost per m^2 for Reno mattresses to just resist motion (at incipient motion condition) as per CSU Test B

| Test run no. | Flow velocity v (m/s) | CSU study (CSU, 1984) | | This thesis | | Maccaferri (Maccaferri, 2004 & Papetti, 1985) | |
|--------------|-------------------------|-----------------------|-----------------|-------------|-----------------|---|-----------------|
| | | t (mm) | Cost/ m^2 (R) | t (mm) | Cost/ m^2 (R) | t (mm) | Cost/ m^2 (R) |
| 1 | 3.310 | 170 | 158.10 | 170 | 158.10 | 170 | 158.10 |
| 2 | 3.965 | 170 | 158.10 | 170 | 158.10 | 170 | 158.10 |
| 3 | 4.530 | 230 | 184.00 | 230 | 184.00 | 230 | 184.00 |
| 4 | 4.656 | 300 | 234.00 | 300 | 234.00 | 300 | 234.00 |
| 5 | 5.058 | 300 | 234.00 | 300 | 234.00 | 500 | 375.00 |
| 6 | 5.622 | 500 | 375.00 | 500 | 375.00 | 500 | 375.00 |
| 7 | 6.156 | 500 | 375.00 | 500 | 375.00 | 600 * | 444.00 |
| 8 | 6.203 | 500 | 375.00 | 600 | 444.00 | 600 * | 444.00 |

* These are assumed extrapolated values and could not be read off directly from the design graphs (see Annexure C, Figure C-2)

- The risk with respect to durability and failure when applying Reno mattresses are much higher than when applying rip rap. Some reasons for this statement are as follows:
 - During high flow conditions debris such as trees, branches, etc. can rip gabion structures apart and could cause failure and severe erosion as a result thereof.
 - Corrosive environments, such as coastal conditions or aggressive soils, could cause corrosion and eventual failure of Reno mattresses.
 - Veld fires could damage the PVC coatings and galvanising of the wire mesh of Reno mattresses, which could lead to short or long term failure.
 - Abrasion of the gabion wire mesh in sediment laden streams with high bed loads could lead to damage, corrosion and / or eventual failure of Reno mattresses.
 - Vandalism is another aspect that could lead to damage and / or failure of Reno mattresses.

8. CONCLUSIONS AND RECOMMENDATIONS

At the conclusion of both the CSU study and this thesis the same question can be asked, namely: “What exactly is the definition of failure of a Reno mattress?”. In the CSU study, it was accepted that even though rock in a Reno mattress had been moved, the mattress would still be serviceable. In this thesis that view point is opposed. This thesis considers two modes of failure, namely serviceability failure and limit state failure, together with the purpose of the Reno mattress. It can be debated that failure occurs as soon as rock starts moving. For example, in the case where a gabion or Reno mattress has been used to protect a pipe, any movement of the gabion or Reno mattress can result in the failure of the pipe, causing failure of the system or failure of the purpose it was intended for. Another example is the case where Reno mattresses have the purpose to protect the underlying ground against erosion. The movement of rock in the mattress to the lower end of the mattress compartment will cause the upper end to be only partly filled. The remaining rock can move more easily because of no support and / or friction previously contributed by the rock that has been moved. Finer particles can also be washed out and the whole system could fail structurally, as well as in the sense of serviceability. Because smaller rock is required for Reno mattresses than for rip rap according to all the methods investigated, except that of the Rooseboom methodology (SANRAL, 1997), the chances of movement of the rock, in the case of damage to the wire mesh, are higher.

This thesis shows that the use of rip rap is economically more beneficial than the use of Reno mattresses and that the risk with respect to durability and / or failure is much lower in the case of rip rap than in the case of Reno mattresses.

It must be reiterated that the results and conclusions of this thesis are based on the CSU study data being used. The accuracy and calibration thereof thus depend on the accuracy of the CSU tests being done. The frame of reference of this thesis is set by the CSU study testing. The calibration achieved, proposals made and accuracy of conclusions in this thesis can thus only be made within those limits.

This thesis concludes with the following recommendations:

- For the design of mean rock size, to be used in rip rap and Reno mattresses, in terms of stream power, the applicable recommended Movability numbers are as follows:

Table 8.1: Recommended Movability number, v^*/v_{ss} , for design of mean rock size

| Design In Terms Of Stream Power | |
|--|---|
| Revetment used | Recommended Movability number, v^*/v_{ss} |
| Rip rap | 0,130 |
| Reno mattress | 0,165 |

- For the design of mean rock size, to be used in rip rap and Reno mattresses, in terms of Shield's parameter (shear stress), the applicable recommended Shield's parameters are as follows:

Table 8.2: Recommended Shield's parameter, θ , for design of mean rock size

| Design In Terms Of Shield's Parameter | |
|--|---|
| Revetment used | Recommended Shield's parameter, θ |
| Rip rap | 0,056 [Rooseboom method (SANRAL, 1997), Henderson (1966) & this thesis] |
| Reno mattress | 0,090 |

- Approximately the same mean rock diameter sizes are obtained by using the Shield's parameters, θ , and Movability numbers, v^*/v_{ss} , as recommended in this thesis. Application of the Shield's theory or the Stream power theory, with the design values as suggested in this thesis is recommended for design purposes based on the CSU test data (CSU, 1984).
- The layer thicknesses for rip rap should be at least 2 times the designed mean rock diameter, but never less than 200 mm.

- The layer thicknesses for Reno mattresses should be calculated so that the mattress thicknesses are at least 2 times the designed mean rock diameter (based on at least 1,5 to 2 times the mass of the designed or required mean rock diameter per unit area) with the thicknesses then rounded up to the applicable standard mattress thicknesses, namely 170 mm, 230 mm, 300 mm or 500 mm.

In the event of high flow conditions and required mattress thicknesses of 500 mm or more when using the above method, it is recommended that the Rooseboom method (SANRAL, 1997) for the design of gabions mattresses be applied. The proposals in the Rooseboom method (SANRAL, 1997) are considered to be the safer option with regard to gabion design under high flow conditions, whereby it is suggested that a layer thickness of 2 times the required rock size diameter, as determined for rip rap, is used.

- The nominal wire mesh aperture size generally used is 80 mm x 100 mm. It is thus recommended that rock used in Reno mattresses and gabions should never be smaller than 100 mm in diameter in order to prevent it from being removed from the mattresses.
- Although the wire mesh of Reno mattresses contributes to the stability of the rock in the mattresses, this thesis has shown that rip rap is still the more economical and durable option of the two. Rip rap is thus recommended above Reno mattresses where practically feasible.
- It is recommended that further research be done in this field to provide more accurate and reliable findings on the use of Reno mattresses and rip rap, namely:
 - Finer intervals should be used during testing to more accurately define the point of incipient motion of particles.
 - The study should be extended to include the investigation of motion incipency around bends in channels, on channel side slopes, and on very steep longitudinal slopes.

9. REFERENCES

1. Armitage, Neil P. (2002). A Unit Stream Power Model for the Prediction of Local Scour (Thesis for the degree of Doctor of Philosophy, University of Stellenbosch).
2. Armitage, Neil and Caroline McGahey (2003). WRC Report No. 1098/1/03, A Unit Stream Power Model for the Prediction of Local Scour in Rivers, Cape Town.
3. Burcharth, Hans F. and Steven A. Hughes (2003). Draft Fundamentals of Design, Chapter 5, Coastal and Engineering Manual (EM 1110-2-1100), U.S. Army Corps of Engineers, Washington, D.C.
4. Chadwick, Andrew and John Morfett (1998). Hydraulics in Civil and Environmental Engineering, 3rd Edition, E & FN SPON.
5. Chow, Ven Te (1959). Open-Channel Hydraulics, International Student Edition, McGraw-Hill.
6. Course Notes (2003). Floods and Stormwater 2003, Volume 1: River Flows: 2 - 4 April 2003: Institute of Water and Environmental Engineering: Department of Civil Engineering University of Stellenbosch.
7. CSU (1984). Hydraulic Test To Develop Design Criteria For The Use Of Reno Mattresses, Prepared by the Civil Engineering Department, Engineering Research Centre, Colorado State University, Fort Collins, Colorado.
8. Henderson, F.M. (1966). Open channel Flow, Macmillan.
9. Maccaferri (2004). Brochures on African Gabions Environmental Solutions.

10. Papetti, Andrea (1985). Flexible Linings in Reno Mattress and Gabions for Canals and Canalised Water Courses, Maccaferri, Bologna.
11. Rooseboom, A (1992). Water Research Commission Report No. 297/1/92, Sediment Transport in Rivers and Reservoirs – A Southern African Perspective, Pretoria.
12. Rooseboom, A (1974). Technical Report No. 62, Open Channel Fluid Mechanics, Department of Environment Affairs, Pretoria.
13. SANRAL (1997). Road Drainage Manual, Fourth Print of 1986 Version, Pretoria (First edition published by the former National Transport Commission, 1981).
14. Simons, Daryl B. and Fuat Şentürk (1977). Sediment Transport Technology, Water Resources Publications, Fort Collins, Colorado 80522, USA.
15. Simpson, Richard (1997). Critical Hydraulic Conditions for the Mobilisation of Sediments in a Cape River (Thesis for the degree of Master of Engineering, University of Stellenbosch).
16. U.S. Army Corps of Engineers (1984). Drainage and erosion control, Chapter 14, Engineering Manual (EM) No. 1110-3-136, Washington, D.C.

ANNEXURES

ANNEXURE A

**Table A-1: Dimensions of Model-Scale and Full-Scale
Mattresses Tested in CSU Study**

Table A-1: Dimensions of Model-Scale and Full-Scale Mattresses Tested in CSU Study

| Test | Prototype | | | | | Model | | | | | | |
|--------------------------|------------------------|----------------|----------------|---------------------------|------------------------|----------------|----------------|---------------------------|------------------------|----------------|----------------|---------------------------|
| | Nominal Thickness (mm) | Mesh type (mm) | Wire Dia. (mm) | Nominal Filling Rock (mm) | Nominal Thickness (mm) | Mesh type (mm) | Wire Dia. (mm) | Nominal Filling Rock (mm) | Nominal Thickness (mm) | Mesh type (mm) | Wire Dia. (mm) | Nominal Filling Rock (mm) |
| 1,22 m Flume | | | | | | | | | | | | |
| A | 150 | 60 x 80 | 2 – 2.2 | 75 – 150 | 50 | 19.5 – 31.75 | 0.6 – 0.7 | 25 – 50 | | | | |
| B | 230 | 60 x 80 | 2 – 2.2 | 75 – 150 | 75 | 19.5 – 31.75 | 0.6 – 0.7 | 25 – 50 | | | | |
| C | 300 | 60 x 80 | 2 – 2.2 | 100 – 150 | 100 | 19.5 – 31.75 | 0.6 – 0.7 | 38 – 50 | | | | |
| D | 450 | 80 x 100 | 2.4 – 2.7 | 100 – 200 | 150 | 25.4 – 38.1 | 0.8 – 0.9 | 38 – 63.5 | | | | |
| 2,44 m Flume | | | | | | | | | | | | |
| | 230 | 80 x 100 | 2.4 – 2.7 | 75 – 150 | 75 | 25.4 – 38.1 | 0.8 – 0.9 | 38 – 50 | | | | |
| Outdoor Prototype | | | | | | | | | | | | |
| | 150 | 60 x 80 | 2 | 75 – 150 | - | - | - | - | | | | |
| | 230 | 60 x 80 | 2 | 75 – 150 | - | - | - | - | | | | |

ANNEXURE B

Relationship between Reno Mattress Thickness and Rock Particle Diameter

Relationship between Reno Mattress Thickness and Rock Particle Diameter

According to Rooseboom (SANRAL, 1997), the mass of an individual gabion or Reno mattress must be at least 1,5 to 2 times that of the median rock particle diameter calculated.

The following explanation is proof that a minimum required mattress thickness of 2 times the median rock particle diameter will fall within the range of the required minimum required mass for a Reno mattress, namely at least 1,5 to 2.0 times that of the mean rock diameter calculated (SANRAL, 1997).

The assumed porosity, λ , of the rock matrix in Reno mattresses is 0,45 (see paragraph 4.2).

Assume the Reno mattress thickness = t

$$\begin{aligned} \text{Thus, the volume of Reno mattress per m}^2: \quad \text{Volume / m}^2 &= 1 \times 1 \times t \times (1-0,45) \\ &= 0,55 t \end{aligned} \quad (\text{B.1})$$

$$\text{The projected area of a rock particle:} \quad A = \frac{\pi d^2}{4}$$

$$\begin{aligned} \text{The number of particles per m}^2: \quad \text{No / m}^2 &= \left(\frac{1 \times 1}{\frac{\pi d^2}{4}} \right) \\ &= \frac{4}{\pi d^2} \end{aligned}$$

$$\begin{aligned} \text{The volume of this number of particles per m}^2: \quad \text{Volume / m}^2 &= \frac{4}{\pi d^2} \times \frac{\pi d^3}{6} \\ &= \frac{2 d}{3} \end{aligned}$$

$$\text{The mass of the volume of particles per m}^2: \quad \text{Mass / m}^2 = \frac{2 d (2650)}{3} \quad (\text{B.2})$$

- **1,5 times the mass of Reno mattress**

$$\text{from (B.2): } 1,5 \times \text{Mass} / \text{m}^2 = \frac{1,5[2d(2650)]}{3} = 2650d$$

$$\therefore \text{Volume of } (1,5 \times \text{mass}) / \text{m}^2 = d \quad (\text{B.3})$$

$$\text{Set (B.1) = (B.3): } 0,55t = d$$

$$\therefore t = 1,818d \quad (\text{B.4})$$

- **2 times the mass of Reno mattress**

$$\text{from (B.2): } 2 \times \text{Mass} / \text{m}^2 = \frac{2[2d(2650)]}{3} = \frac{4d(2650)}{3}$$

$$\therefore \text{Volume of } (2 \times \text{mass}) / \text{m}^2 = \frac{4d}{3} \quad (\text{B.5})$$

$$\text{Set (B.1) = (B.5): } 0,55t = \frac{4d}{3}$$

$$\therefore t = 2,424d \quad (\text{B.6})$$

$$\text{From (B.4) and (B.6): } 1,818d < 2d < 2,424d \quad (\text{B.7})$$

ANNEXURE C

**Maccaferri Design Criteria for revetments using Reno
Mattresses (Maccaferri, 2004 and Papetti, 1985)**

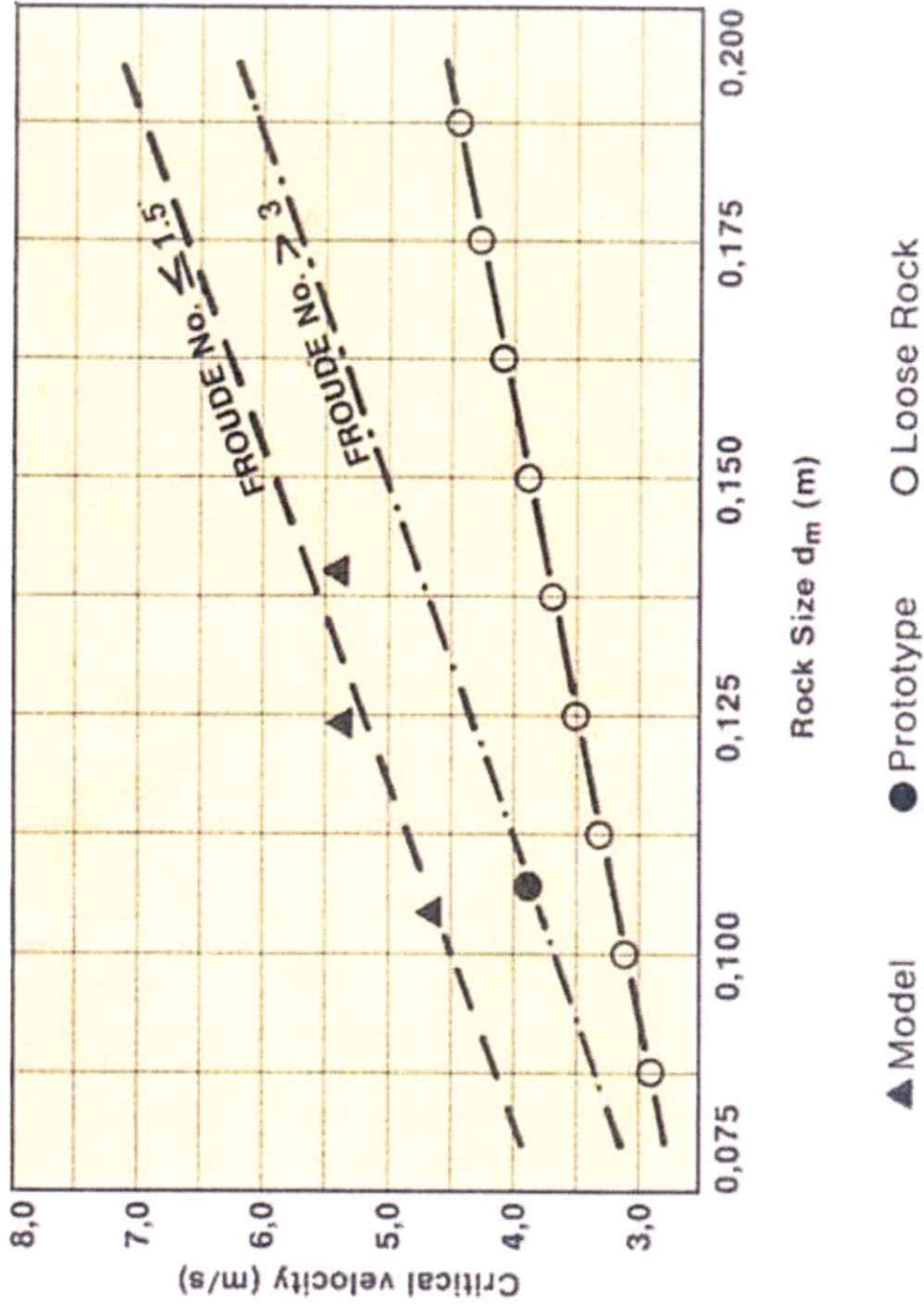


Figure C-1: Critical velocity that initiates rock movement as a function of rock size (CSU, 1984; Maccaferri, 2004 and Papetti, 1985)

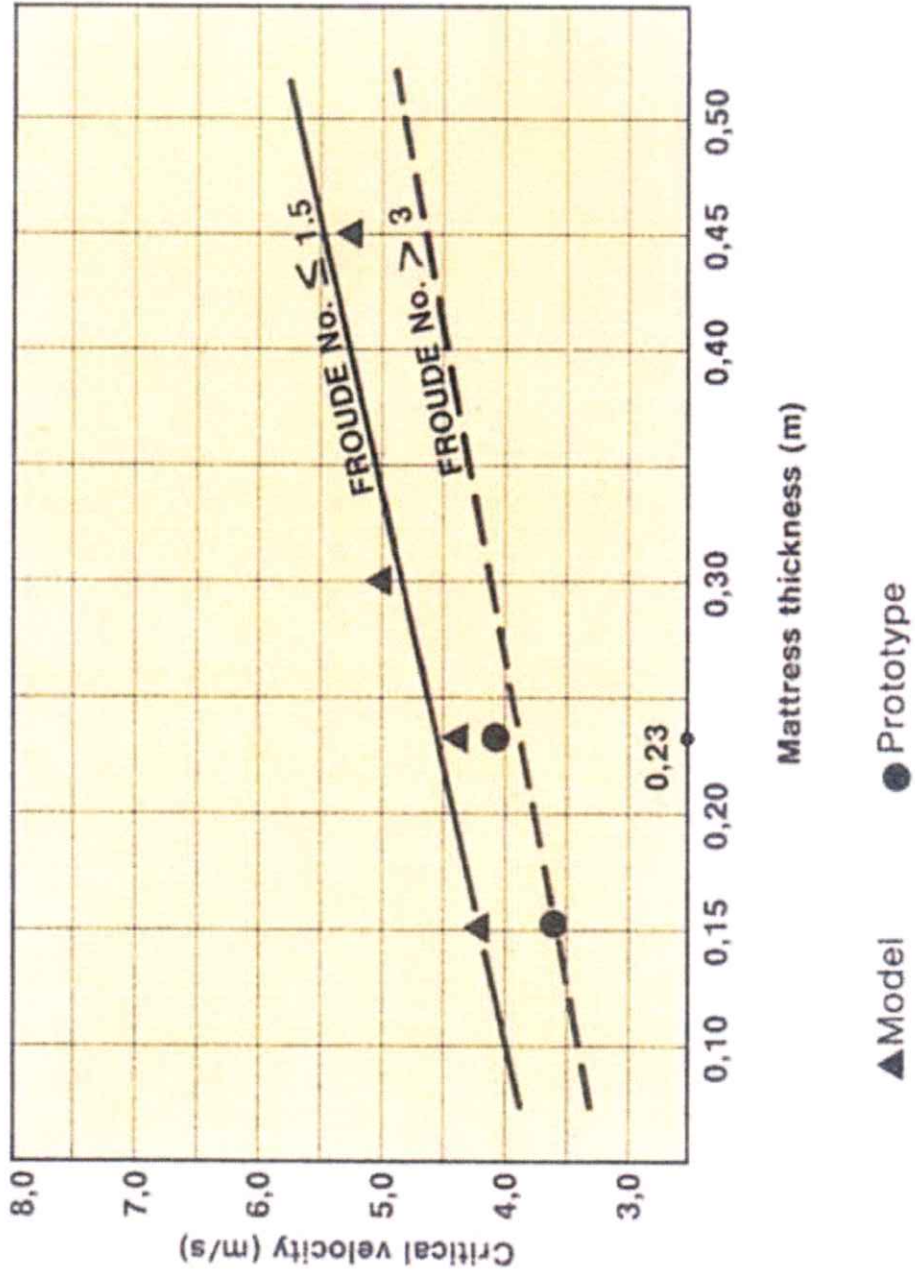


Figure C-2: Critical velocity that initiates rock movement as a function of Reno mattress thickness (CSU, 1984; Maccaferri, 2004 and Papetti, 1985)

| Type Type Tipo | Thickness Epaisseur Espesor m | Filling stones Pierraille de remplissage Pedrisco de relleno | | Critical velocity (*) Vitesse critique (*) Velocidad crítica (*) m/s | Limit velocity (*) Vitesse limite (*) Velocidad límite (*) m/s |
|---|--|--|-----------------|---|---|
| | | Stone size Granulométrie Dimensiones mm | d ₅₀ | | |
| Reno mattresses Matelas Reno Colchones Reno | 0.15-0.17 | 70-100 | 0.085 | 3.5 | 4.2 |
| | | 70-150 | 0.110 | 4.2 | 4.5 |
| | 0.23-0.25 | 70-100 | 0.085 | 3.6 | 5.5 |
| | | 70-150 | 0.120 | 4.5 | 6.1 |
| | 0.30 | 70-120 | 0.100 | 4.2 | 5.5 |
| | | 100-150 | 0.125 | 5.0 | 6.4 |
| 0.50 | 100-200 | 0.150 | 5.8 | 7.6 | |
| | 120-250 | 0.190 | 6.4 | 8.0 | |

(*) The values of velocity reported were obtained experimentally for Froude numbers ≤ 1 (see page 33); values > 1 are intended as purely indicative and approximated.

(*) Les valeurs des vitesses indiquées sont tirées expérimentalement des nombres de Froude ≤ 1 (voir page 33); les valeurs > 1 sont purement indicatives.

(*) Los valores de velocidad indicados han sido calculados experimentalmente para números de Froude ≤ 1 (pág. 33); para valores > 1 , deben considerarse como puramente indicativos y muy en general.

Table C-1: Indicative Reno mattress and gabion thicknesses in relation to water velocities
(CSU, 1984; Maccaferri, 2004 and Papetti, 1985)

ANNEXURE D

Figures D-1 to D-4: Comparison of Rip Rap Layer and Reno Mattress Thicknesses between Various Methods Used for CSU Tests A to D to Just Resist Particle Motion

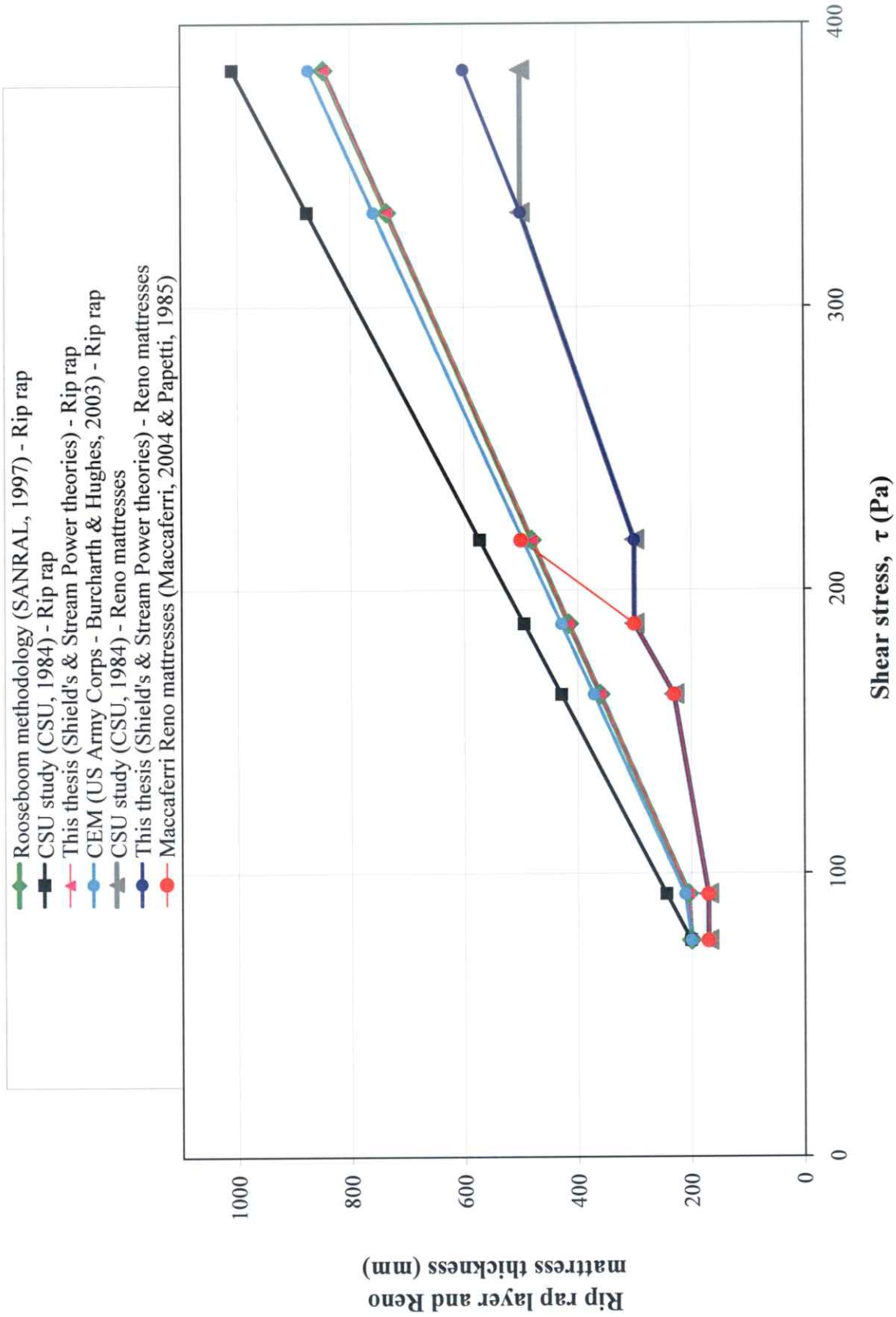


FIGURE D-1: COMPARISON OF RIP RAP LAYER AND RENO MATTRESS THICKNESSES BETWEEN VARIOUS METHODS USED FOR CSU TEST A

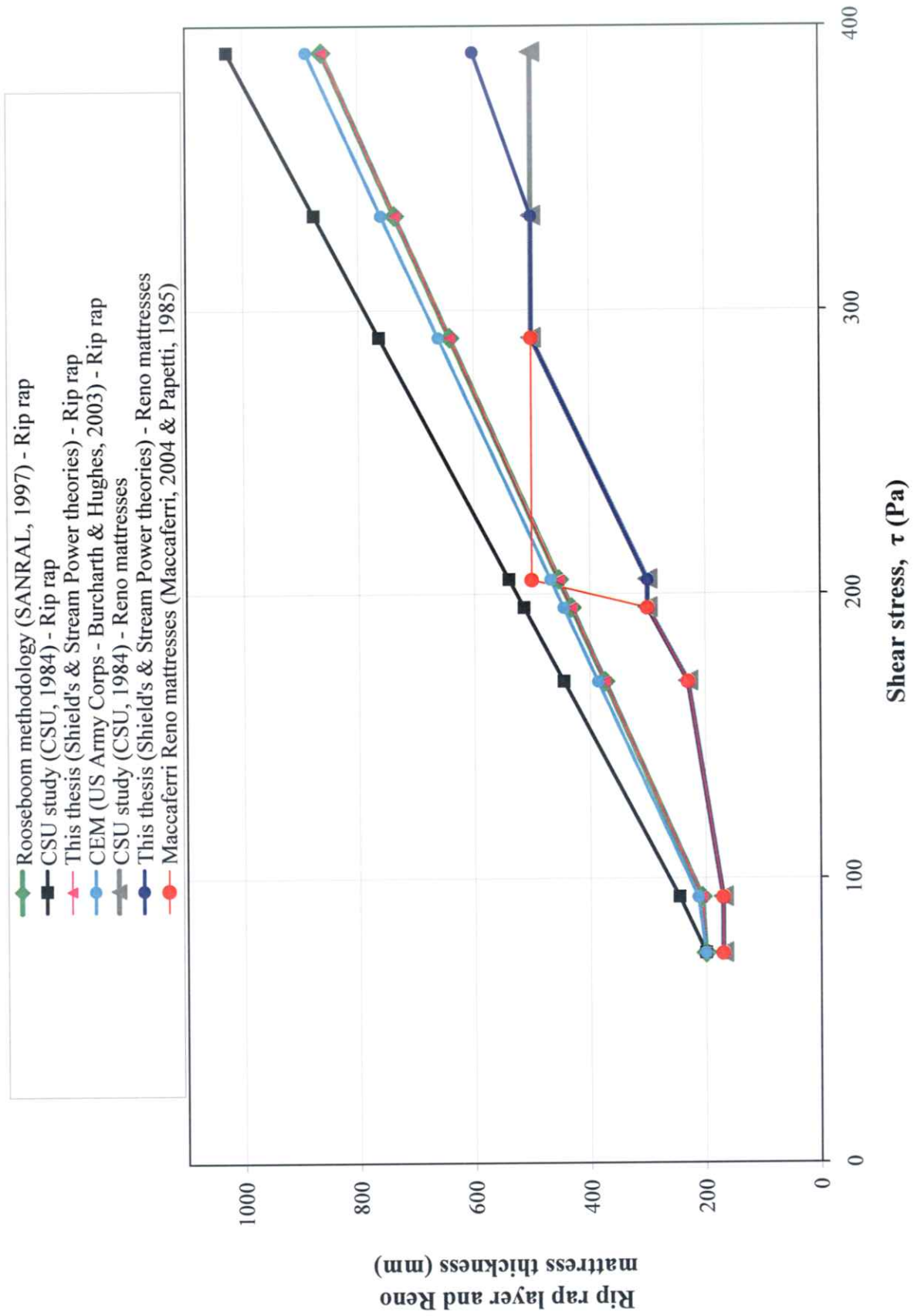


FIGURE D-2: COMPARISON OF RIP RAP LAYER AND RENO MATTRESS THICKNESSES BETWEEN VARIOUS METHODS USED FOR CSU TEST B

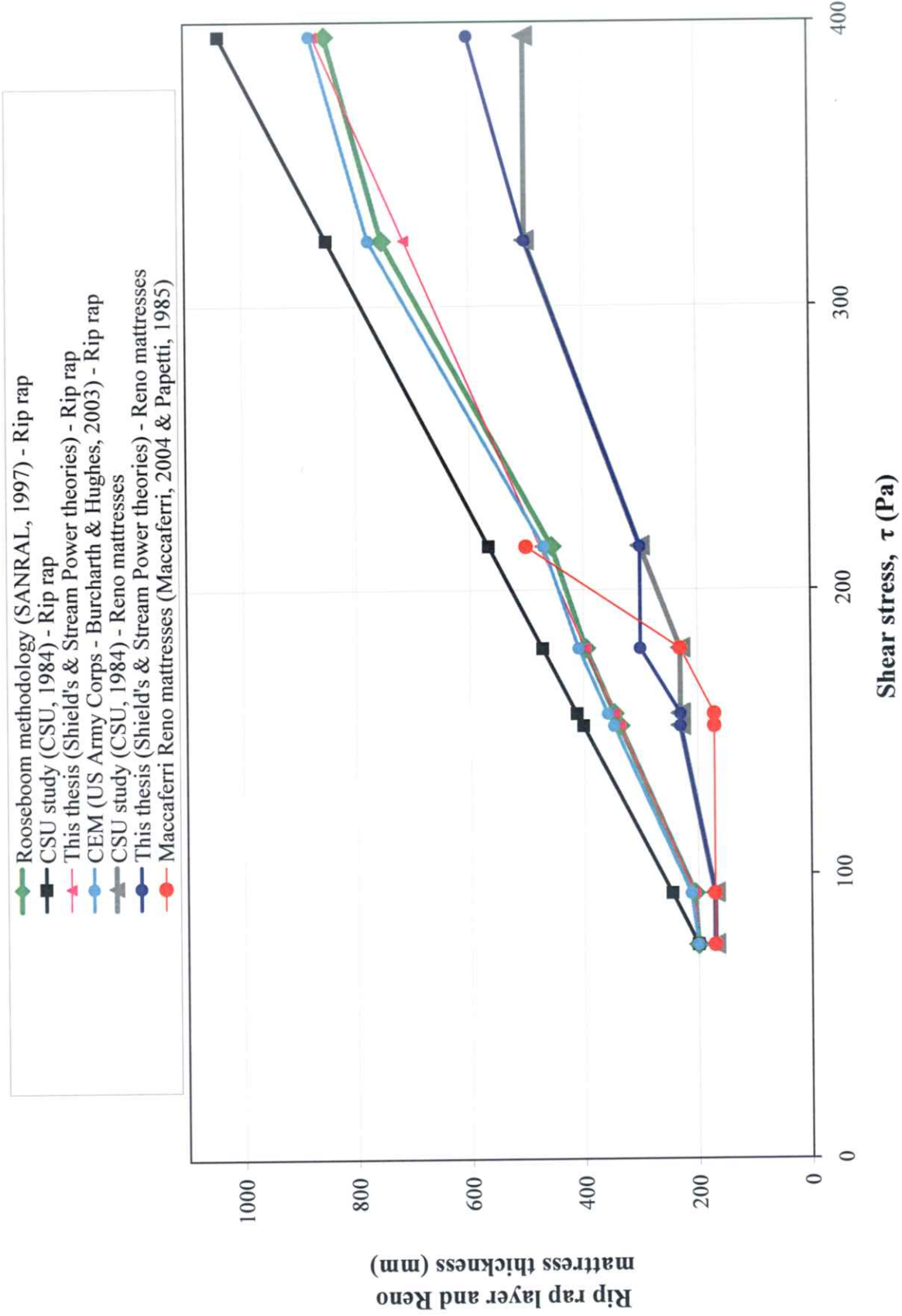


FIGURE D-3: COMPARISON OF RIP RAP LAYER AND RENO MATTRESS THICKNESSES BETWEEN VARIOUS METHODS USED FOR CSU TEST C

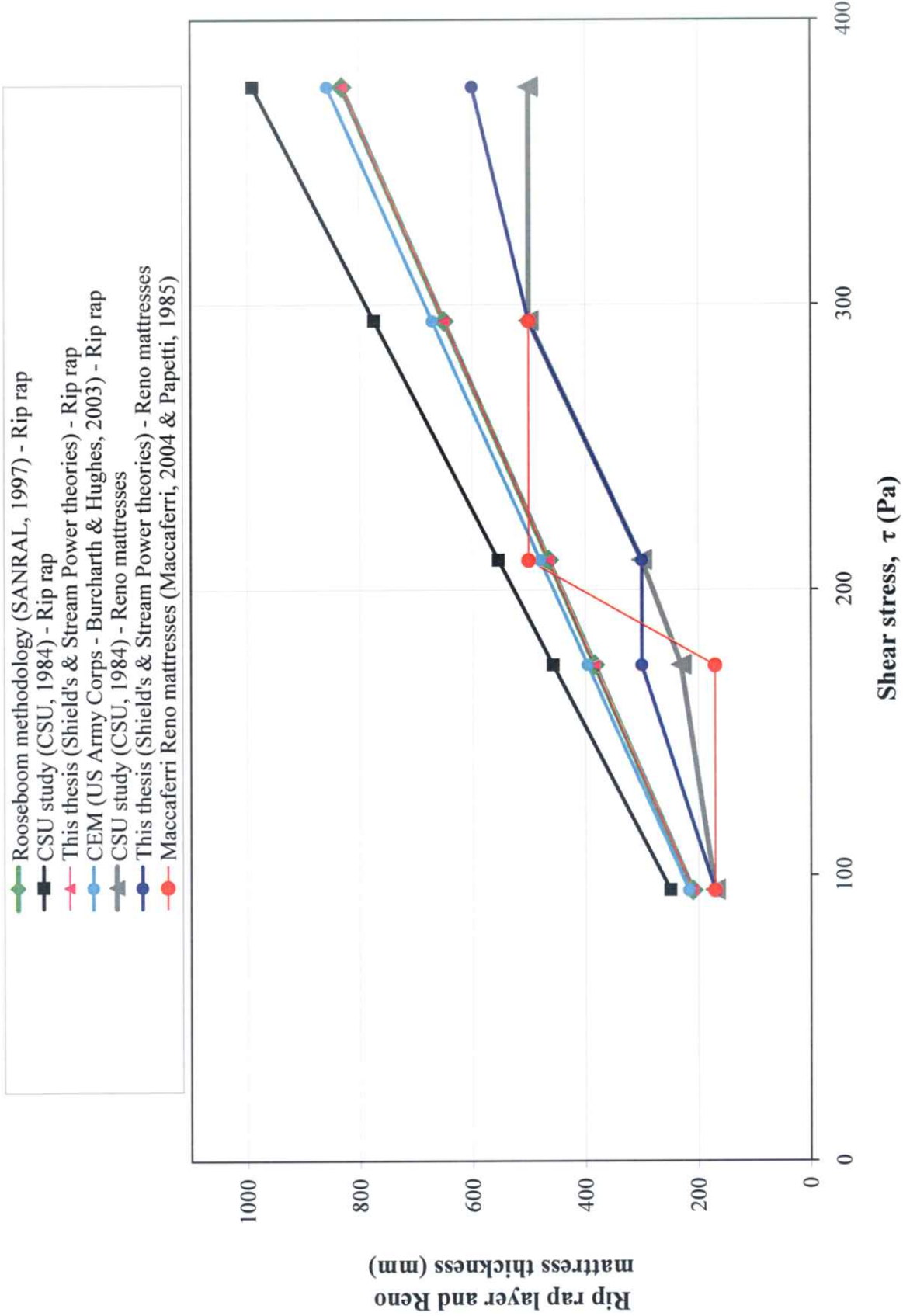


FIGURE D-4: COMPARISON OF RIP RAP LAYER AND RENO MATTRESS THICKNESSES BETWEEN VARIOUS METHODS USED FOR CSU TEST D

ANNEXURE E

Figures E-1 to E-4: Relationship of Sensitive Parameters to Each Other for Minimum Conditions to Just Resist Particle Motion Based on Data of CSU Tests A to D

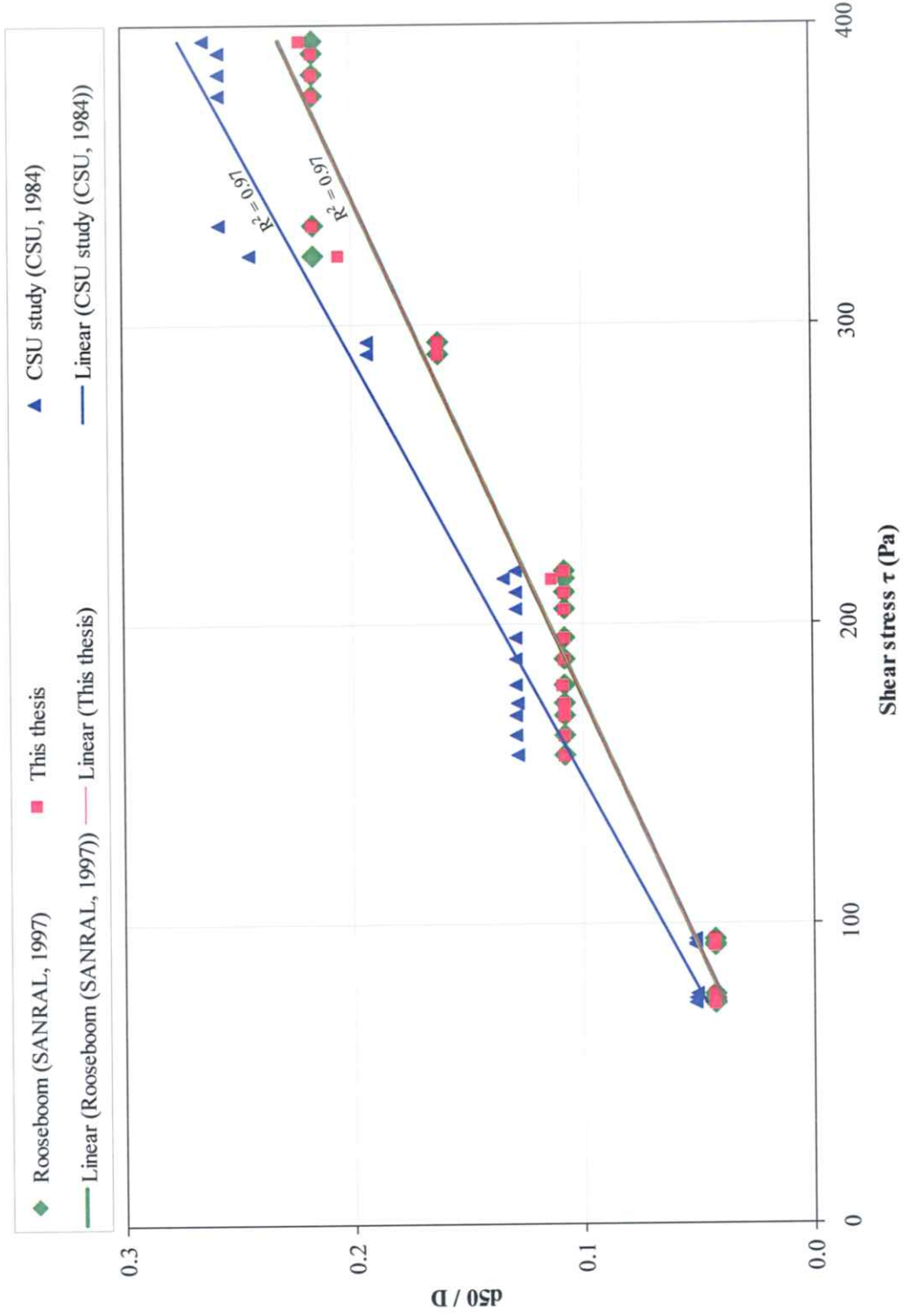


Figure E-1: The relationship of d_{50} / D to bed shear stress for minimum conditions to just resist particle motion (at point of motion incipency) for rip rap, based on data of CSU tests A to D (also see Tables 4.8 to 4.11 and Figures 4.4 to 4.7)

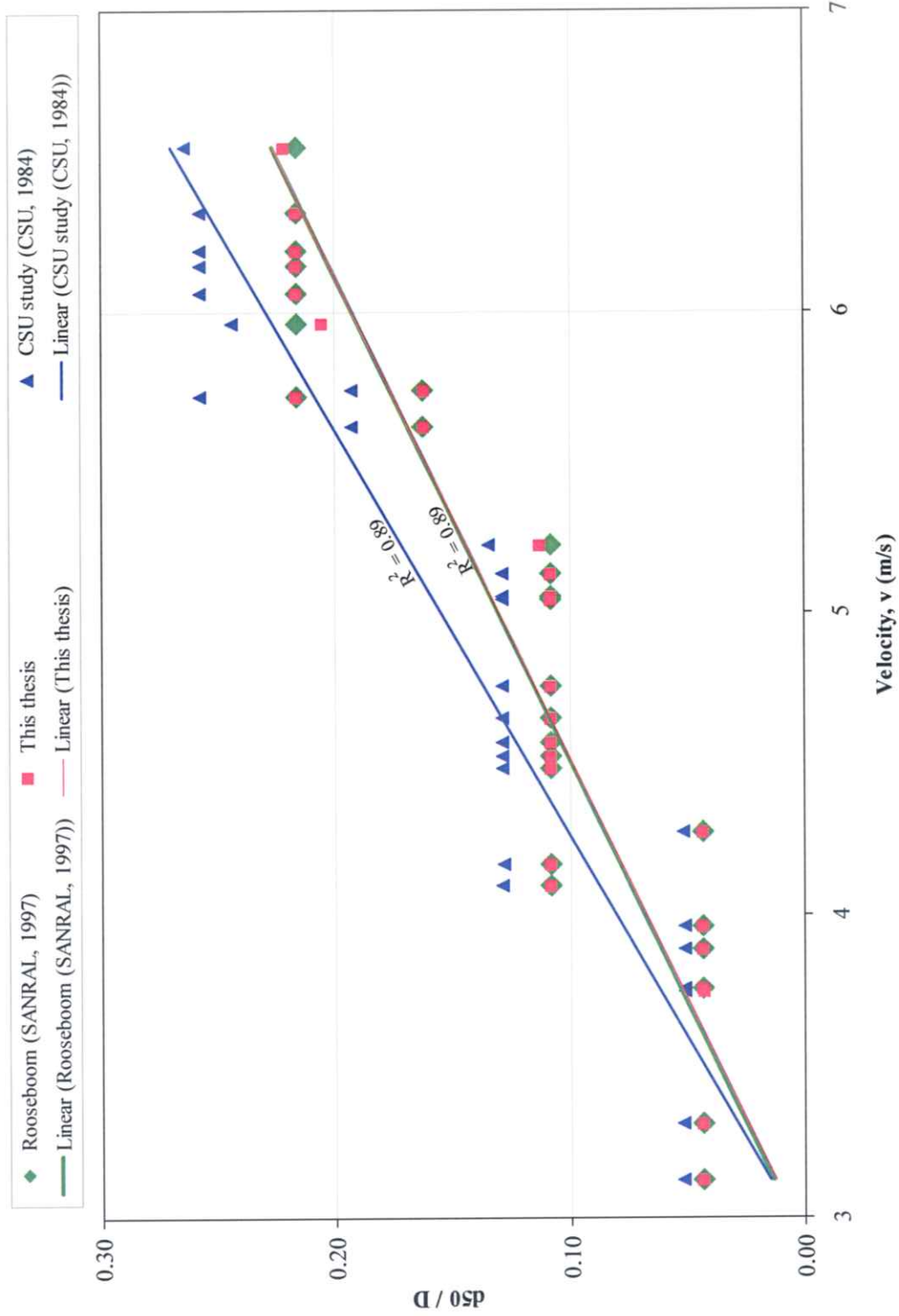


Figure E-2: The relationship of d_{50} / D to flow velocity for minimum conditions to just resist particle motion (at point of motion incipency) for rip rap, based on data of CSU tests A to D (also see Tables 4.8 to 4.11 and Figures 4.4 to 4.7)

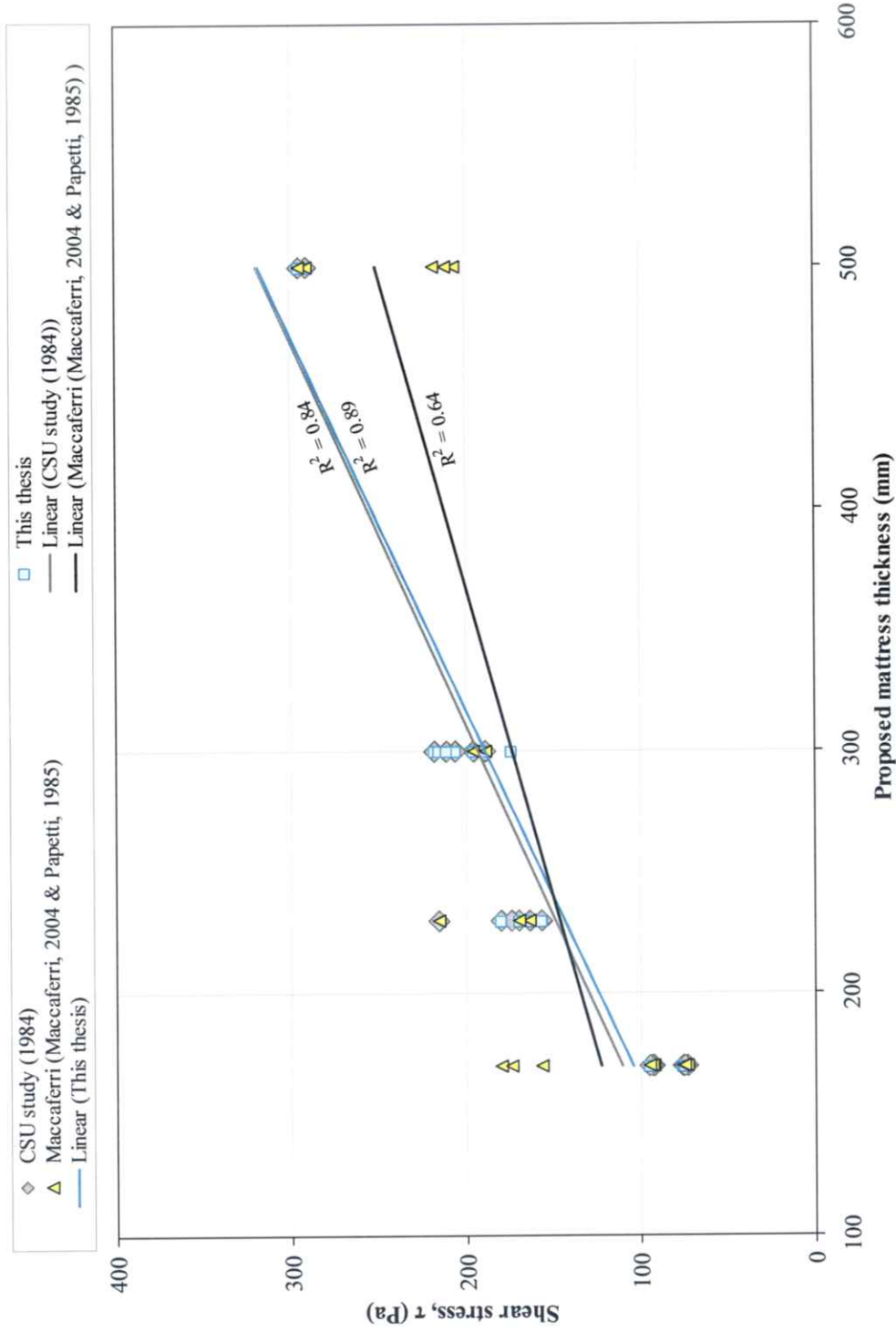


Figure E-3: The relationship of bed shear stress to proposed Reno mattress thickness for minimum conditions to just resist particle motion (at point of motion incipency), based on data of CSU tests A to D (also see Tables 4.12 to 4.15 and Figures 4.11 to 4.14)

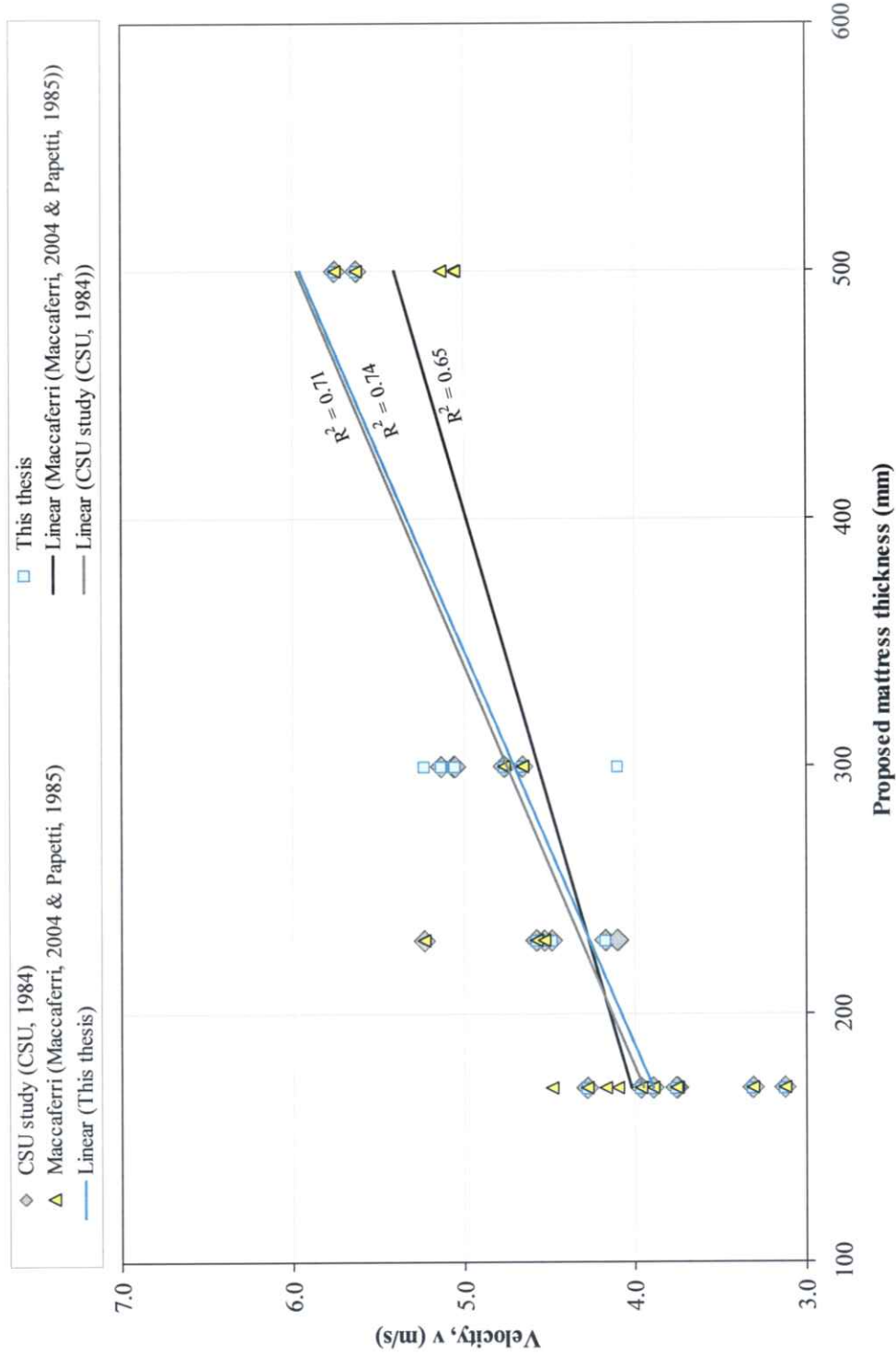


Figure E-4: The relationship of flow velocity to proposed Reno mattress thickness for minimum conditions to just resist particle motion (at point of motion incipency), based on data of CSU tests A to D (also see Tables 4.12 to 4.15 and Figures 4.11 to 4.14)

ANNEXURE F

**Figures F-1 to F-4: Comparative Costs for Rip Rap
and Reno Mattresses Based
on CSU Tests A to D**

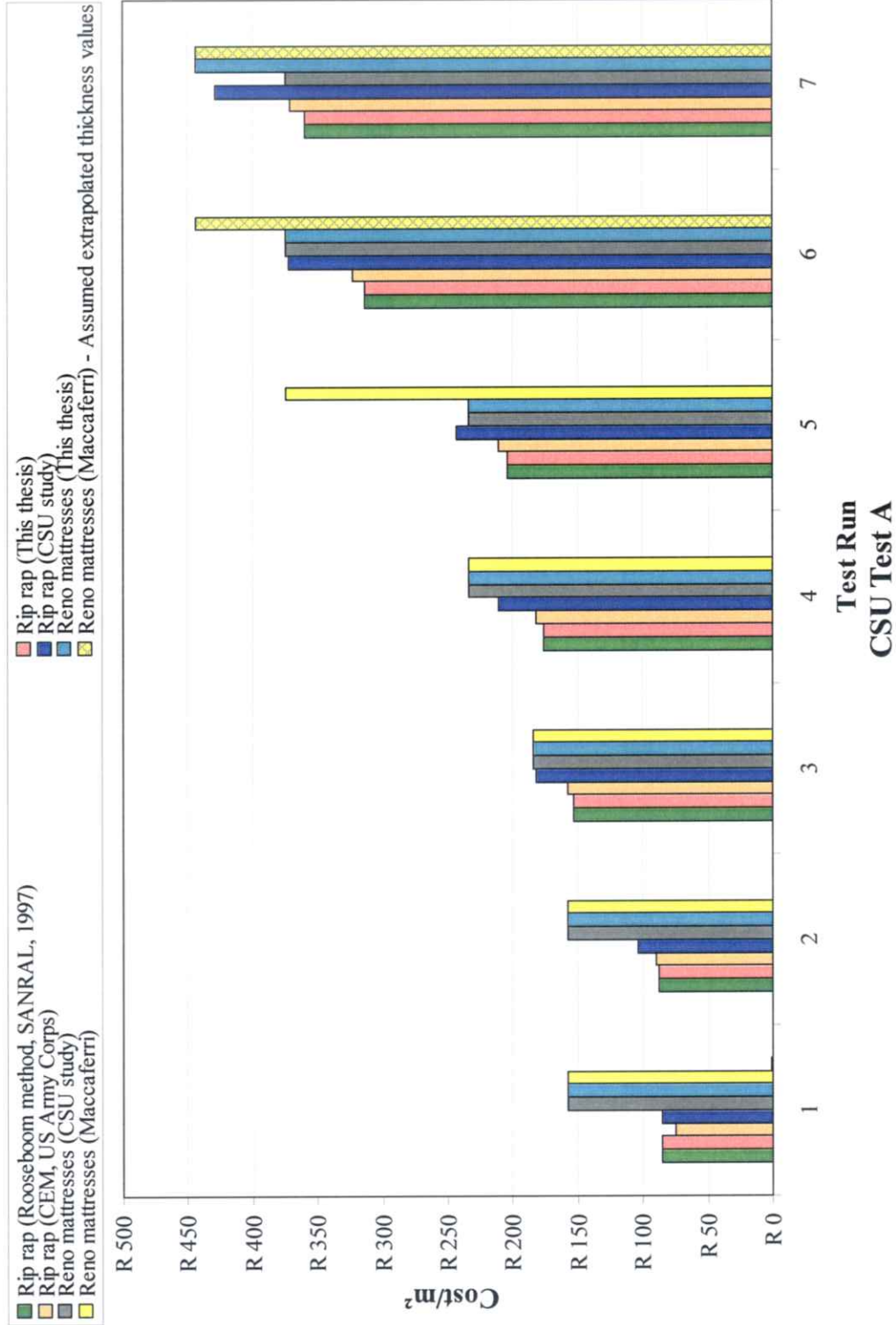


Figure F-1: Comparative costs for rip rap and Reno mattresses for minimum required layer thicknesses to just resist motion (at incipient motion condition) as per CSU Test A (see Tables 3.4, 4.1, 4.8 and 4.12, as well as Figures 4.4 and 4.11)

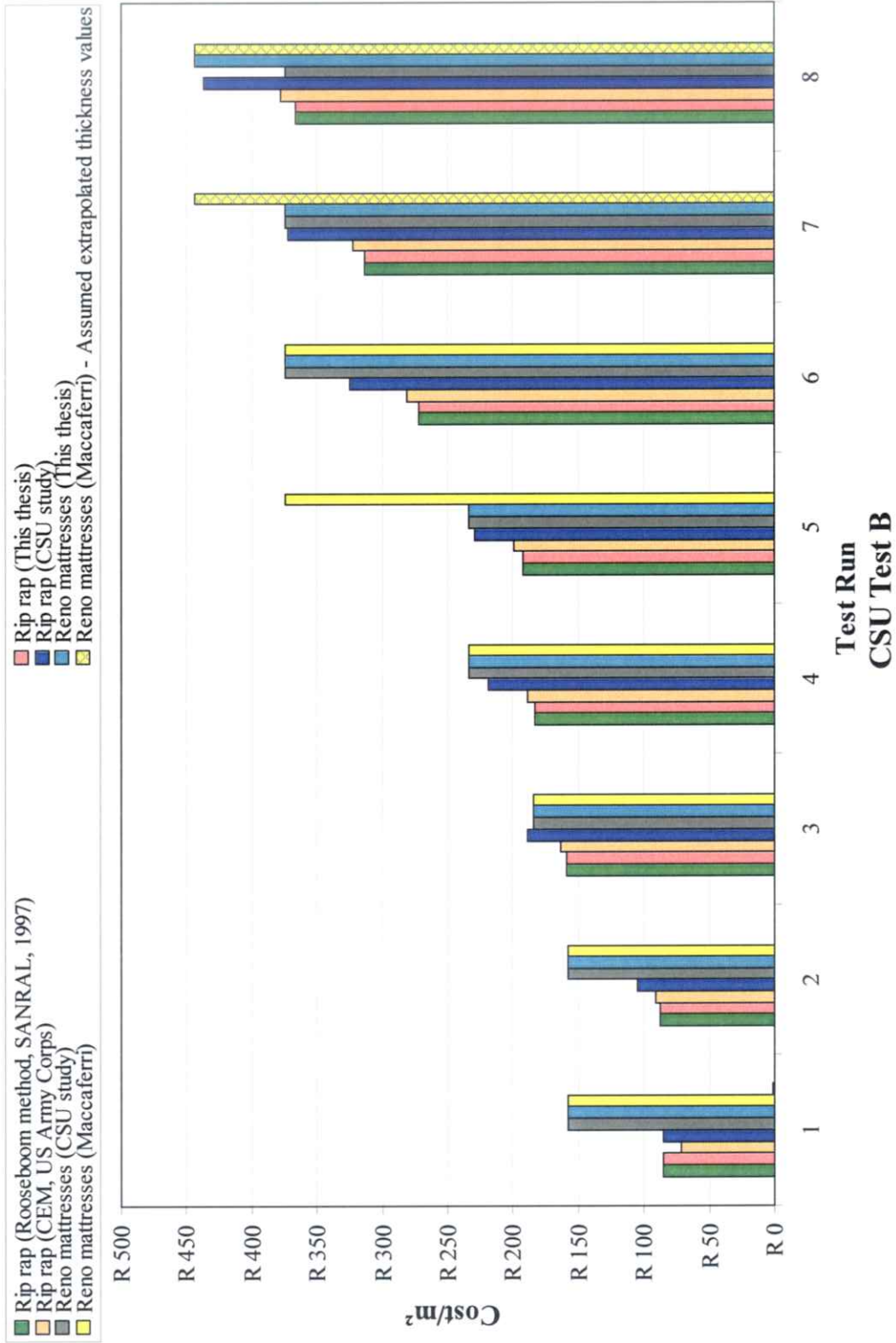


Figure F-2: Comparative costs for rip rap and Reno mattresses for minimum required layer thicknesses to just resist motion (at incipient motion condition) as per CSU Test B (see Tables 3.5, 4.2, 4.9 and 4.13, as well as Figures 4.5 and 4.12)

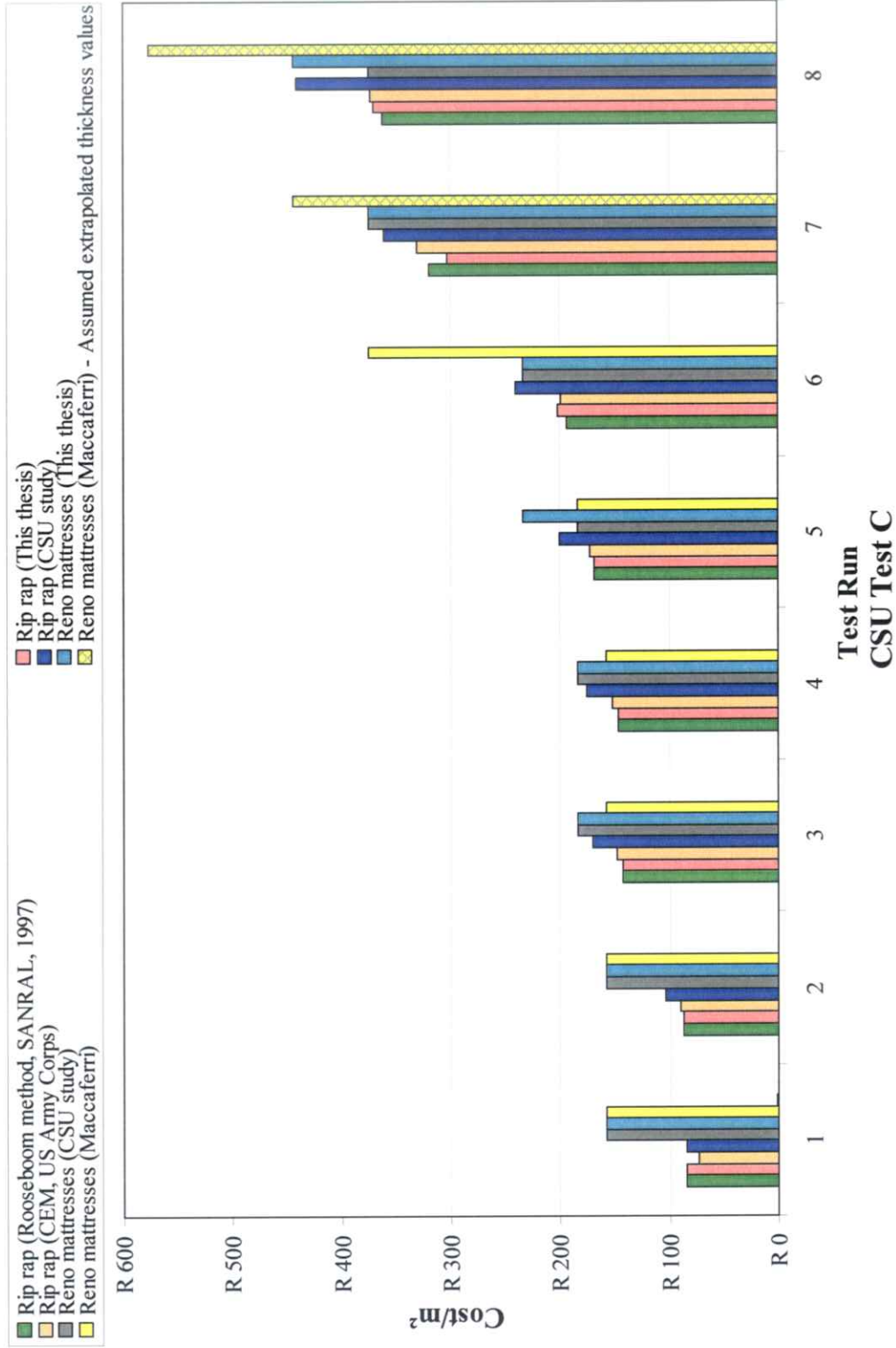


Figure F-3: Comparative costs for rip rap and Reno mattresses for minimum required layer thicknesses to just resist motion (at incipient motion condition) as per CSU Test C (see Tables 3.6, 4.3, 4.10 and 4.14, as well as Figures 4.6 and 4.13)

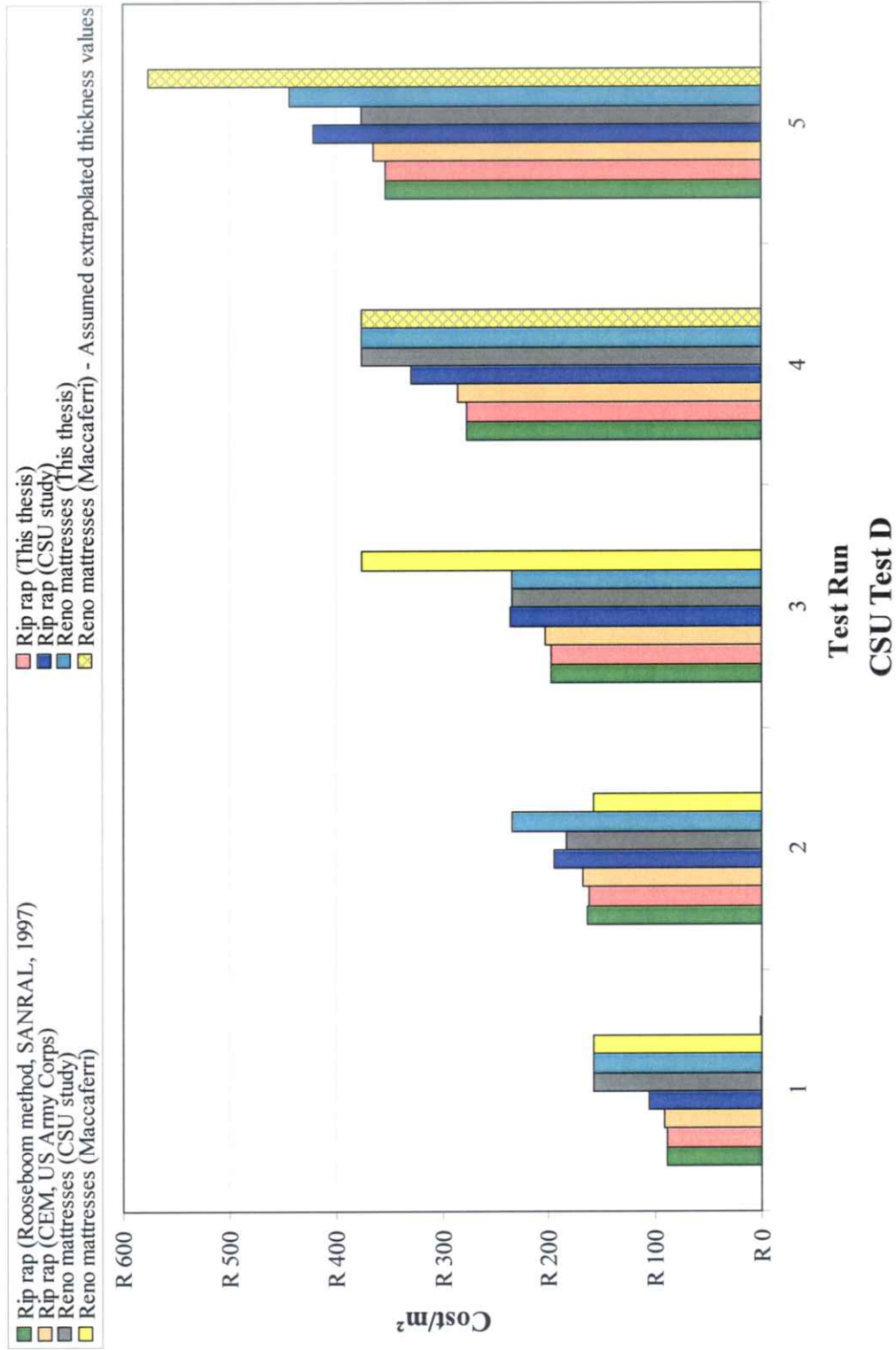


Figure F-4: Comparative costs for rip rap and Reno mattresses for minimum required layer thicknesses to just resist motion (at incipient motion condition) as per CSU Test D (see Tables 3.7, 4.4, 4.11 and 4.15, as well as Figures 4.7 and 4.14)

